

UNIVERSITÄT BREMEN

FACHBEREICH 04

DEUTSCHES ZENTRUM FÜR LUFT- UND RAUMFAHRT (DLR)

Master Thesis Report

Analysis of Hydrogen and Methane as a Fuel for Electrically Augmented Expander Cycle Engine

by

Taha Merchant

First Examiner: Dr. -Ing. Peter Rickmers

Second Examiner: Prof. Dr. -Ing. Andreas Rittweger

Submitted: April 24th, 2023

Offizielle Erklärungen von

Nachname: Merchant Vorname: Taha
Matrikelnr.: 6017989

A) Eigenständigkeitserklärung

Ich versichere, dass ich die vorliegende Arbeit selbstständig verfasst und keine anderen als die angegebenen Quellen und Hilfsmittel verwendet habe.

Alle Teile meiner Arbeit, die wortwörtlich oder dem Sinn nach anderen Werken entnommen sind, wurden unter Angabe der Quelle kenntlich gemacht. Gleiches gilt auch für Zeichnungen, Skizzen, bildliche Darstellungen sowie für Quellen aus dem Internet.

Die Arbeit wurde in gleicher oder ähnlicher Form noch nicht als Prüfungsleistung eingereicht.

Die elektronische Fassung der Arbeit stimmt mit der gedruckten Version überein.

Mir ist bewusst, dass wahrheitswidrige Angaben als Täuschung behandelt werden.

B) Erklärung zur Veröffentlichung von Bachelor- oder Masterarbeiten

Die Abschlussarbeit wird zwei Jahre nach Studienabschluss dem Archiv der Universität Bremen zur dauerhaften Archivierung angeboten. Archiviert werden:

- 1) Masterarbeiten mit lokalem oder regionalem Bezug sowie pro Studienfach und Studienjahr 10 % aller Abschlussarbeiten
- 2) Bachelorarbeiten des jeweils ersten und letzten Bachelorabschlusses pro Studienfach u. Jahr.

Ich bin damit einverstanden, dass meine Abschlussarbeit im Universitätsarchiv für wissenschaftliche Zwecke von Dritten eingesehen werden darf.

Ich bin damit einverstanden, dass meine Abschlussarbeit nach 30 Jahren (gem. §7 Abs. 2 BremArchivG) im Universitätsarchiv für wissenschaftliche Zwecke von Dritten eingesehen werden darf.

Ich bin nicht damit einverstanden, dass meine Abschlussarbeit im Universitätsarchiv für wissenschaftliche Zwecke von Dritten eingesehen werden darf.

C) Einverständniserklärung über die Bereitstellung und Nutzung der Bachelorarbeit / Masterarbeit / Hausarbeit in elektronischer Form zur Überprüfung durch Plagiatsoftware

Eingereichte Arbeiten können mit der Software *Plagscan* auf einen hauseigenen Server auf Übereinstimmung mit externen Quellen und der institutionseigenen Datenbank untersucht werden. Zum Zweck des Abgleichs mit zukünftig zu überprüfenden Studien- und Prüfungsarbeiten kann die Arbeit dauerhaft in der institutionseigenen Datenbank der Universität Bremen gespeichert werden.

Ich bin damit einverstanden, dass die von mir vorgelegte und verfasste Arbeit zum Zweck der Überprüfung auf Plagiate auf den *Plagscan*-Server der Universität Bremen hochgeladen wird.

Ich bin ebenfalls damit einverstanden, dass die von mir vorgelegte und verfasste Arbeit zum o.g. Zweck auf dem *Plagscan*-Server der Universität Bremen hochgeladen u. dauerhaft auf dem *Plagscan*-Server gespeichert wird.

Ich bin nicht damit einverstanden, dass die von mir vorgelegte u. verfasste Arbeit zum o.g. Zweck auf dem *Plagscan*-Server der Universität Bremen hochgeladen u. dauerhaft gespeichert wird.

Mit meiner Unterschrift versichere ich, dass ich die oben stehenden Erklärungen gelesen und verstanden habe. Mit meiner Unterschrift bestätige ich die Richtigkeit der oben gemachten Angaben.

24.04.2023, Bremen

Datum, Ort



Unterschrift



Abstract

With the increase in activity and momentum towards Lunar and Martian exploration and habitation, there is a need for a reliable, reusable and versatile engine which can also use a propellant that can be produced in situ. The Osiris Electrically Augmented Expander Cycle Engine, developed in an earlier Masters Project work, can fill that role; however, one of the important parameters to be considered for this implementation is the choice of the right fuel. Liquid hydrogen and liquid methane are the two fuels being considered for this engine due to their potential for in situ production, but which of these two would be the ideal choice? The objective of this study is to understand the effects of hydrogen and methane as fuel in a spacecraft with the Osiris Electrically Augmented Expander Cycle Engine for Lunar and interplanetary missions. The study will create two specific use case envelopes for a mission to the Moon and Mars for which a spacecraft with the two versions of the engine will be defined. The study will then look at six different aspects and how these two fuel versions compare against each other and then look at the merits of hydrogen and methane as a fuel for exploration missions as a whole at the end.

Acknowledgements

I would like to thank my thesis supervisor, Dr. Peter Rickmers, for his support during the course of my thesis and for being a constant source of inspiration and encouragement. I would also like to thank my supervisor at my workplace, Christian Hessel, whose advice was always invaluable, as well as, all my colleagues at the propulsion department at ArianeGroup Bremen.

The support of my friends and family through this journey is of course an integral part of making any of this possible, so I'd like to thank my parents, sister, grandparents, uncle and aunt for all their love and prayers, along with Jesaiah, Dhruv, Sahana, Jugal and Giuditta for always standing by my side.

Contents

List of Abbreviations	13
1 Introduction	14
1.1 Motivation	14
1.2 Research Question	15
2 Theoretical background and State of The Art	16
2.1 Pressure Fed Engines	16
2.2 Pump Fed Engines	16
2.2.1 Gas Generator Cycle	16
2.2.2 Staged Combustion Cycle	17
2.2.3 Expander Cycle	17
2.2.4 Electric Pump Cycle	17
2.3 Electrically Augmented Expander Cycle	18
3 Osiris Rocket Engine	19
3.1 Introduction	19
3.2 Description	19
4 Approach	24
5 Use Case Envelopes	27
5.1 LEO-Mars Orbit Mission	27
5.1.1 Approach	28
5.1.2 Results	32
5.1.2.1 ΔV Required	35
5.1.2.2 Time of Flight	35
5.2 LEO-Moon Orbit Mission	35
5.2.1 Approach	36
5.2.2 Results	38
5.2.2.1 ΔV Required	39
5.2.2.2 Time of Flight	39
6 Efficiency of the Fuels	40
6.1 Introduction	40
6.2 Specific Impulse and Chemistry of Combustion	41
6.2.1 Hydrolox Combustion	43
6.2.2 Methalox Combustion	44
6.3 Conclusion and Scoring	45

7	System Mass and Fuel Budget	47
7.1	Introduction	47
7.2	System Mass Estimation Tool	48
7.2.1	Approach	48
7.2.1.1	Tool Logic	51
7.3	Results	55
7.3.1	For Moon Mission with Hydrolox Osiris Engine	55
7.3.2	For Moon Mission with Methalox Osiris Engine	56
7.3.3	For Mars Mission with Hydrolox Osiris Engine	57
7.3.4	For Mars Mission with Methalox Osiris Engine	58
7.3.5	Trends	58
7.3.5.1	ΔV Trend for Hydrolox Engine	59
7.3.5.2	ΔV Trend for Methalox Engine	60
7.3.5.3	Oxidiser to Fuel Ratio Trend for Hydrolox Engine for Moon Mission	61
7.3.5.4	Oxidiser to Fuel Ratio Trend for Methalox Engine for Moon Mission	62
7.3.5.5	Oxidiser to Fuel Ratio Trend for Hydrolox Engine for Mars Mission	63
7.3.5.6	Oxidiser to Fuel Ratio Trend for Methalox Engine for Mars Mission	64
7.3.5.7	Specific Impulse Trend for Hydrolox Engine for Moon Mission	65
7.3.5.8	Specific Impulse Trend for Methalox Engine for Moon Mission	66
7.3.5.9	Specific Impulse Trend for Hydrolox Engine for Mars Mission	67
7.3.5.10	Specific Impulse Trend for Methalox Engine for Mars Mission	68
7.3.6	Summary	69
7.4	Conclusion and Scoring	70
8	Pump Power Requirements	74
8.1	Osiris Hydrogen and Methane Pump Overview	74
8.2	Start Up Power	78
8.3	Conclusion and Scoring	80
9	Storability and Long-Term Use	82
9.1	Introduction	82
9.2	Factors affecting storability and long-term use	82
9.2.1	Molecule Size	82

9.2.2	Cryogenic Temperature	83
9.2.3	Interaction with Materials	83
9.2.4	Handling on Earth and other Planetary bodies	84
9.2.5	Toxicity	84
9.2.6	Boil Off	85
9.3	Conclusion and Scoring	85
10	Boil Off Behaviour	87
10.1	Introduction	87
10.2	Boil Off Estimate with Heat Flux Input Estimation Tool	87
10.2.1	Approach	87
10.3	Results	93
10.3.1	Power inputs to the Spacecraft Tanks using Matlab Tool	93
10.3.1.1	Solar Heat Flux Distribution Graph	93
10.3.1.2	For Moon mission	94
10.3.1.3	For Mars mission	103
10.3.2	Boil Off calculation using BoilFAST	111
10.3.2.1	For Liquid Hydrogen Tank for Moon Mission	111
10.3.2.2	For Liquid Methane Tank for Moon Mission	115
10.3.2.3	For Liquid Hydrogen Tank for Mars Mission	118
10.3.2.4	For Liquid Methane Tank for Mars Mission	122
10.4	Summary	125
10.4.1	Heat Flux Estimation using Matlab Tool	125
10.4.2	Boil Off Estimation using BoilFAST	126
10.5	Conclusion and Scoring	126
11	In Situ Production	128
11.1	Introduction	128
11.2	Mars	129
11.2.1	Resources	129
11.2.2	ISRU for Hydrogen on Mars	132
11.2.2.1	Electrolysis	132
11.2.2.2	Magnetite / Wustite Redox Cycle Method to Produce Hydrogen	136
11.2.2.3	Water Gas Shift Reaction	136
11.2.2.4	Liquid Hydrogen Storage	137
11.2.3	ISRU for Methane on Mars	137
11.2.3.1	Natural Methane	137
11.2.3.2	Sabatier Process	138
11.2.3.3	Liquid Methane Storage	139
11.3	The Moon	139

11.3.1 Resources	139
11.3.2 ISRU for Hydrogen on the Moon	142
11.3.3 ISRU for Methane on the Moon	142
11.4 Conclusion and Scoring	143
12 Evaluation of Results	145
13 Conclusion	150
Appendix A	151
Appendix B	155
Appendix C	162
List of Figures	169
List of Tables	173
References	174

List of Abbreviations

Abbreviation	Description
AEM	Anion Exchange Membrane
AU	Astronomical Unit
CH ₄	Liquid Methane
ESA	European Space Agency
GC	Glassy Carbon
GMAT	General Mission Analysis Tool
ISRU	In-situ resource utilization
LCROSS	Lunar Crater Observation and Sensing Satellite
LEO	Low-Earth-Orbit
LH ₂	Liquid Hydrogen
LOx	Liquid Oxygen
LRO	Lunar Reconnaissance Orbiter
MER	Mass Estimation Relation
MOXIE	Mars Oxygen In-Situ Resource Utilization Experiment
MRO	Mars Reconnaissance Orbiter
NASA	National Aeronautics and Space Administration
OF Ratio	Oxidiser to Fuel Ratio
SpaceX	Space Exploration Technologies Corporation
ULA	United Launch Alliance

1. Introduction

In 1903, Konstantin Eduardovitch Tsiolkovsky published an article in the journal “Scientific Review” in Russia called “Exploration of Space with Reactive Devices” [1].

The summarised key points of this article were as follows:

1. Space travel is possible.
2. This can be accomplished by means of, and only by means of, rocket propulsion since a rocket is the only known propulsive device which will work in empty space.
3. Gunpowder rockets cannot be used since gunpowder simply does not have enough energy to do the job.
4. Certain liquids do possess the necessary energy.
5. Liquid hydrogen would be a good fuel and liquid oxygen a good oxidiser, and the pair would make a nearly ideal propellant combination.

Today, 120 years later, mankind has gone through a number of technological breakthroughs and stands on the precipice of the next phase of space exploration. What Tsiolkovsky wrote about in 1903 has been realised now, and in fact, liquid hydrogen and liquid oxygen are indeed one of the most efficient propellant combinations used in spacecraft today [1]. But when performance is not the only goal, then other propellants start to become significant contenders.

For Lunar and interplanetary exploration, especially with long-term goals in mind, there are new priorities for a spacecraft. Space systems are needed that are rapidly reusable, reliable, versatile and self-sustaining to a large extent. This is why this analysis aims to look at propellant selection from a system level point of view for an engine that meets these demands in the context of Lunar and interplanetary exploration.

1.1. Motivation

In the last decade, the momentum for space exploration, and especially human space exploration, has built up significantly. This trend is also seen in the current decade and the foreseeable future. With human exploration missions to the Moon scheduled for a couple of years from now and significant advancements in the preparations for Mars missions, the demand for a fleet of vehicles and transport capabilities to the Moon and the Red Planet is at an all-time high. It is, therefore,

crucial that fuel selection is a part of the development phase of engines as for in this chapter of space exploration, the technological and design choices for space technology would be especially driven by its intended scenario [2][3].

The Osiris Electrically Augmented Expander Cycle Engine is poised to be an excellent candidate to fill this role for a multi-restart, multi-use and highly throttleable in-space engine. It is an engine developed for a master project for these capabilities specifically [4]. During the development of the Osiris engine, the fuel initially considered was hydrogen. But as the design progressed, many drawbacks started to appear with hydrogen as the fuel. As an alternate investigation, the engine design study was also conducted with liquid methane as a fuel and a lot of the drawbacks of hydrogen were mitigated. Nonetheless, there were still some aspects of liquid hydrogen that were superior in one aspect of the design compared to others. Therefore a need arose to analyse both Methane and Hydrogen as a fuel for its intended interplanetary use from different aspects and all relevant factors and compare them to come to a conclusion as to with which fuel the engine development should continue.

1.2. Research Question

The main research question that is aimed to be answered is as follows:

For a given set of use case envelopes, whether Hydrogen or Methane is a better fuel option for the Osiris Electrically Augmented Expander Cycle engine?

2. Theoretical background and State of The Art

For missions beyond Earth Orbit, the propellant considered is usually a storable liquid type [5]. The reasons for this are the easy storage and the long-term reliability of these propellants. But considering the rate of growth of longer exploration missions, not only is a more efficient propulsion system required, but also a sustainable one where the propellant can be sourced from their destination. It is for this reason that methane and hydrogen are also being considered for future exploration missions.

Current studies looking at methane and hydrogen tended to focus on their application here on Earth as a source of fuel [6]. In terms of directly comparing methane and hydrogen as a rocket fuel, a lot of studies have considered basic factors for comparison of these two fuels, such as specific impulse, density etc. But what they have not considered, are many aspects on a system level and especially with having a specific engine in mind [7]. Therefore this study intends to bridge that gap.

To have an understanding of the gap the Osiris Electrically Augmented Expander Cycle engine intends to fill, below is a brief look at the state-of-the-art liquid engines.

2.1. Pressure Fed Engines

In a pressure fed liquid rocket engine, the propellant is forced into the combustion chamber using a pressurised gas, such as helium or nitrogen, rather than relying on an engine-driven fuel pump. This is a relatively simple system and is cost-effective [8].

One of the state-of-the-art pressure fed engines used today is the SuperDraco engine onboard SpaceX's Dragon 2 capsule [9].

2.2. Pump Fed Engines

2.2.1. Gas Generator Cycle

In a gas generator system for a rocket engine, a portion of the fuel and oxidiser is redirected to a separate chamber known as the Gas Generator Chamber. Within this chamber, the propellants undergo combustion and generate high-pressure, high-velocity gases that drive the turbine responsible for powering the fuel and oxidiser pumps [8].

The Merlin engine, which is considered a cutting-edge Gas Generator propulsion system, is currently utilised on SpaceX's Falcon 9 rocket [10].

2.2.2. Staged Combustion Cycle

Staged combustion involves diverting a portion of the oxidiser to a separate chamber, as in the gas generator cycle. However, in staged combustion, all of the fuel is directed to the pre-burner, where it is ignited with the oxidiser. The resulting combustion products are then utilised to drive the turbine, which generates power for the fuel and oxidiser pumps [8].

Currently, one of the most advanced full-flow staged combustion engines available is the Raptor engine, which is set to provide propulsion for SpaceX's Starship rocket [11].

2.2.3. Expander Cycle

The Expander cycle operates without initial combustion. Rather than igniting the fuel, it is passed alongside the combustion chamber, where it absorbs the chamber's heat and expands. This expanded fuel is then directed through a turbine, which powers the fuel pump before finally being redirected to the combustion chamber [8].

The RL10 rocket engine is widely recognized as one of the most dependable expander cycle engines in use today. It is currently employed by United Launch Alliance (ULA) to power their Atlas V and Delta IV rockets, as well as by other companies for their rocket's upper stages [12].

2.2.4. Electric Pump Cycle

The Electric Pump cycle replaces the conventional turbine-driven pump mechanism with an electric motor, which is powered by batteries. A driveshaft connects the electric motor to the pump, enabling the transfer of power. This design offers a straightforward, low-complexity solution with fewer moving parts and fewer losses [8].

The best example of an Electric Pump Engine is the Rutherford engine used by Rocket Lab for their Electron rocket [13].

2.3. Electrically Augmented Expander Cycle

The Electrically Augmented Expander cycle engine is a fusion between the Expander and the Electric Pump cycle engine combining the advantages of both. This cycle has a heat exchanger system around the nozzle and turbine that runs with the expanded gas at the higher throttle range, and an electrical pump that powers the motor during startup and lower throttle [4].

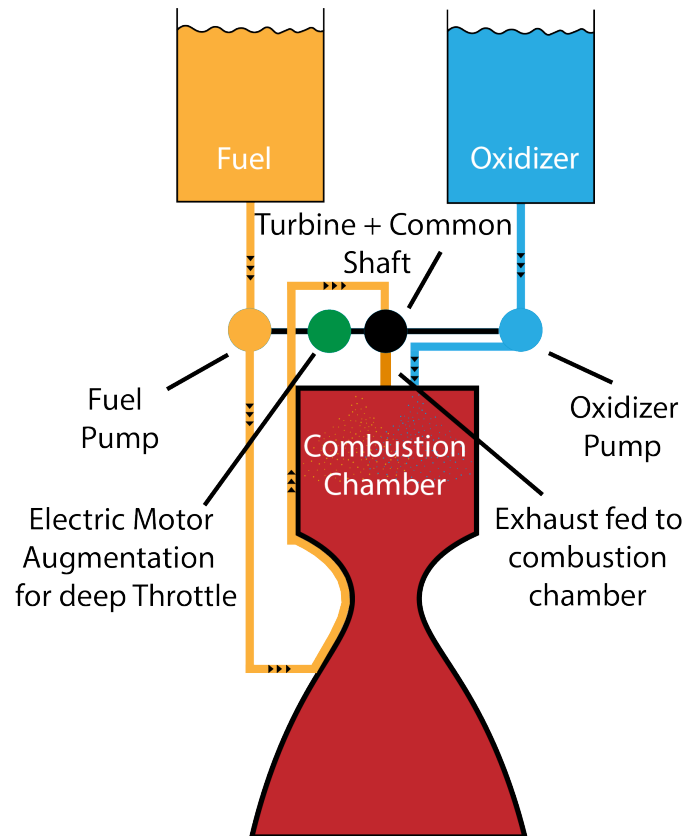


Figure 1: Electrically Augmented Expander Cycle [4]

The Osiris Engine is designed as an Electrically Augmented Expander Cycle engine. For the general understanding of the Osiris Engine, the Masters Project report on the Phase A design of the Electrically Augmented Expander Cycle Engine is a good starting point [4]. In this, the initial design process is detailed, and the general design is laid out. This thesis builds on the work done in this report.

3. Osiris Rocket Engine

3.1. Introduction

The Osiris Electrically Augmented Expander cycle is a liquid bipropellant engine developed to fill in the gaps created due to the drawbacks of a traditional Expander cycle engine by leveraging the potential of advancements in electrical motors and battery technology. The ability of the engine to be easily restartable and deep throttle makes it an excellent engine perfectly suited for high-frequency interplanetary missions. It was intentionally designed to use propellants that could be sourced in situ on destinations such as the Moon and Mars and therefore the design considered hydrogen and methane as its options [4].

3.2. Description

The Osiris Electrically Augmented Expander Cycle engine was designed for two versions, Hydrolox and Methalox [4].

Engine Specifications

Hydrolox Version:

- Thrust: 50 kN
- \dot{m}_{ox} : 8.94 kg/s
- \dot{m}_{fuel} : 1.79 kg/s
- \dot{m} : 10.73 kg/s
- Chamber Pressure: 20 bar
- Oxidiser to Fuel Ratio: 5.0
- Theoretical Specific Impulse: 475 s
- Realistic Specific Impulse (90% efficiency assumed) : 427.5 s

Methalox Version:

- Thrust: 50 kN
- \dot{m}_{ox} : 10.36 kg/s
- \dot{m}_{fuel} : 2.88 kg/s

- \dot{m} : 13.236 kg/s
- Chamber Pressure: 20 bar
- Oxidiser to Fuel Ratio: 3.6
- Theoretical Specific Impulse: 385 s
- Realistic Specific Impulse (90% efficiency assumed) : 346.54 s

The design philosophy of the Osiris engine was based on RL10 A-3 Expander cycle engine as it was similar in performance and had a base architecture of the expander cycle, which is close to the new cycle [40].

The engine consists of a turbine which drives the pumps using the expanded gases during higher throttle phases of operation, one oxidiser pump connected to a shaft, and one fuel pump also connected to a shaft. For the Hydrolox version of the engine, the fuel pump is two stages and, for the Methalox version, it is one stage. The two pump shafts are connected by a gearing mechanism. For the start-up and lower throttle phases, there is an electric motor, which is connected with the help of a clutching mechanism to the gearing mechanism connecting the two pump shafts. Subsequently, there is the combustion chamber and nozzle assembly, along with inbuilt cooling channels built into an inner copper shell and surrounded by a second steel shell. These propellant-feeding driving mechanisms were the main focus of the initial Osiris design. Apart from these, there are all the other standard parts in a liquid engine design. Below are the figures for the general design layout and engine CAD model developed in the project.

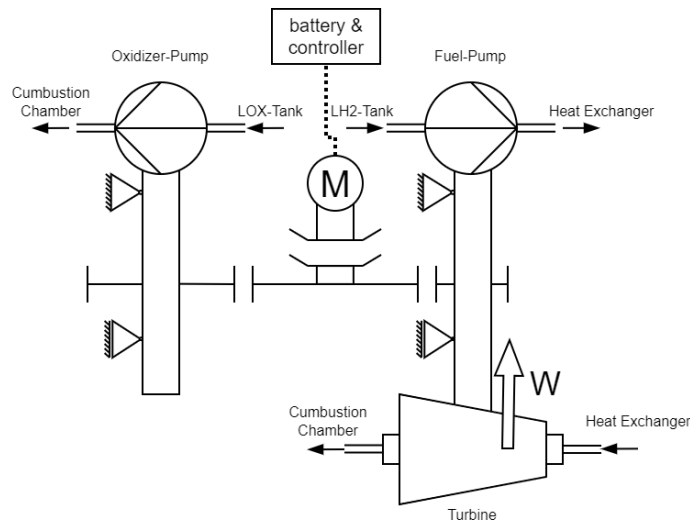
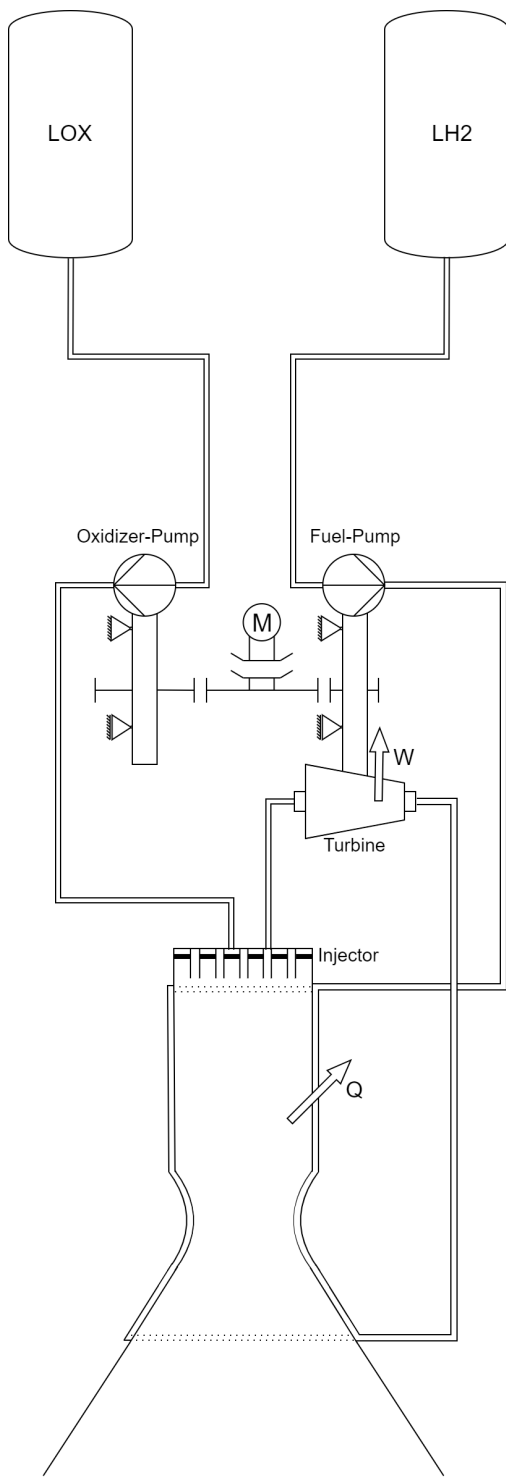
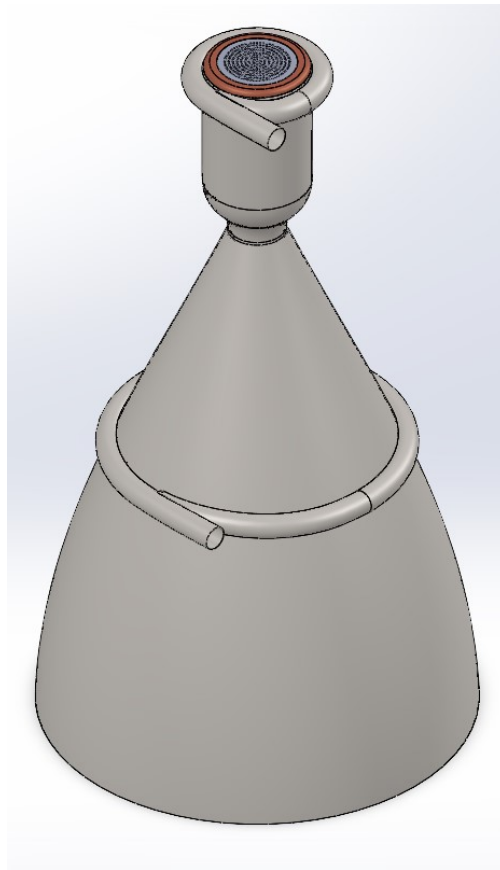


Figure 2: General Turbo Pump Configuration for Osiris Engine [4]



((a)) Complete System Diagram for Osiris Engine [4]



((b)) Final Engine Model (Hydrolox Version) [4]

Figure 3: Osiris Engine System Diagram and Model

The following is the Engine Mass breakdown for the Osiris Engine.

Hydrolox Version:

Part	Mass(kg)
Inner Copper Nozzle and Combustion Chamber with cooling channels	126
Outer Steel Nozzle and Combustion Chamber Shell	85
Injector Plate	1.1
Electric Motor	28.2
Transmission Shafts and Gears	30
Battery and Controller	143
Turbine and Housing	15
Fuel Pump and Housing	50
Oxidiser Pump and Housing	15
Mounts and Other connection hardware	4
Ignition System	3
Valves	21
Tubing and Piping	20
Miscellaneous	5
Total	546.3

Table 1: Hydrolox Version Mass Breakdown

Chapter 3 Osiris Rocket Engine

Methalox Version:

Part	Mass(kg)
Inner Copper Nozzle and Combustion Chamber with cooling channels	141
Outer Steel Nozzle and Combustion Chamber Shell	95
Injector Plate	1.1
Electric Motor	12
Transmission Shafts and Gears	30
Battery and Controller	45
Turbine and Housing	15
Fuel Pump and Housing	20
Oxidiser Pump and Housing	15
Mounts and Other connection hardware	4
Ignition System	3
Valves	21
Tubing and Piping	16
Miscellaneous	5
<u>Total</u>	<u>425.1</u>

Table 2: Methalox Version Mass Breakdown

4. Approach

This study will use a simplified approach to compare the two fuels on a system level with the Osiris engine specifically in mind. This means that the conditions within which it would be compared would give a good representation of the actual environment and provide an equivalent platform for comparison but not necessarily detailed in any specific direction. The aim is to look at both versions of the Osiris engine and put them next to each other comparing them based on certain factors but with having the spacecraft and a specific target mission in mind. This will give a better understanding of which version of Osiris Engine to develop further.

To compare the two engine versions, there will be a sample mission defined that the spacecraft will perform. This will give us an equivalent base for comparison. The two missions chosen are Low Earth Orbit (LEO) to Moon Orbit and LEO to Mars Orbit. These two target destinations were selected since, in the following decades, exploration activities on these bodies are expected to be rampant.

For this study, some assumptions and simplifications will be made.

- First of all, the spacecraft that will be used with the engine for comparison can be considered as a kickstage or a service module for a capsule.
- This spacecraft will have a certain payload on top of it. For example, it could be a lander segment or, in the case of a service module as the spacecraft, the payload would be the capsule it is transporting.
- The spacecraft's mission for the study will be from LEO to Target Body Orbit.
- This is the only segment of operation that will be considered for the study.

For comparing the two fuels for the Osiris engine, different aspects will be looked into that would be important for a space exploration mission, propellant selection and spacecraft design.

They are as follows:

- Efficiency of the Fuels
- System Mass and Fuel Budget
- Pump Power Requirement
- Storability and Long Term Use

Chapter 4 Approach

- Boil Off Behaviour
- In Situ Production



Figure 4: Topics for Comparison

These aspects are interconnected with each other, and software tools will be used to study some of them.

These tools, their inputs, and their outputs will be explained in the following chapters.

They interact with each other as follows:

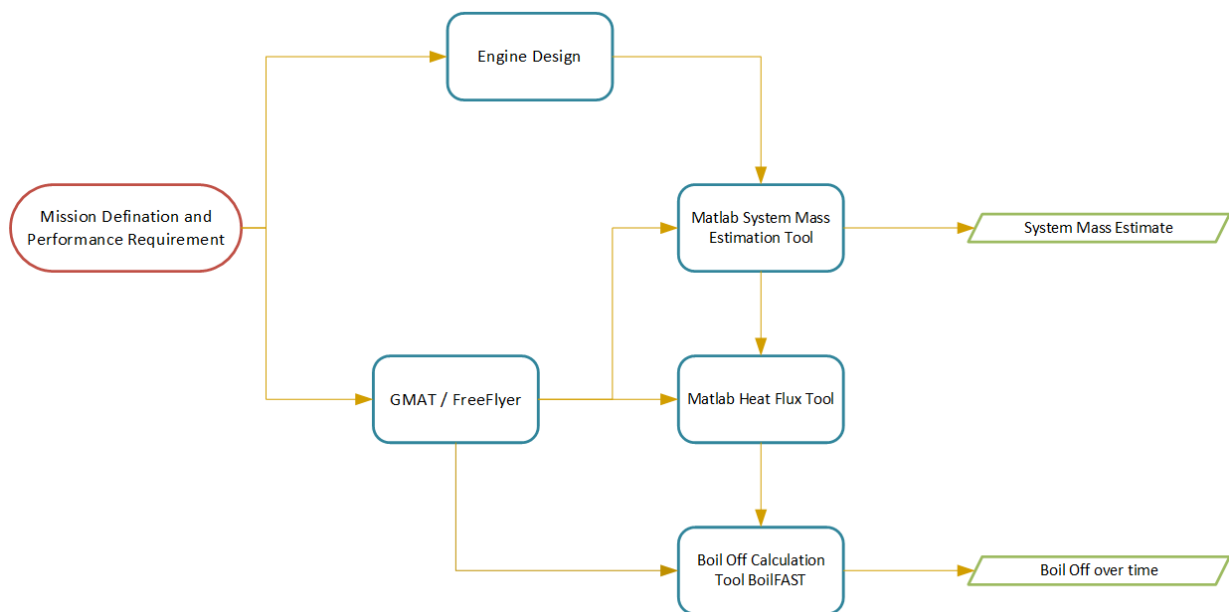


Figure 5: Top Level Logic flow for the Tools used

GMAT, FreeFlyer, BoilFAST, and Matlab are publicly available software, and the Mass Estimation and Heat Flux Estimation tools were created using Matlab for this study. More about these softwares will be discussed in the coming sections, and the code for the Matlab tools are available in the Appendix.

Scoring System

To have an understanding of how the fuels stack up against each other, a scoring system will be used. First, for each aspect of comparison, a score will be given from 0 to 10 for each fuel for each mission type. This will then be multiplied to a certain weight. This would depend on how impactful that factor would be in the overall propellant selection. This would then be added together for each fuel for each mission, and this would give a score to compare.

$$\text{Score for X fuel for Y mission} = \sum(\text{Weight} \times \text{Score})$$

5. Use Case Envelopes

For comparing the different aspects of the two fuels, hydrogen and methane, a reference mission has to be established first. This can be done by selecting certain mission characteristics and then finding out its performance and trajectories and using that information to analyse the fuels.

For this study, two mission types have been considered.

- LEO-Mars Orbit
- LEO-Lunar Orbit

These mission types are considered because, keeping the multirestart and deep throttle capabilities of the Osiris Engine in mind, it is best suited for exploration Missions to the Moon or Mars. To simplify the orbital requirement and not include complicated landing manoeuvres that differ vastly between the Moon and Mars, as well as to provide similar engine burn scenarios (Transfer Burn and Orbit Insertion Burn), the trajectory from the LEO to the Planetary Body orbit was selected.

5.1. LEO-Mars Orbit Mission

In this mission, the spacecraft will start in a LEO and will perform a manoeuvre for Mars Transfer Orbit and, after the encounter with Mars, will perform a Mars Orbit Insertion Manoeuvre.

The assumed orbit data is as follows:

- Spacecraft LEO Altitude: 500 km
- Spacecraft LEO Eccentricity: 0
- Spacecraft LEO Inclination: 23.5°
- Spacecraft LEO Longitude of the Ascending Node: 0°
- Spacecraft LEO Argument of Periapsis: 0°
- Spacecraft LEO True Anomaly: 0°

- Desired Mars Orbit Altitude: 250 km

The orbit of the Mars Reconnaissance Orbiter was used as a reference for assuming these orbital altitudes [14]. Some of the orbital parameters have been chosen as 0 for a simplified Patched Conics approach. This will be further explained in the next section.

Other assumptions made for this analysis:

- A simplified patched conics approach will be used.
- Earth and Mars have perfectly circular and co-planar orbits.
- Newtonian physics is considered.
- Atmospheric Perturbations will not be considered.
- Planetary bodies affecting the spacecraft are the Earth, the Sun, the Moon and Mars
- The journey is assumed perfect; therefore, ΔV required for correction burns is not included.

5.1.1. Approach

The analysis of the trajectory requirements for this mission was done in FreeFlyer® Astrodynamics Software with a student license [15]. This is a commercial off-the-shelf software for Mission Analysis and has been in use since 1997 [16]. The approach followed is based on a modified version of a software tutorial for Patched Conics Transfer [17].

1. First, the Phase Angle is calculated between the two planets so that the spacecraft reaches Mars at the right time and the epoch at which this phase angle occurs. The spacecraft is then propagated to this epoch 6.

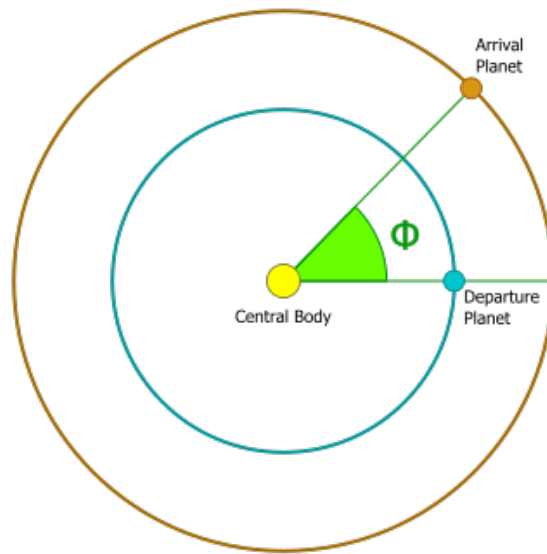


Figure 6: Phase Angle Diagram [17]

2. To have a hyperbolic planet departure, the necessary manoeuvre that the spacecraft would have to make in LEO is then calculated. For this, the hyperbolic excess velocity of departure is then calculated 7.

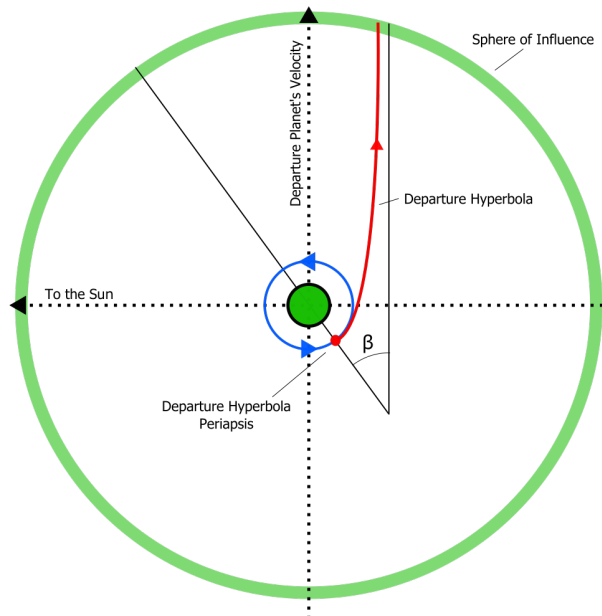


Figure 7: Hyperbolic Escape Trajectory of the spacecraft from Earth [17]

$$v_{\infty} = |v_{TransE} - v_E| \quad (1)$$

v_{∞} = Hyperbolic Excess Speed of Departure Hyperbola
 v_{TransE} = Velocity of Transfer Orbit at Earth (Periapsis)
 v_E = Orbital Velocity of Earth

3. To calculate the hyperbolic excess velocity of departure, the Orbital Velocity of Earth with respect to the Sun is to be calculated first.

$$v_E = \sqrt{\frac{\mu_{Sun}}{r_E}} \quad (2)$$

μ_{Sun} = Gravitational Parameter of the Sun
 r_E = Radius of Earth's Orbit around Sun

4. As well as the velocity of transfer at Earth.

$$v_{TransE} = \sqrt{\mu_{Sun} \left(\frac{2}{r_E} - \frac{1}{a_{Trans}} \right)} \quad (3)$$

a_{Trans} = Semi - Major Axis of Transfer Orbit

Therefore from equation 2 and 3

$$v_{\infty} = \sqrt{\frac{\mu_{Sun}}{r_E} \left(\sqrt{2 - \frac{r_E}{a_{Trans}}} - 1 \right)} \quad (4)$$

5. Once the hyperbolic excess velocity is calculated, the velocity at periapsis can be found.

$$a_{hyp} = \left(\frac{2}{r_{EarthSOI}} - \frac{v_{\infty}^2}{\mu_{Earth}} \right)^{-1} \quad (5)$$

a_{hyp} = Semi - Major Axis of Escape Hyperbola
 $r_{EarthSOI}$ = Radius of Earth's SOI
 μ_{Earth} = Standard Gravitational Parameter of Earth

$$v_p = \sqrt{\mu_{Earth} \left(\frac{2}{r_p} - \frac{1}{a_{hyp}} \right)} \quad (6)$$

v_p = Velocity at Periapsis of the Hyperbola
 r_p = Radius of the Parking Orbit

6. Therefore, the Δv needed by the spacecraft to escape Earth can be calculated by subtracting the parking orbit velocity from the velocity at periapsis.

$$\Delta v_1 = \left| v_p - \sqrt{\frac{\mu_{Earth}}{r_p}} \right| \quad (7)$$

$\Delta v_1 = \text{Magnitude of First Burn}$

7. After calculating where in the spacecraft's trajectory around Earth the burn would be needed to be performed, the β angle is calculated.

$$\beta = \cos^{-1} \left(\frac{1}{1 + \frac{r_p \cdot v_\infty^2}{\mu_{Earth}^2}} \right) \quad (8)$$

8. It can be calculated similarly for a Hyperbolic Planetary Arrival 8.

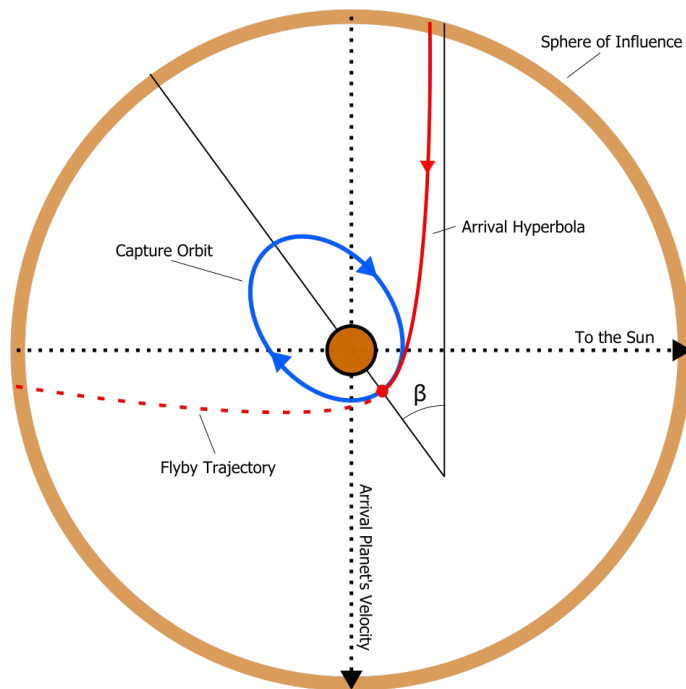


Figure 8: Hyperbolic Arrival Trajectory of the spacecraft to Mars [17]

$$\Delta v_2 = \left| v_p - \sqrt{\frac{\mu_{Mars}}{r_p}} \right| \quad (9)$$

$\Delta v_2 =$ Magnitude of Second Burn

$v_p =$ Velocity at Periapsis of the Arrival Hyperbola

$\mu_{Mars} =$ Gravitational Parameter of Mars

$r_p =$ Radius of the Arrival Parking Orbit/Periapsis

This gives the Δv required to insert the spacecraft into a circular Mars Orbit.

5.1.2. Results

The following were the results of the Trajectory Simulation on FreeFlyer Astrodynamics Software:

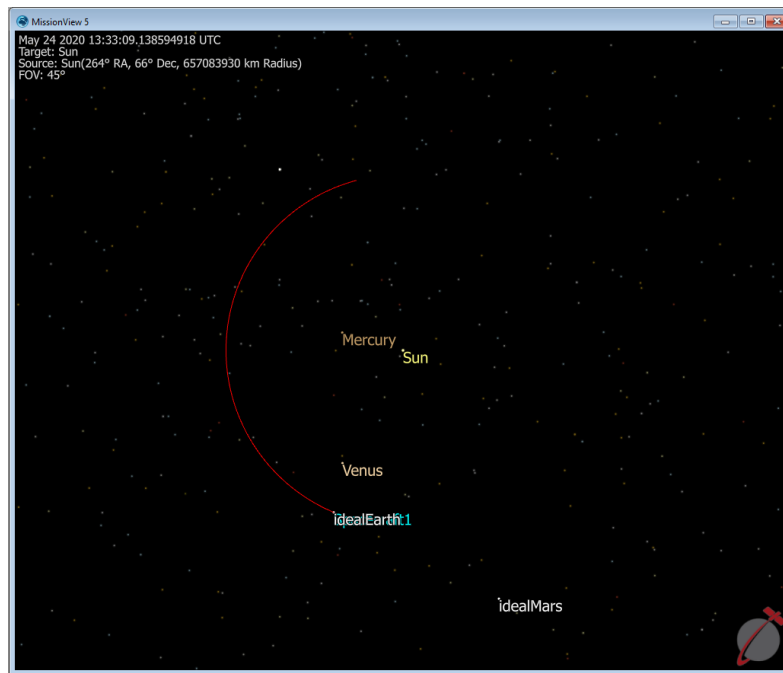


Figure 9: Trajectory simulation of the Spacecraft at Earth Departure

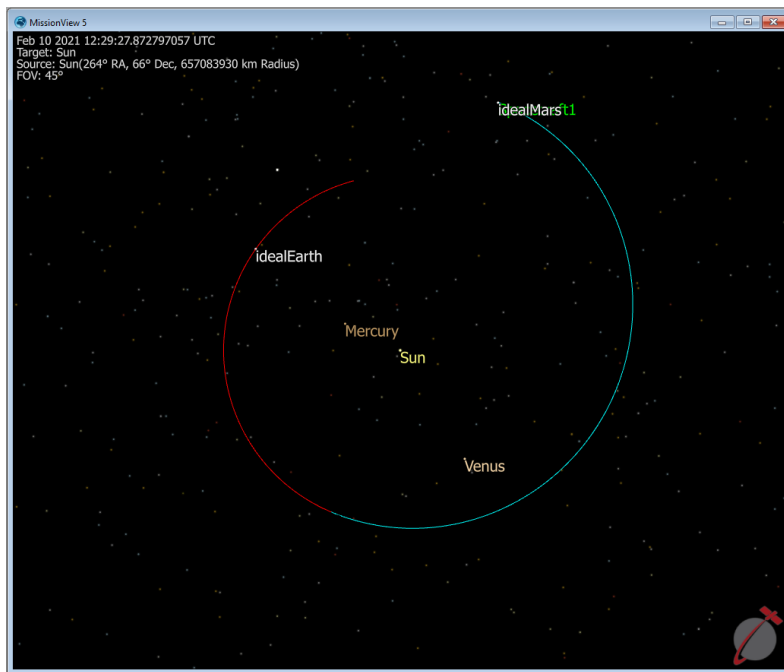


Figure 10: Trajectory simulation of the Spacecraft Transfer Trajectory

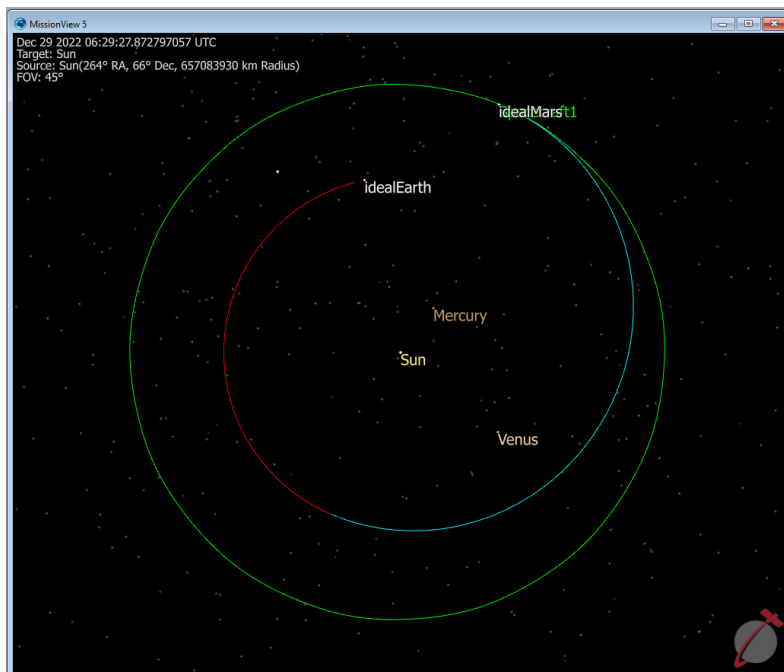
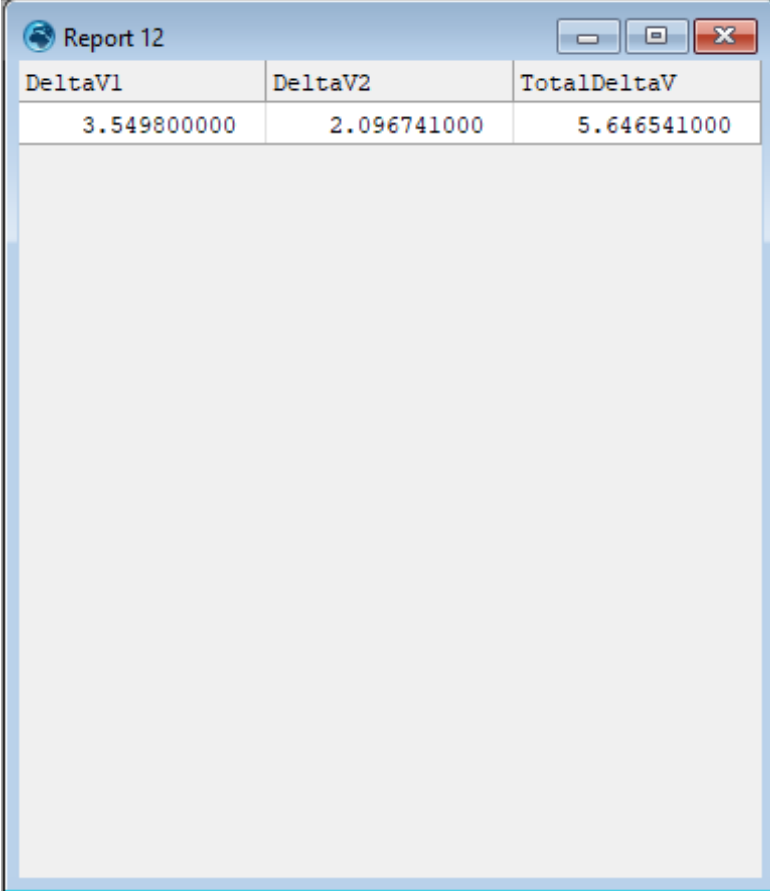


Figure 11: Trajectory simulation of the Spacecraft in its final trajectory around Mars



DeltaV1	DeltaV2	TotalDeltaV
3.549800000	2.096741000	5.646541000

Figure 12: Final ΔV Requirements

In the trajectories of the spacecraft shown in figures 9, 10 & 11, the red path is the trajectory of the spacecraft around the solar system while it is in Earth Orbit, the blue path is the trajectory of the spacecraft on its transfer trajectory to Mars, and the green path is the trajectory of the spacecraft around the solar system in Mars Orbit.

Therefore our main outputs from the simulation are:

1. ΔV Required
2. Time of Flight

5.1.2.1 ΔV Required

$$\begin{aligned}\Delta V1 &= 3.5498 \text{ km/s} \\ \Delta V2 &= (-)2.0967 \text{ km/s} \\ \underline{\Delta V_{Total}} &= 5.6465 \text{ km/s}\end{aligned}$$

The total ΔV required for the two burns is 5.6465 km/s.

5.1.2.2 Time of Flight

$$\begin{aligned}T_{travel} &= t_{arrival} - t_{departure} \\ T_{travel} &= \text{February 10, 2021, 09 : 30} - \text{May 24, 2020, 13 : 30} \\ T_{travel} &= 261 \text{ days, 20 hours} \\ &= 6284 \text{ hours}\end{aligned}$$

5.2. LEO-Moon Orbit Mission

In this mission, the spacecraft will be in a Low Earth Orbit and will perform a manoeuvre for Lunar Transfer Orbit and, after the encounter with the Moon, will perform a Lunar Orbit Insertion Manoeuvre.

The assumed orbit data is as follows:

- Spacecraft LEO Altitude: 170 km
- Spacecraft LEO Eccentricity: 0
- Spacecraft LEO Inclination: 28.5°
- Spacecraft LEO Longitude of the Ascending Node: 329.48°
- Spacecraft LEO Argument of Periapsis: 30.83°
- Spacecraft LEO True Anomaly: 99.88°

- Desired Lunar Orbit Altitude: 110 km

The orbits of the Apollo 15 mission was used as a reference for assuming these orbital altitudes [18].

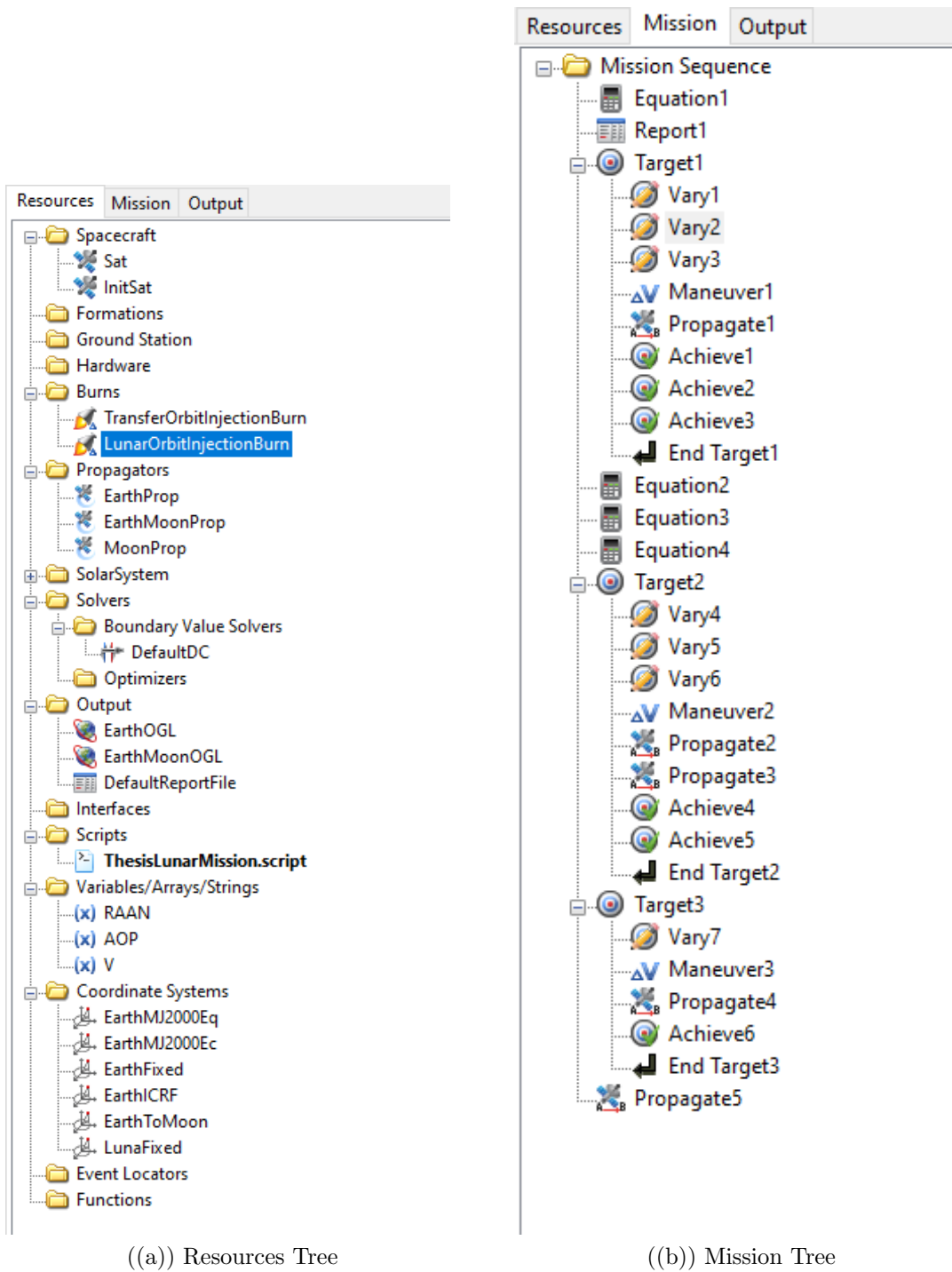
Other assumptions made for this analysis:

- Earth and the Moon have realistic orbits simulated for this mission. The information on the motion of planetary bodies is a part of the software.
- Newtonian physics is considered.
- Atmospheric Perturbations will not be considered.
- The JGM-2 gravitational Model was used for Earth.
- The LP-165 gravitational Model was used for the Moon.
- Planetary bodies that affect the spacecraft are the Earth, the Sun, and the Moon.

5.2.1. Approach

The analysis of the trajectory requirements for this mission was done in NASA's General Mission Analysis Tool (GMAT) version R2020a [19]. GMAT is a publicly available and open-source Mission Analysis software. The mission was modelled based on an existing example script, with modifications made to suit the mission requirements.

For this simulation, first, the resources were initialised and set up for the desired mission. And then, the mission sequence was set up.



((a)) Resources Tree

((b)) Mission Tree

Figure 13: GMAT Mission definition

5.2.2. Results

The following were the results of the Trajectory Simulation on GMAT Software:

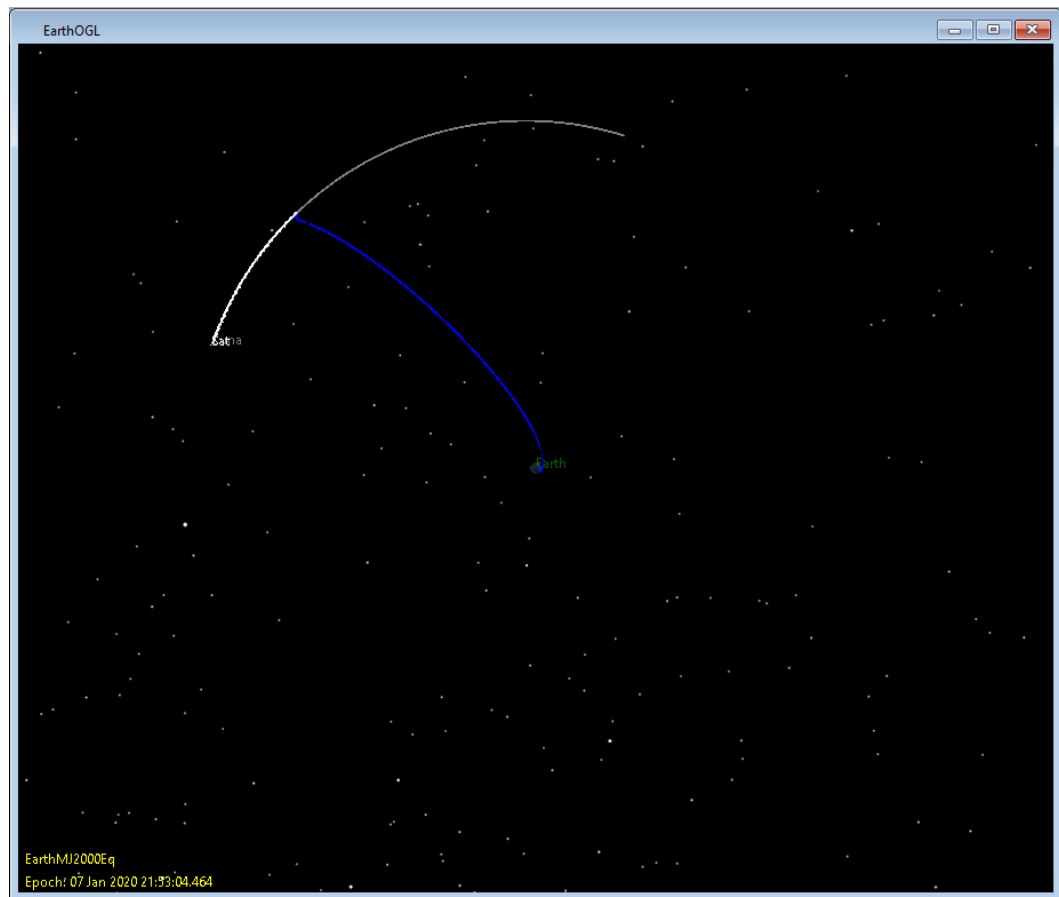


Figure 14: Moon Transfer Trajectory

```

Maneuver Summary
-----
Impulsive Burn:      TransferOrbitInjectionBurn
Spacecraft:         Sat
Origin:             Earth
Axes:              VNB
Delta V Vector:
Element 1:          3.1461673330229 km/s
Element 2:          0.0000000000000 km/s
Element 3:          0.0000000000000 km/s

```

Figure 15: ΔV Required for First Burn

```

Maneuver Summary
-----
Impulsive Burn:    LunarOrbitInjectionBurn
Spacecraft:       Sat
Origin:           Luna
Axes:             VNB
Delta V Vector:
  Element 1:      -0.8007477937600 km/s
  Element 2:       0.0000000000000 km/s
  Element 3:       0.0000000000000 km/s
    
```

Figure 16: ΔV Required for Second Burn

In the trajectories of the spacecraft shown in figure 14, the blue path is the trajectory of the spacecraft on its way to the Moon, and the white path is the trajectory of the spacecraft in Moon Orbit.

Therefore our Main Outputs from the simulation are:

1. ΔV Required
2. Time of Flight

5.2.2.1 ΔV Required

$$\begin{aligned} \Delta V1 &= 3.1461 \text{ km/s} \\ \Delta V2 &= (-)0.8007 \text{ km/s} \\ \underline{\Delta V_{Total}} &= 3.9469 \text{ km/s} \end{aligned}$$

The total ΔV required for the two burns is 3.9469 km/s.

5.2.2.2 Time of Flight

$$\begin{aligned} T_{travel} &= t_{arrival} - t_{departure} \\ T_{travel} &= \text{January 05, 2020, 20 : 59} - \text{January 01, 2020, 00 : 00} \\ T_{travel} &= 4 \text{ days, 20 hours, 59 minutes} \\ &= 117 \text{ hours} \end{aligned}$$

6. Efficiency of the Fuels

6.1. Introduction

When modern rocket propulsion was first being developed in the early 20th century, one of the very first propellant combinations proposed of liquid hydrogen and liquid oxygen, was initially not further developed. This was because of the low density of hydrogen and the handling hazards associated with dealing with cryogenic fluids. Apart from this, the availability of liquid hydrogen was also quite low as the technology for liquefaction was not very advanced. The equipment required for that was also only able to produce liquid hydrogen in small quantities. So, for all intents and purposes, liquid hydrogen was not used as a fuel for early rocket engines for practical reasons [1].

In the late 1930's Walter Thiel conducted some of the first experiments with liquid hydrogen and liquid oxygen as rocket propellants. But even during his experiments, hydrogen posed many handling challenges and would leak very readily due to its small molecular size [20].

The Centaur rocket was the first rocket which used liquid hydrogen and liquid oxygen as its propellants. Its development started in 1956, and its first flight attempt was in 1962, with the first successful attempt in 1963 [21].

Since then, liquid hydrogen and liquid oxygen have been the workhorse of some of the aerospace industry's most important rockets. It is especially preferred in the upper stages of rockets due to its mass advantage and its higher energy density. Today it is used in the Vinci engine for Ariane 6, several versions of RL-10, RS-25 for the Space Launch System, Vulcain 2 engine for Ariane 5 and many other Russian, Chinese, Indian and Japanese engines [22] [12] [23] [24].

Methane as a rocket fuel was not initially considered. This was because, many more easily available hydrocarbons were accessible, and these were used in rocket engine development.

In the early 1900's Herman Oberth wanted to build a rocket with methane but decided against it as methane was difficult to obtain in Germany then. However, in 1930, Johannes Winkler another German rocket engineer, built a liquid methane and liquid oxygen rocket engine. But his results were not very exciting as the performance of his Methalox engine was just marginally better than other hydrocarbons [1].

But as time went by, methane was no longer an exotic fuel. A lot of Liquefied Natural Gas reserves were discovered, and with this, methane became readily available. By 1970, NASA had started to experiment with methane as a rocket fuel. They took the RL-10 engine, which used liquid hydrogen and liquid oxygen and modified

it to use FLOX (Fluorine and oxygen) as oxidiser and methane as fuel [25]. Recently, there has been a renewed interest in methane as a fuel, and this is being driven by companies such as SpaceX and Blue Origin. Methane poses as a better alternative to hydrogen in terms of long-term storage for interplanetary missions. Additionally, the advantage of methane being able to be produced in situ on Mars is definitely a driving factor. Some of the methane and oxygen engines that are being developed are the Raptor engine to be used on Starship, the BE-4 engine to be used on New Glenn and Vulcan, the M10 for the Vega-E, and some other Chinese and American engines [11] [26] [27].

6.2. Specific Impulse and Chemistry of Combustion

Specific Impulse is defined as the thrust per unit propellant mass flow rate per acceleration due to gravity [8].

$$I_{sp} = \frac{\int_0^t F dt}{g_0 \int_0^t \dot{m} dt} \quad (10)$$

Here in Equation 10, the specific impulse is represented as the variation of thrust and mass flow rate with time t . The acceleration due to gravity is considered constant, and the value for standard gravity g_0 is used.

Therefore, it will be equal to the total Impulse by the total mass of propellant consumed into acceleration due to gravity.

$$I_{sp} = I_t / (m_p g_0) \quad (11)$$

For constant thrust and constant propellant mass flow rates, specific impulse can be represented as:

$$I_{sp} = F / (\dot{m} g_0) = F / \dot{w} = I_t / w \quad (12)$$

With this notation, the unit of specific impulse is seconds. This is the SI unit.

But another value often used to measure the performance of the propulsion system is the effective exhaust velocity v_e . This is essentially the same as specific impulse but without the standard gravity denominator.

$$v_e = I_{sp} g_0 = F / \dot{m} \quad (13)$$

The unit for this is m/s, and for this study, specific impulse (I_{sp}) and exhaust velocity (v_e) will be used interchangeably to indicate performance.

Specific Impulse is an integral part of an engine's characteristics and indicates its performance. In a way, it represents how efficient the engine is with its use of its fuel and oxidiser. An engine with a higher specific impulse will be able to provide more ΔV for the same quantity of fuel and oxidiser compared to an engine with a lower specific impulse. Therefore a higher specific impulse is always desirable.

Specific Impulse represents the energy stored in the propellants, which is released when it is combusted. To understand the theoretical maximum specific impulse for any propellant combination, the chemical energy of the propellants must be equated to the kinetic energy of the exhaust products. This is because, under ideal condition assumptions, all of this stored energy, is converted into fast-moving gases, and the kinetic energy of the exhaust gas particles is what propels the spacecraft. The calculations made, will be for Vacuum Specific Impulse [28].

$$E = \frac{1}{2}mv_e^2 \quad (14)$$

$$\sqrt{\frac{2E}{m}} = v_e \quad (15)$$

$$\frac{\sqrt{\frac{2E}{m}}}{g} = \frac{v_e}{g} = I_{sp} \quad (16)$$

E = Total Chemical Energy Stored

m = Mass of the Propellant

v_e = Exhaust Velocity

g = Acceleration due to Gravity

I_{sp} = Specific Impulse

The energy stored per unit mass can be represented as u , called the chemical energy density.

$$u = \frac{E}{m} \quad (17)$$

Therefore,

$$I_{sp} = \frac{\sqrt{2u}}{g} \quad (18)$$

6.2.1. Hydrolox Combustion

The chemical reaction for the combustion of hydrogen and oxygen is as follows [28]:

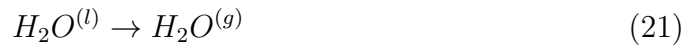


Therefore the chemical energy density u must be found.

Since the enthalpy change of combustion ΔH is for the reaction,



The enthalpy of vaporisation ΔH_{vap} also needs to be accounted for.



Therefore, for the reaction where the product is water in its gaseous form [28]:

$$u = \frac{(\Delta H - \Delta H_{vap})}{m_m} \quad (22)$$

Where m_m is the Molar Mass of the combustion product

Therefore the I_{sp} is:

$$I_{sp} = \frac{\sqrt{\frac{2(\Delta H - \Delta H_{vap})}{m_m}}}{g} \quad (23)$$

Putting in the values for our reaction [29],

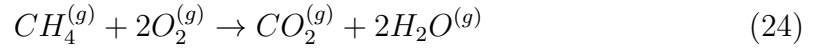
$$\begin{aligned} \Delta H &= 285.8kJ/mol \\ \Delta H_{vap} &= 40.2kJ/mol \\ m_m &= 18g/mol \\ g &= 9.81m/s^2 \end{aligned}$$

Hence, the maximum theoretical I_{sp} is:

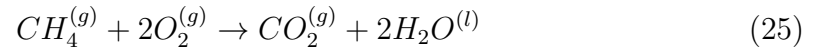
$$\underline{I_{sp} = 532.5 s}$$

6.2.2. Methalox Combustion

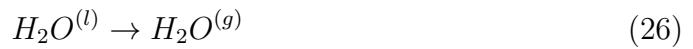
The chemical reaction for the combustion of methane and oxygen is as follows [28]:



Similar to the hydrogen and oxygen combustion, the enthalpy change of combustion ΔH is for the following reaction:



And here as well, phase change in water needs to be accounted for;



But here, since there are 2 moles of water, the ΔH_{vap} is doubled. Also, for molar mass, carbon dioxide also has to be included.

Therefore, calculating I_{sp} :

$$u = \frac{(\Delta H - \Delta H_{vap})}{m_m} \quad (27)$$

$$I_{sp} = \frac{\sqrt{\frac{2(\Delta H - \Delta H_{vap})}{m_m}}}{g} \quad (28)$$

Putting in the values for our reaction [29],

$$\begin{aligned} \Delta H &= 890.6kJ/mol \\ \Delta H_{vap} &= 2 \times 40.2kJ/mol \\ m_m &= 44 + 2 \times 18 = 80g/mol \\ g &= 9.81m/s^2 \end{aligned}$$

Hence, the maximum theoretical I_{sp} is:

$$\underline{I_{sp} = 458.7 s}$$

In reality, the theoretical I_{sp} is not achieved. This is due to the combination of various factors, such as:

- The propellants are not always being burnt at their optimal stoichiometric ratio
- Mechanical losses due to vibrations

- Thermal losses such as heat escaping as well as heating up parts of the spacecraft
- Intramolecular Vibrations and rotations
- Non-axial exhaust gas kinetic motion

After all of the possible losses, the kinetic energy of the exhaust gases in the axial direction is what remains and that gives the actual specific impulse.

For the Osiris Engine, the Hydrolox version has a theoretical specific impulse of 475 seconds and the Methalox version has a theoretical specific impulse of 385 seconds before considering reduction during operations due to engine efficiency [4].

6.3. Conclusion and Scoring

Below is a diagram representing the specific impulses of LH_2/LOx , LCH_4/LOx and $\text{RP-1}/\text{LOx}$.

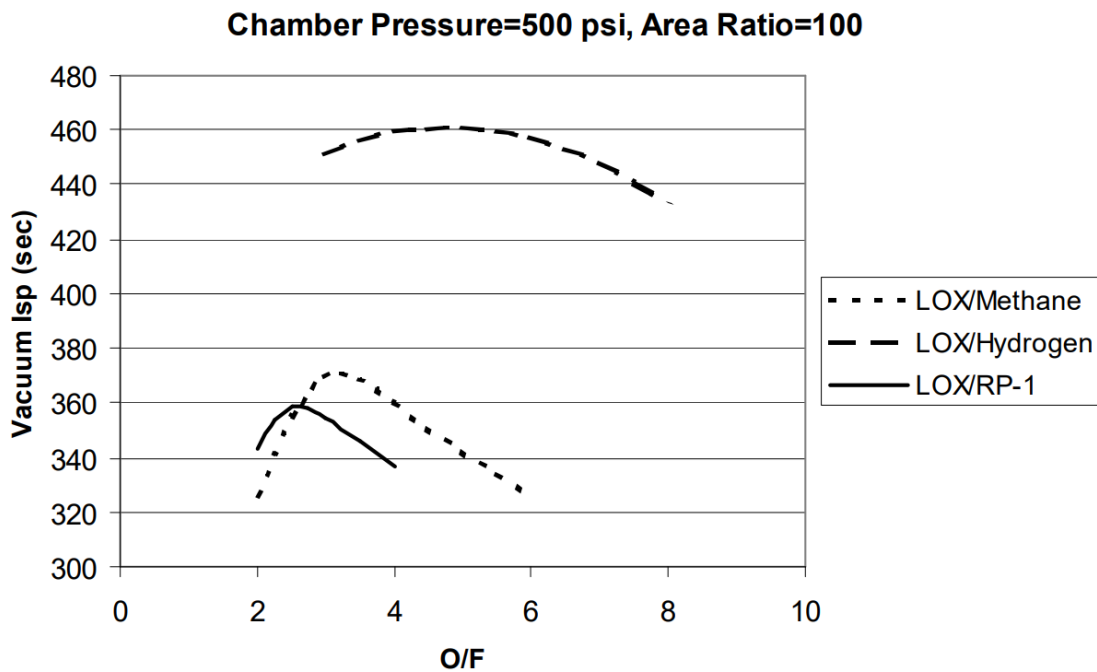


Figure 17: Graph of Vacuum Specific Impulse vs O/F ratio for LH_2/LOx , LCH_4/LOx and $\text{RP-1}/\text{LOx}$ [30]

It can be observed that LH_2/LOx outshines its propellant competitors with respect to specific impulse. Apart from some experimental propellant combinations with

fluorine, hydrogen and oxygen is the best-known combination of propellants for chemical propulsion.

Comparatively, methane and oxygen have a much lower I_{sp} , but it is high enough to be a considerable propellant choice for a chemical combustion engine.

To score hydrogen and methane as fuels with respect to Specific Impulse, the difference in I_{sp} of the two fuels with oxygen can be looked at.

Hydrogen can first be assigned 10 points on a scale of 0 to 10 as liquid hydrogen and liquid oxygen has the highest known specific impulse for a practical chemical propulsion engine. (Fluorine can be excluded as an oxidiser due to its toxicity and due to its difficulty to handle).

The difference in the two I_{sp} 's can then be considered.

$$\begin{aligned}
 I_{sp}Hydrolox - I_{sp}Methalox &= 90s \\
 \text{Difference Percentage} &= 90/475 \times 100 \\
 &= 18.94\%
 \end{aligned}$$

Therefore, methane can be scored an 18.94% lower score.

The score for methane is then 8.105.

Part	Moon-Hydrolox	Moon-Methalox	Mars-Hydrolox	Mars-Methalox
Score	10	8.105	10	8.105

Table 3: Scoring for Efficiency of Fuels

7. System Mass and Fuel Budget

7.1. Introduction

In space travel, mass is one of the most important design factors. Due to the rocket equation 29, the heavier the spacecraft or the launcher is, the more fuel it requires to get to its destination. The additional weight of the extra fuel, in turn, increases the mass of the spacecraft, therefore, further fuel is required, and so on. Thus, it is of utmost importance that all space hardware is of the minimum possible mass. It is so essential to the spacecraft development procedure, that sometimes, for cost estimation, the cost is measured in kilograms instead of a currency. This is because, the mass is the greatest driving factor for putting the spacecraft into space [8].

The mass of the spacecraft can be broadly divided into its propellant mass and the dry mass, which is the mass of the spacecraft minus its propellant. The change in fuel for the engine will affect both, the propellant mass and dry mass. Therefore, in this section, it will be analysed how the fuel mass and dry mass of the spacecraft will look like for the two different fuels.

Before looking at the comparison, it is important to understand the difference between hydrogen and methane in terms of their density.

In terms of density, methane is denser than hydrogen. At standard temperature and pressure, the density of methane gas is approximately 0.717 kg/m^3 , while the density of hydrogen gas is only 0.0899 kg/m^3 . This means that for the same volume, a tank of methane will contain more mass than a tank of hydrogen. However, it is important to note that both hydrogen and methane can be liquefied at low temperatures, which increases their density significantly. Liquid hydrogen has a density of 70.88 kg/m^3 , while liquid methane has a density of 422.6 kg/m^3 at 1 bar. Despite this increase in density, liquid methane is still denser than liquid hydrogen, which means that it would be stored in smaller tanks and requires less volume on the rocket for the same mass of hydrogen [31] [32].

However, when considering the specific impulse of a Hydrolox engine vs a Methalox engine, things are again put into perspective. Due to the Hydrolox engine having a higher specific impulse for the same amount of ΔV required, a smaller mass of propellant would be needed as compared to the Methalox engine version. In this section, it will be observed how specific impulse affects the mass on the system level.

7.2. System Mass Estimation Tool

7.2.1. Approach

For comparing the system mass of the spacecraft using different fuels, a method needs to be first established to calculate system mass. It is important to note that this would be a comparative study where the rough estimates of system mass would suffice as long as the approach for the elements of comparison remains the same. Therefore, with this in mind, the estimation was made using Mass Estimation Relations (MER).

For this, a Matlab tool with an interactive approach was made to estimate the inert mass, fuel mass and oxidiser mass and, therefore, the total system mass using MERs [58]. The source for the MERs used in the tool was from Principles of Space Systems Design by David Akin [33]. This is a compilation and formulation from the works of C. R. Glatt, I. O. MacConochie, and W. Heineman [34] [35] [36] [37]. All the MERs in the following section will be from this source. All assumptions made will be mentioned as required.

The System is broken down into these main components:

- Payload Mass
- Propellant Mass
 - Fuel Mass
 - Oxidiser Mass
- Propellant Tanks
 - Fuel Tank Mass
 - Oxidiser Tank Mass
 - Fuel Tank Insulation Mass
 - Oxidiser Tank Insulation Mass
- Engine Mass
- Thrust Bearing Structure Mass
- Gimbal System Mass
- Structural Mass
- Avionics Mass

- Wiring Mass

Payload Mass

The payload mass would be taken from the user input directly. For this mission, a payload mass of 3900 kg will be used. This assumption is based on 2 example missions. The Chandrayaan 2 Moon orbiter and lander had a combined wet mass of 3850 kg [38]. The Curiosity Mars Science Lab had a payload wet mass of 3893 kg [39].

Propellant Mass

This is essentially calculated using the rocket equation by assuming the inert mass fraction for the first iteration [8].

$$\Delta V = v_e \ln \frac{m_0}{m_f} \quad (29)$$

$\Delta V = \text{Change in Velocity}$

$v_e = \text{Exhaust Velocity}$

$m_0 = \text{Initial Mass}$

$m_f = \text{Final Mass}$

Propellant Tank Mass

The following MER was used for the propellant tanks [33]:

$$\text{For Liquid Hydrogen Tanks : } M_{LH_2Tank}(kg) = 9.09 V_{LH_2Tank} (m^3) \quad (30)$$

$$\text{For all Methane and Oxygen Tanks : } M_{Tank}(kg) = 12.16 V_{PropellantTank} (m^3) \quad (31)$$

The tank diameters for both engine versions was assumed to be 3.5 m for the calculations.

Propellant Tank Insulation Mass

The fuel tanks are assumed as cylindrical with insulation on all sides.

The following MER was used for the propellant tank insulation [33]:

$$\text{For Liquid Hydrogen Tanks : } M_{LH_2Insulation}(kg) = 2.88 A_{Tank} (kg/m^2) \quad (32)$$

$$\text{For all Methane and Oxygen Tanks : } M_{Tank}(kg) = 1.123 A_{Tank} (kg/m^2) \quad (33)$$

Engine Mass

The engine mass is from the Osiris Engine design for Methalox and Hydrolox versions. (Table 1 & 2)

Thrust Bearing Structure Mass

The MER for this is as follows [33]:

$$M_{Thrust\ Structure}(kg) = 2.55 \times 10^{-4} \times T(N) \quad (34)$$

Gimbal System Mass

The MER for this is as follows [33]:

$$M_{Gimbals}(kg) = 237.8 \left[\frac{T(N)}{P_{cc}(Pa)} \right]^{0.9375} \quad (35)$$

Structural Mass

Here, the MER for interstage structure is being used [33]:

$$M_{Interstage}(kg) = 4.95 \times (A_{Interstage})^{1.15} (m^2) \quad (36)$$

The interstage height for both engine versions was assumed to be 1.0 m for the calculations.

Avionics Mass

The MER for this is as follows [33]:

$$M_{Avionics}(kg) = 10 \times (M_{Total})^{0.361} (kg) \quad (37)$$

Wiring Mass

The MER for this is as follows [33]:

$$M_{Wiring}(kg) = 1.058 \times \sqrt{M_{Total}}(kg) \times (L_{Stage})^{0.25}(m) \quad (38)$$

7.2.1.1 Tool Logic

The Matlab tool was written with an interactive approach, with the ability to take user input and then generate the mass estimate. In this section, the operational logic of the tool will be explained.

1. First, the following is asked for user input:
 - ΔV
 - Thrust
 - Combustion Chamber Pressure
 - Oxidiser - Fuel Ratio
 - Fuel
 - If the fuel is not known to the tool, then also Fuel Density
 - Inert Mass Fraction Initial Assumption
 - Specific Impulse
 - Payload Mass
 - Engine Mass
 - Oxidiser Tank Diameter
 - Fuel Tank Diameter
 - Interstage Height

The default oxidiser for this tool was set to oxygen.

2. From the Rocket Equation, the mass ratio is obtained first. The initial inert mass fraction assumption is then used to get the payload fraction, and this is used for the first iteration. 29
3. Then, the initial total mass estimate is obtained from the payload mass and the payload fraction. and the inert mass from the inert mass fraction.
4. An error counter is set to an arbitrary number larger than 1 and the condition is set for the loop to continue as long as the error counter is more than 1. This error counter is the difference between the total mass in the consecutive iterations. The main solving loop is then entered.
5. The propellant mass for this iteration is calculated using the mass ratios, Payload mass and Inert mass.

6. The separate fuel and oxidiser masses are calculated using the oxidiser to fuel ratio.
7. The total mass is then calculated by adding the Payload, Inert and Propellant masses. For the first iteration, this will be the same as the initial total mass estimate.
8. Next, the tank masses are calculated. Based on the earlier user input, the appropriate MER is selected to calculate the fuel tank mass. The oxidiser tank mass is calculated similarly.³⁰³¹
9. Then, the tank dimensions are computed. With a known density and mass of fuel, the volume of fuel required is obtained. Assuming 8% ullage volume, the volume of the tank is attained. From this, the height of the tank is extrapolated from the given tank diameter. This is also done for the oxidiser tank.
10. Now, to get the insulation masses, the surface area of the tank is used in the MER. This is chosen accordingly for Liquid Hydrogen, Methane or Oxygen.³²³³
11. The Thrust Bearing structure, Gimbal System, Interstage structure, Avionics and Wiring masses are calculated accordingly using the MERs.³⁴³⁵³⁶³⁷³⁸
12. The total mass calculated for the previous iteration is stored in a temporary variable.
13. A new Total Mass and Inert Mass is obtained by adding the individual masses.
14. The difference is then stored in this new total mass and the previous iteration mass using the temporary variable mentioned previously.
15. Now, if the difference between these two iterations is larger than one kilogram, the loop goes back to step 5 and another iteration is solved.
16. Once the loop condition is satisfied, the tool operation breaks out of it, and the final outputs are displayed.

The following is the schematic of the Matlab tool logic flow and tool inputs and outputs.

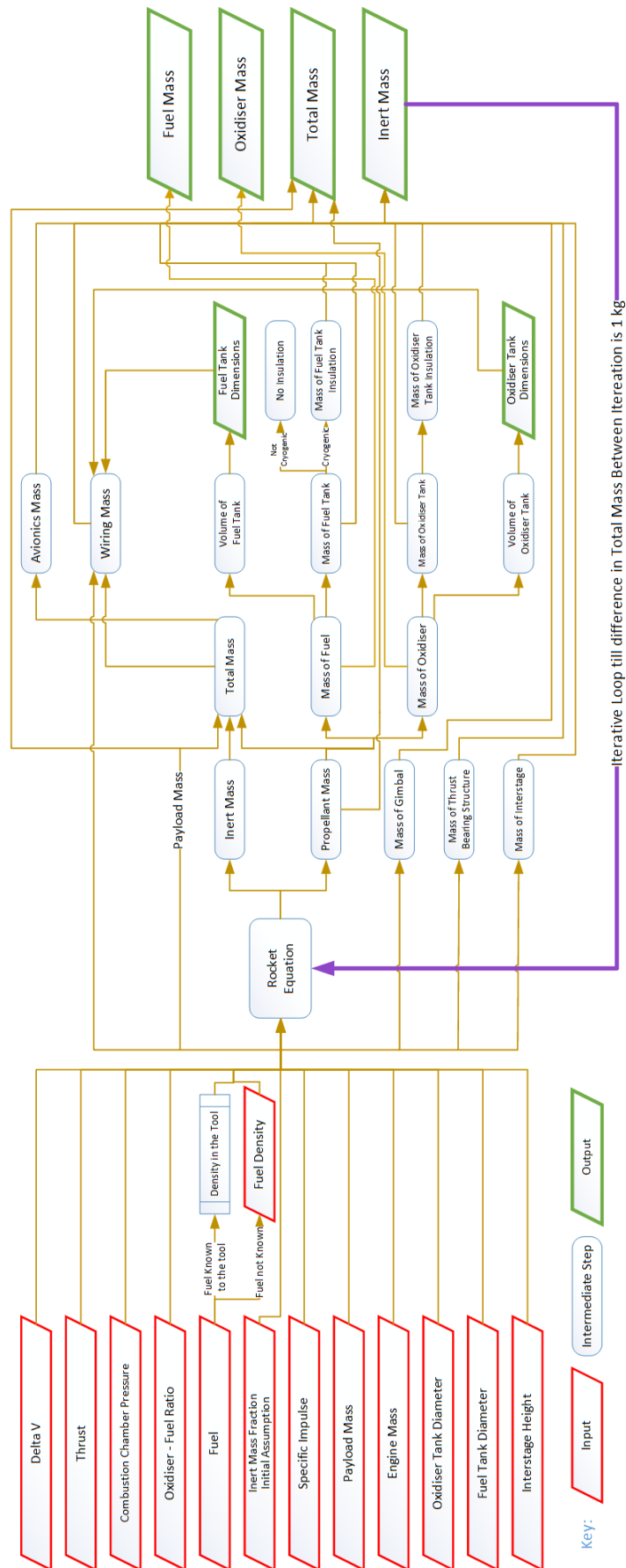


Figure 18: Matlab System Mass Estimation Tool Logic Flow

Input	Unit
ΔV	m/s
Thrust	N
Combustion Chamber Pressure	Pa
Oxidiser to Fuel Ratio	-
Fuel	-
Initial Mass Fraction Assumption	-
Specific Impulse	s
Payload Mass	kg
Engine Mass	kg
Oxidiser Tank Diameter	m
Fuel Tank Diameter	m
Interstage Height	m
Fuel Density	kg/m ³

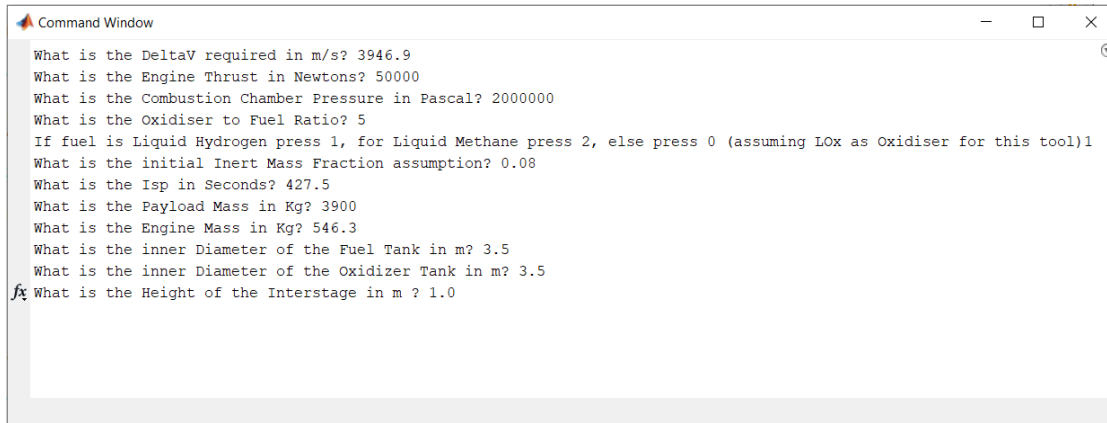
Table 4: Required Inputs for the Mass Estimation Tool and their Units

Output	Unit
Total Mass	kg
Inert Mass	kg
Fuel Mass	kg
Oxidiser Mass	kg
Fuel Tank Height	m
Oxidiser Tank Height	m

Table 5: Outputs from the Mass Estimation tool and their units

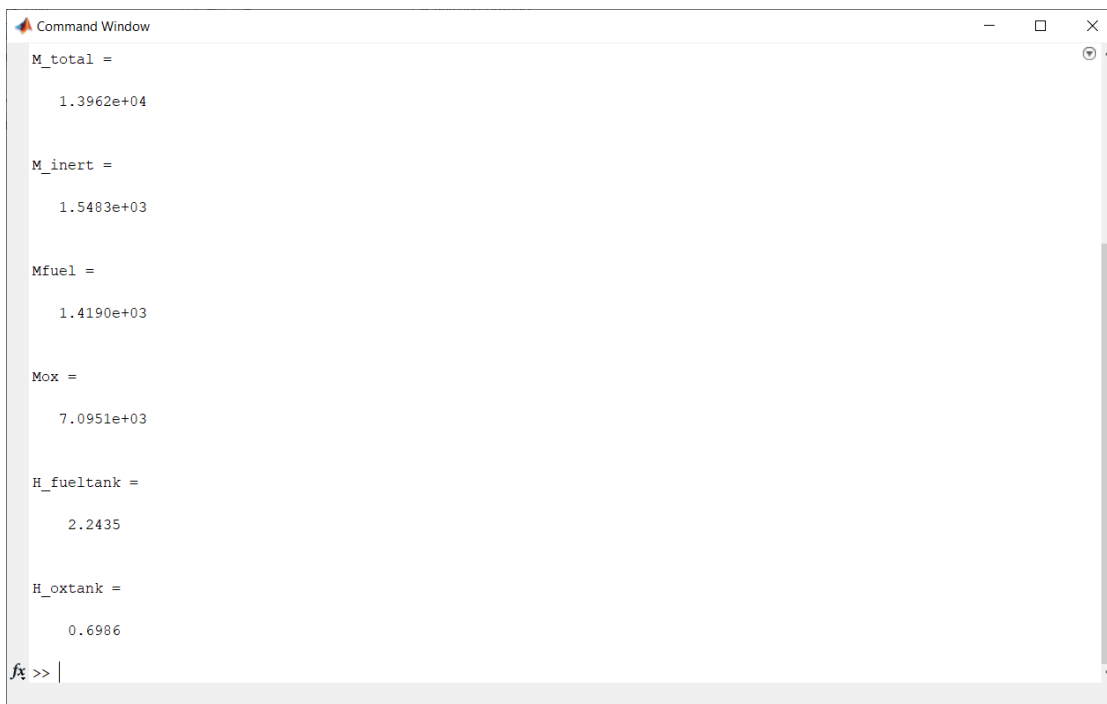
7.3. Results

7.3.1. For Moon Mission with Hydrolox Osiris Engine



```
Command Window
What is the DeltaV required in m/s? 3946.9
What is the Engine Thrust in Newtons? 50000
What is the Combustion Chamber Pressure in Pascal? 2000000
What is the Oxidiser to Fuel Ratio? 5
If fuel is Liquid Hydrogen press 1, for Liquid Methane press 2, else press 0 (assuming LOx as Oxidiser for this tool)1
What is the initial Inert Mass Fraction assumption? 0.08
What is the Isp in Seconds? 427.5
What is the Payload Mass in Kg? 3900
What is the Engine Mass in Kg? 546.3
What is the inner Diameter of the Fuel Tank in m? 3.5
What is the inner Diameter of the Oxidizer Tank in m? 3.5
fx What is the Height of the Interstage in m ? 1.0
```

Figure 19: Input for Hydrolox Osiris Engine for Moon Mission



```
Command Window
M_total =
    1.3962e+04

M_inert =
    1.5483e+03

Mfuel =
    1.4190e+03

Mox =
    7.0951e+03

H_fuel tank =
    2.2435

H_ox tank =
    0.6986

fx >> |
```

Figure 20: Output of the tool for Hydrolox Osiris Engine for Moon Mission

7.3.2. For Moon Mission with Methalox Osiris Engine

```

Command Window
What is the DeltaV required in m/s? 3946.9
What is the Engine Thrust in Newtons? 50000
What is the Combustion Chamber Pressure in Pascal? 2000000
What is the Oxidiser to Fuel Ratio? 3.6
If fuel is Liquid Hydrogen press 1, for Liquid Methane press 2, else press 0 (assuming LOx as Oxidiser for this tool)2
What is the initial Inert Mass Fraction assumption? 0.08
What is the Isp in Seconds? 346.54
What is the Payload Mass in Kg? 3900
What is the Engine Mass in Kg? 425.1
What is the inner Diameter of the Fuel Tank in m? 3.5
What is the inner Diameter of the Oxidizer Tank in m? 3.5
fx What is the Height of the Interstage in m ? 1.0|
    
```

Figure 21: Input for Methalox Osiris Engine for Moon Mission

```

Command Window
M_total =
    1.6649e+04

M_inert =
    1.2609e+03

Mfuel =
    2.4974e+03

Mox =
    8.9905e+03

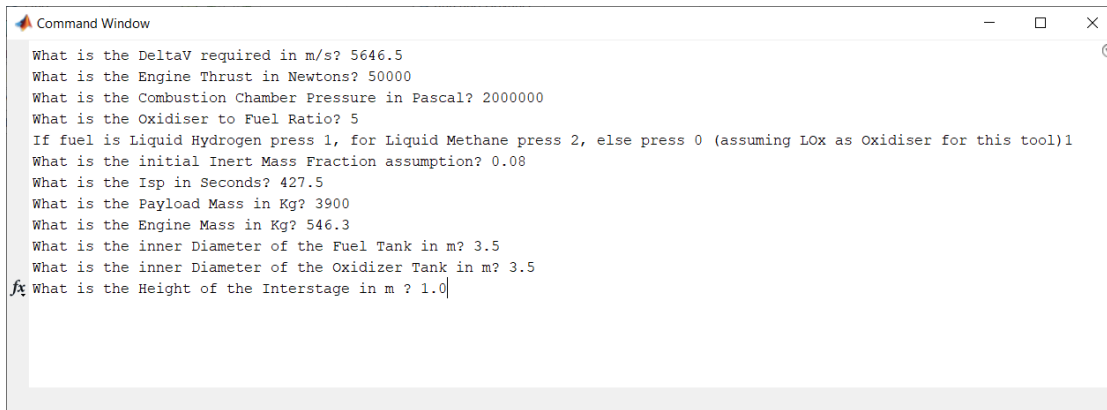
H_fueltank =
    0.6627

H_oxtank =
    0.8853

fx >> |
    
```

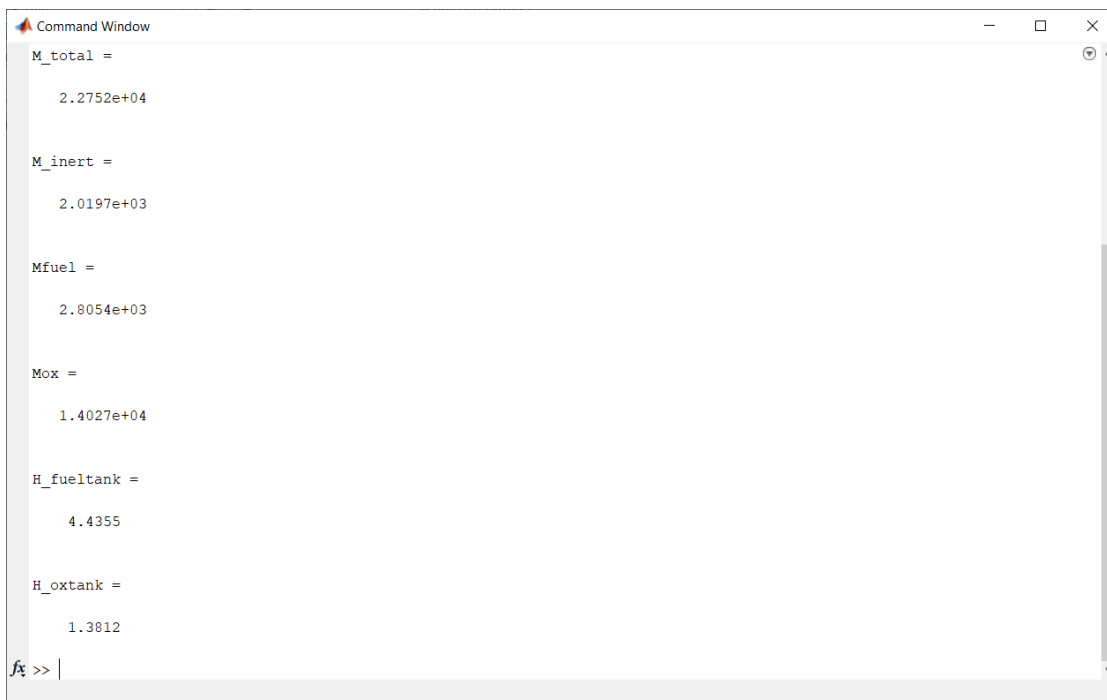
Figure 22: Output of the tool for Methalox Osiris Engine for Moon Mission

7.3.3. For Mars Mission with Hydrolox Osiris Engine



```
Command Window
What is the DeltaV required in m/s? 5646.5
What is the Engine Thrust in Newtons? 50000
What is the Combustion Chamber Pressure in Pascal? 2000000
What is the Oxidiser to Fuel Ratio? 5
If fuel is Liquid Hydrogen press 1, for Liquid Methane press 2, else press 0 (assuming LOx as Oxidiser for this tool)1
What is the initial Inert Mass Fraction assumption? 0.08
What is the Isp in Seconds? 427.5
What is the Payload Mass in Kg? 3900
What is the Engine Mass in Kg? 546.3
What is the inner Diameter of the Fuel Tank in m? 3.5
What is the inner Diameter of the Oxidizer Tank in m? 3.5
fx What is the Height of the Interstage in m ? 1.0
```

Figure 23: Input for Hydrolox Osiris Engine for Mars Mission



```
Command Window
M_total =
    2.2752e+04

M_inert =
    2.0197e+03

Mfuel =
    2.8054e+03

Mox =
    1.4027e+04

H_fueltank =
    4.4355

H_oxtank =
    1.3812

fx >> |
```

Figure 24: Output of the tool for Hydrolox Osiris Engine for Mars Mission

7.3.4. For Mars Mission with Methalox Osiris Engine

```

Command Window
What is the DeltaV required in m/s? 5646.5
What is the Engine Thrust in Newtons? 50000
What is the Combustion Chamber Pressure in Pascal? 2000000
What is the Oxidiser to Fuel Ratio? 3.6
If fuel is Liquid Hydrogen press 1, for Liquid Methane press 2, else press 0 (assuming LOX as Oxidiser for this tool)2
What is the initial Inert Mass Fraction assumption? 0.08
What is the Isp in Seconds? 346.54
What is the Payload Mass in Kg? 3900
What is the Engine Mass in Kg? 425.1
What is the inner Diameter of the Fuel Tank in m? 3.5
What is the inner Diameter of the Oxidizer Tank in m? 3.5
fx What is the Height of the Interstage in m ? 1.0
    
```

Figure 25: Input for Methalox Osiris Engine for Mars Mission

```

Command Window
M_total =
    3.4399e+04

M_inert =
    1.7688e+03

Mfuel =
    6.2458e+03

Mox =
    2.2485e+04

H_fueltank =
    1.6575

H_oxtank =
    2.2140

fx >> |
    
```

Figure 26: Output of the tool for Methalox Osiris Engine for Mars Mission

7.3.5. Trends

In this section, some trends in the Total Mass and Inert Mass of the spacecraft are examined when only one of the key inputs variables is varied. This gives us an understanding of the tool's working and the input sensitivity.

7.3.5.1 ΔV Trend for Hydrolox Engine

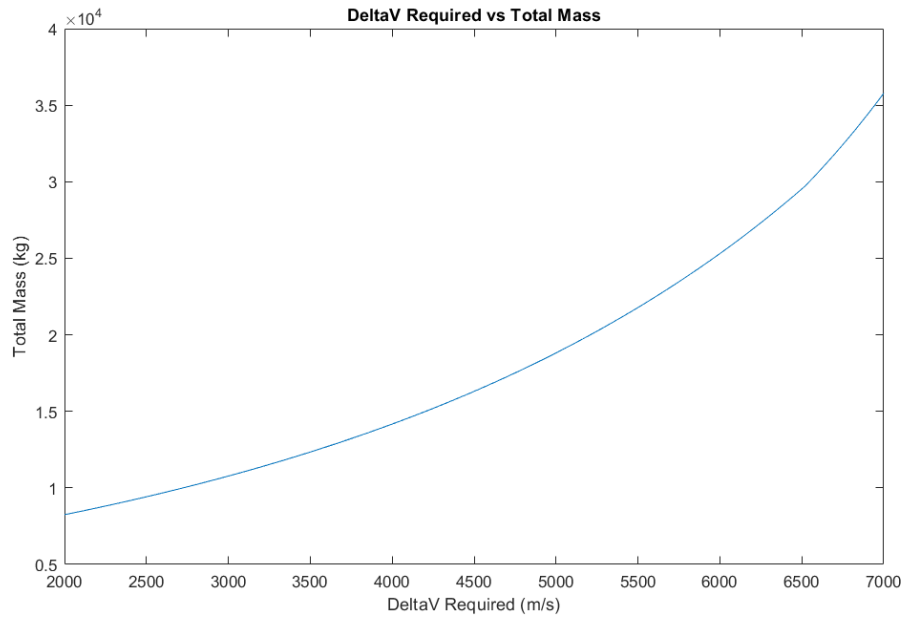


Figure 27: Plot of ΔV Total Mass plot for Hydrolox Engine

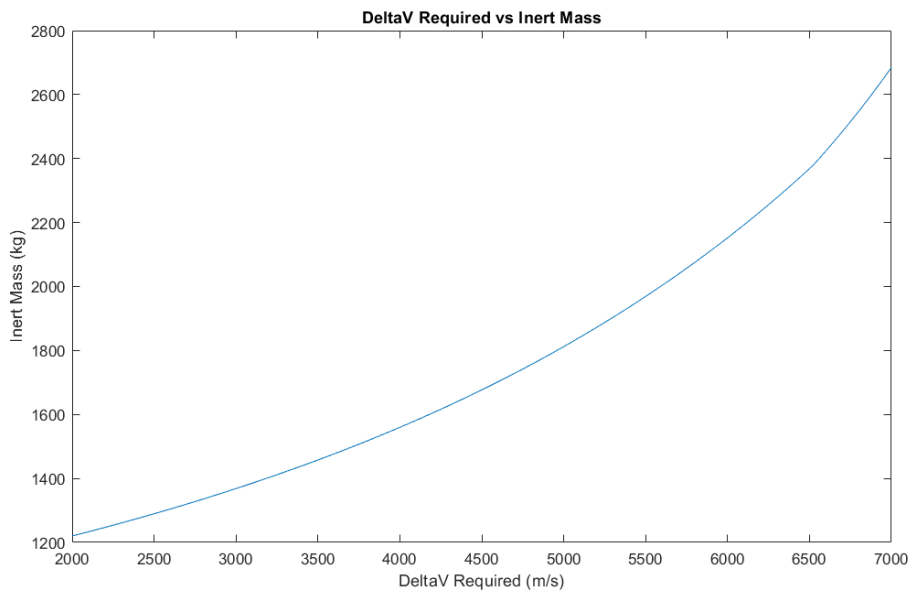


Figure 28: Plot of ΔV vs Inert Mass plot for Hydrolox Engine

7.3.5.2 ΔV Trend for Methalox Engine

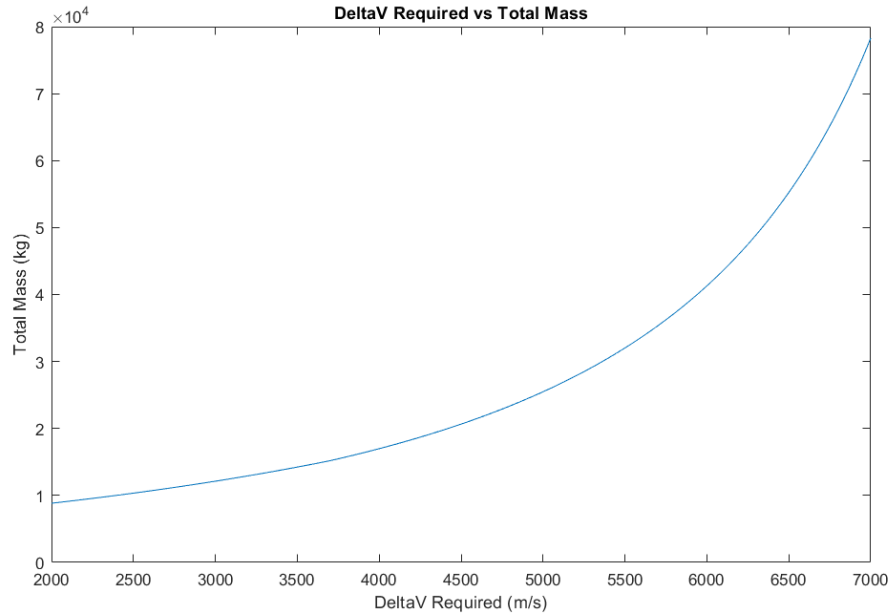


Figure 29: Plot of ΔV vs Total Mass plot for Methalox Engine

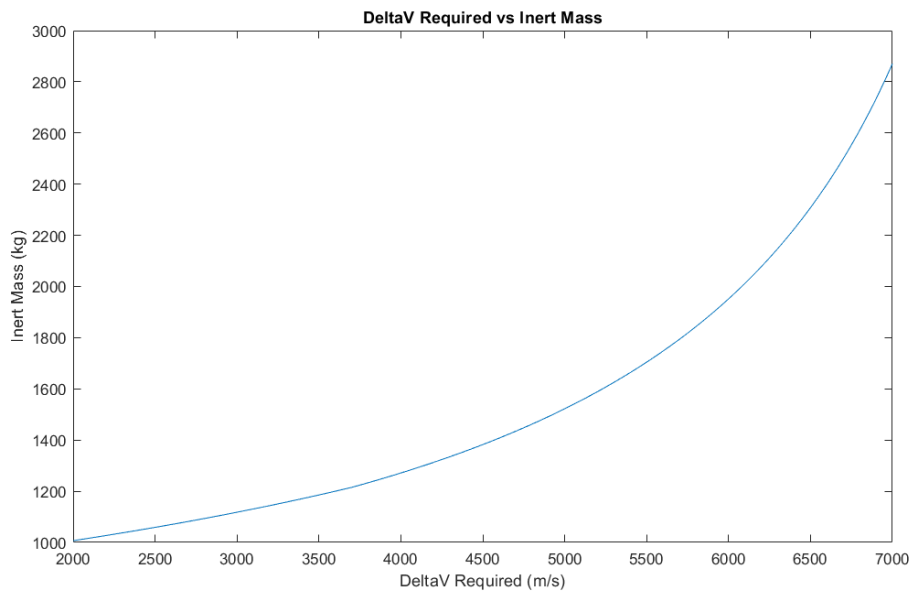


Figure 30: Plot of ΔV vs Inert Mass plot for Methalox Engine

7.3.5.3 Oxidiser to Fuel Ratio Trend for Hydrolox Engine for Moon Mission

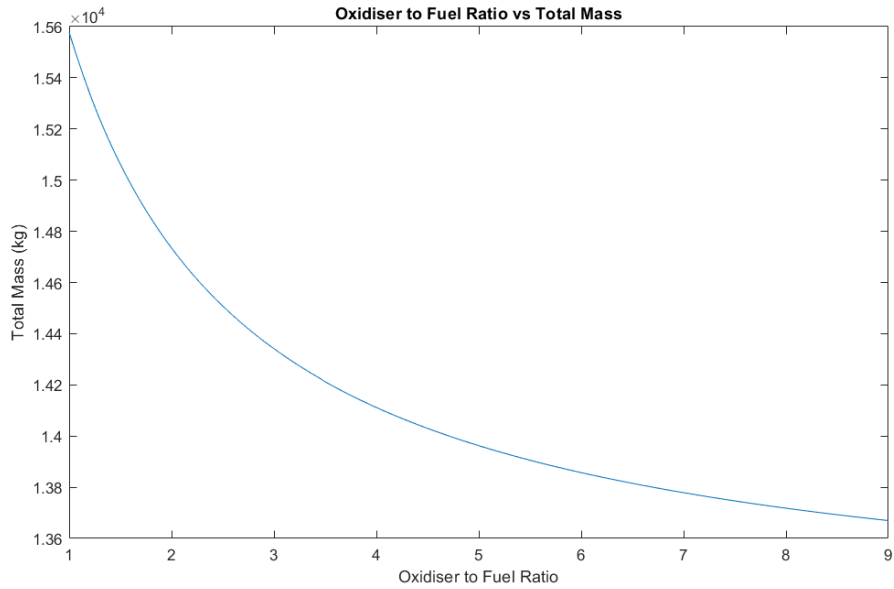


Figure 31: Plot of OF Ratio vs Total Mass for Hydrolox Engine for Moon Mission

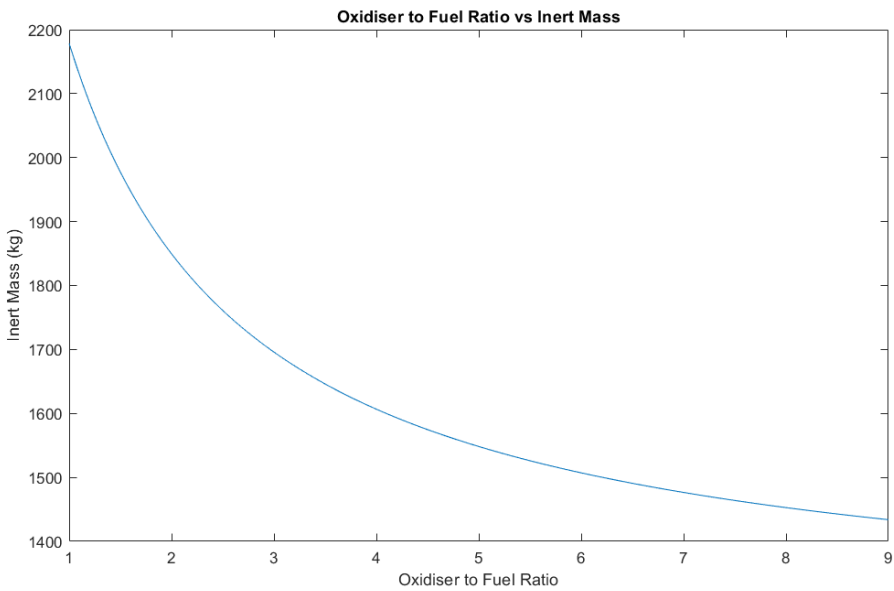


Figure 32: Plot of OF Ratio vs Total Mass for Hydrolox Engine for Moon Mission

7.3.5.4 Oxidiser to Fuel Ratio Trend for Methalox Engine for Moon Mission

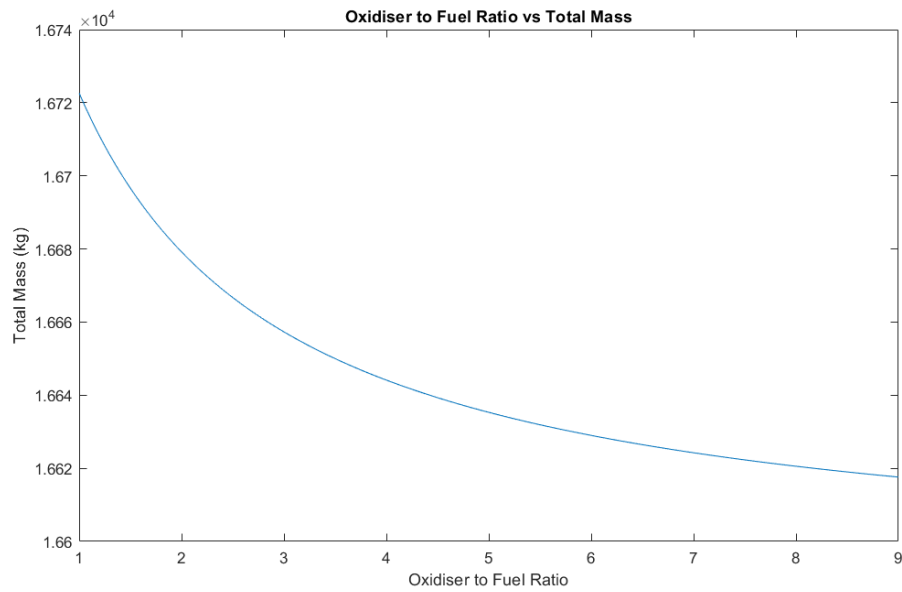


Figure 33: Plot of OF Ratio vs Total Mass for Methalox Engine for Moon Mission

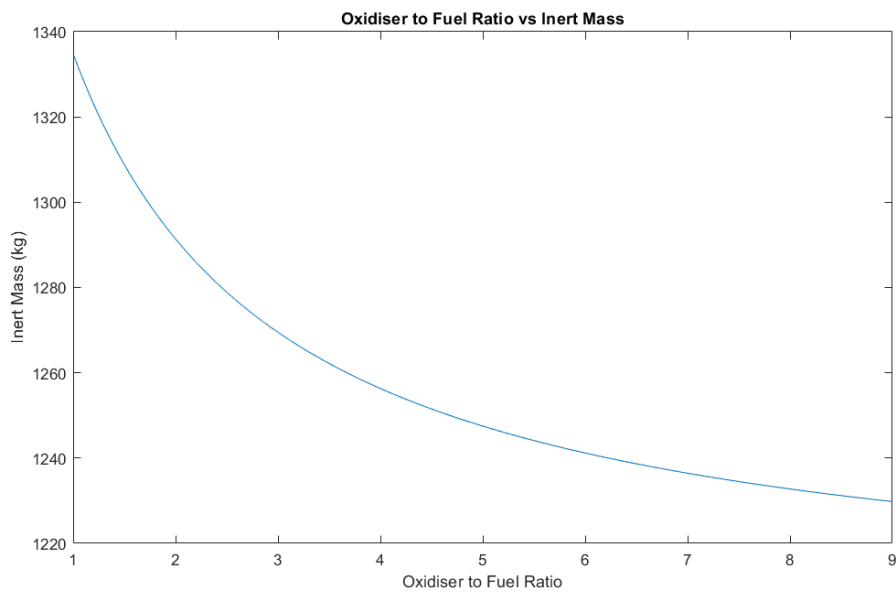


Figure 34: Plot of OF Ratio vs Inert Mass for Methalox Engine for Moon Mission

7.3.5.5 Oxidiser to Fuel Ratio Trend for Hydrolox Engine for Mars Mission

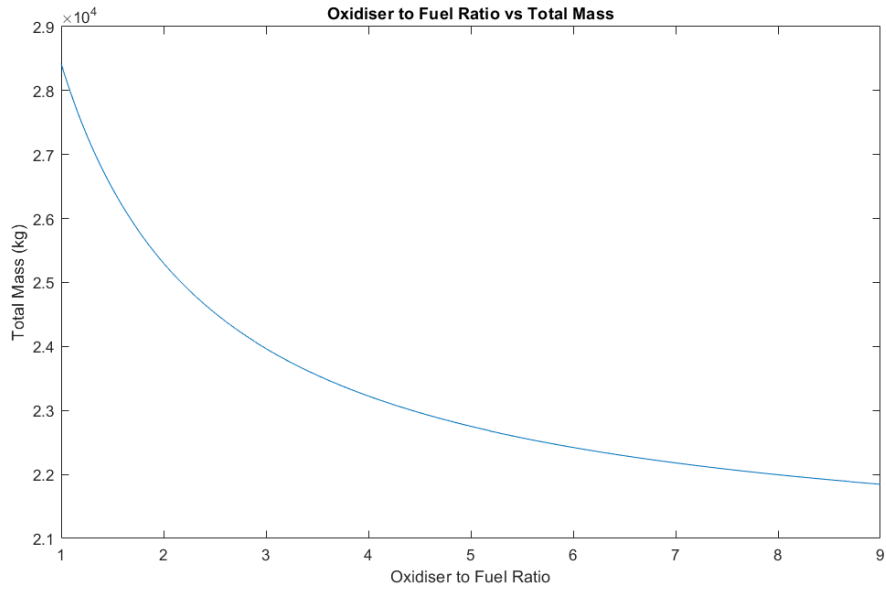


Figure 35: Plot of OF Ratio vs Total Mass for Hydrolox Engine for Mars Mission

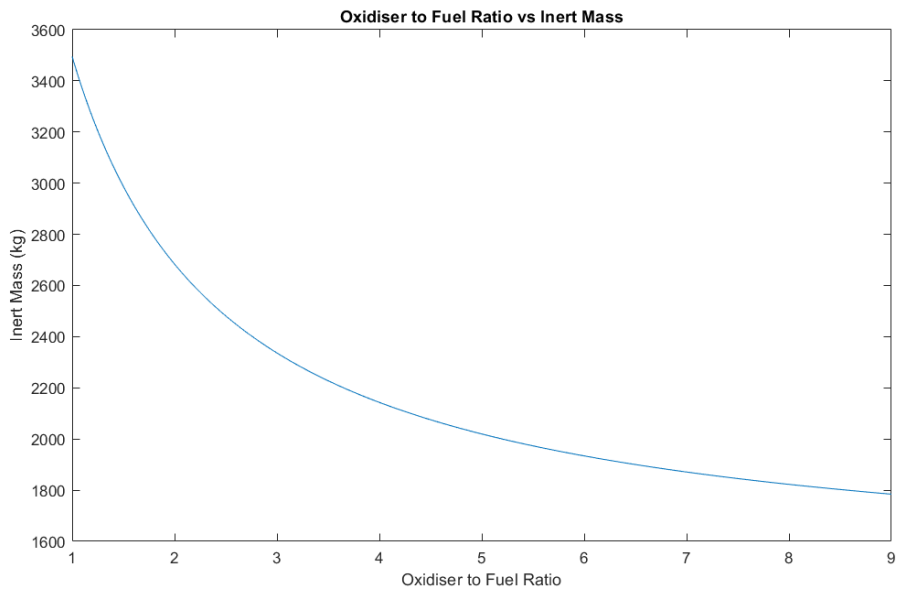


Figure 36: Plot of OF Ratio vs Inert Mass for Hydrolox Engine for Mars Mission

7.3.5.6 Oxidiser to Fuel Ratio Trend for Methalox Engine for Mars Mission

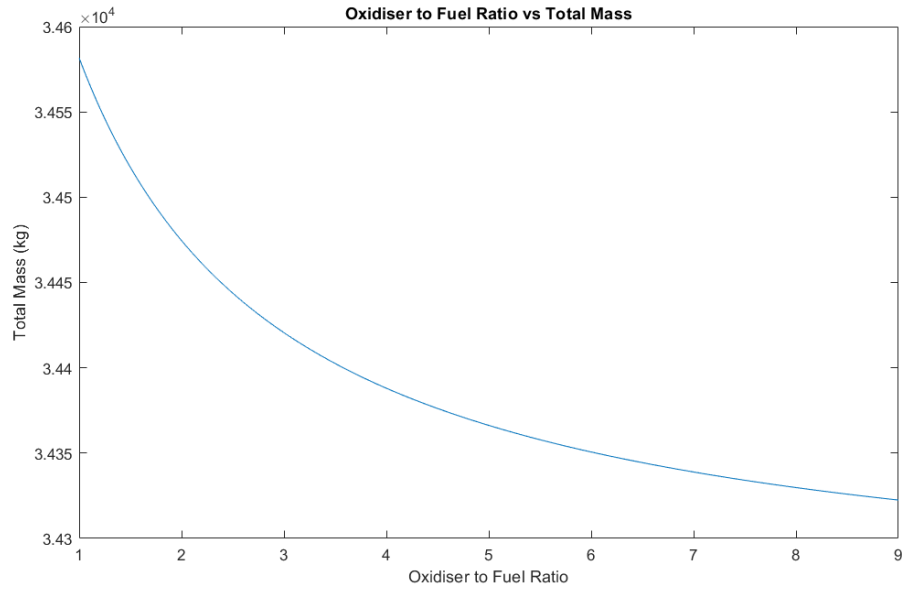


Figure 37: Plot of OF Ratio vs Total Mass for Methalox Engine for Mars Mission

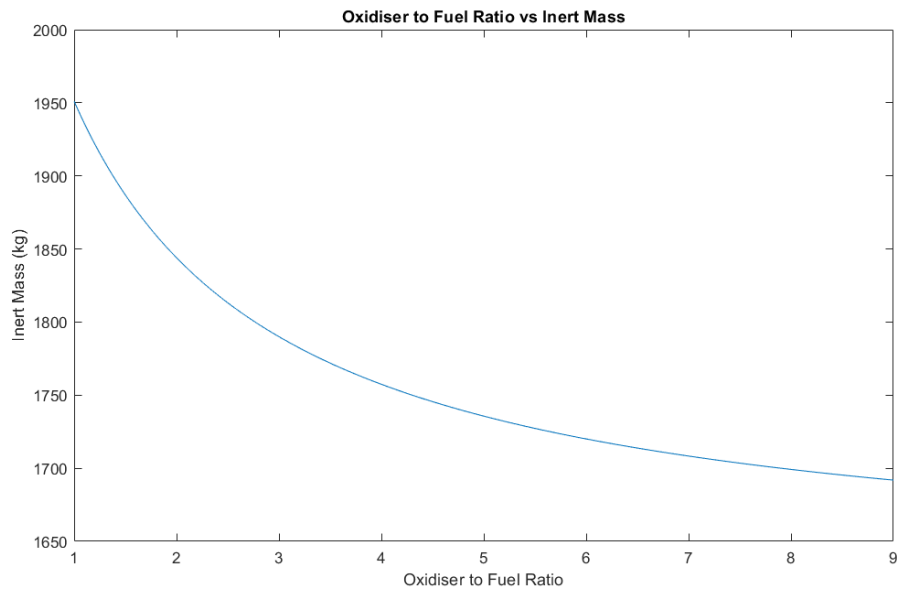


Figure 38: Plot of OF Ratio vs Inert Mass for Methalox Engine for Mars Mission

7.3.5.7 Specific Impulse Trend for Hydrolox Engine for Moon Mission

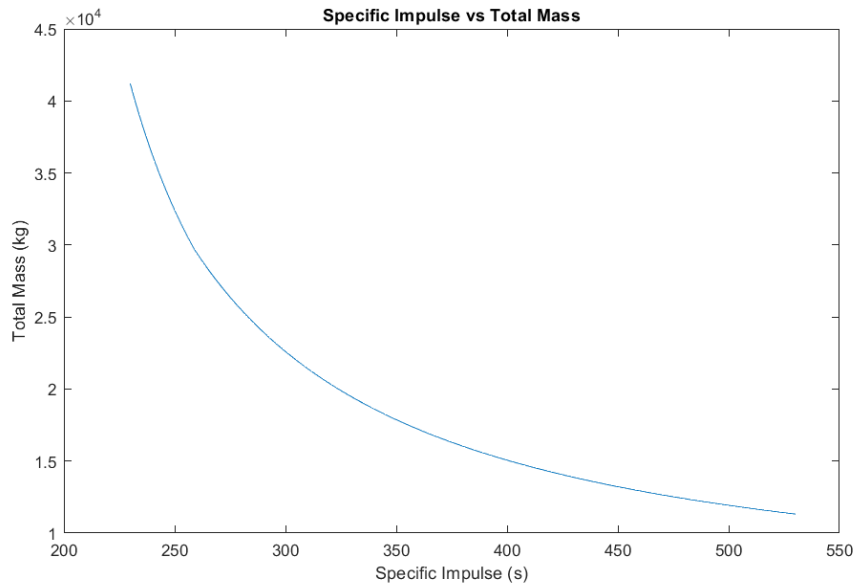


Figure 39: Plot of I_{sp} vs Total Mass for Hydrolox Engine for Moon Mission

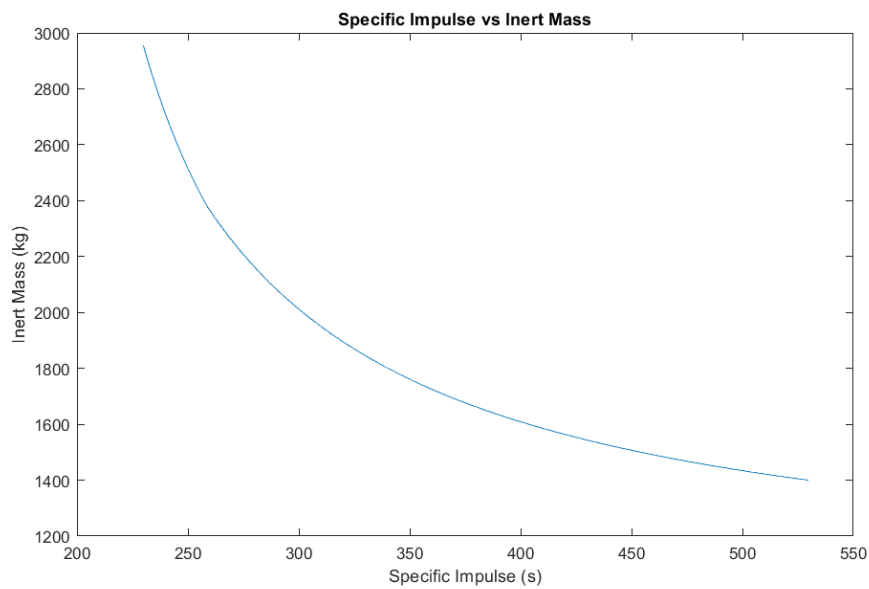


Figure 40: Plot of I_{sp} vs Inert Mass for Hydrolox Engine for Moon Mission

7.3.5.8 Specific Impulse Trend for Methalox Engine for Moon Mission

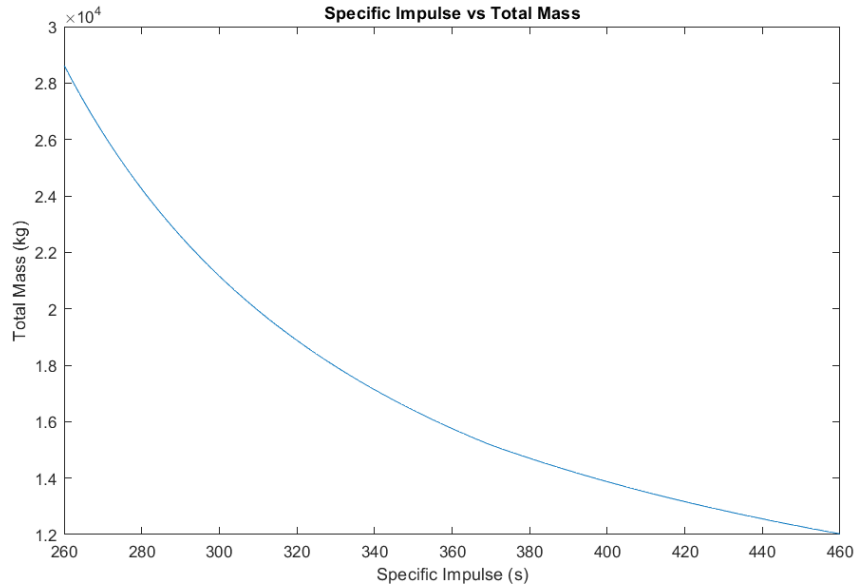


Figure 41: Plot of I_{sp} vs Total Mass for Methalox Engine for Moon Mission

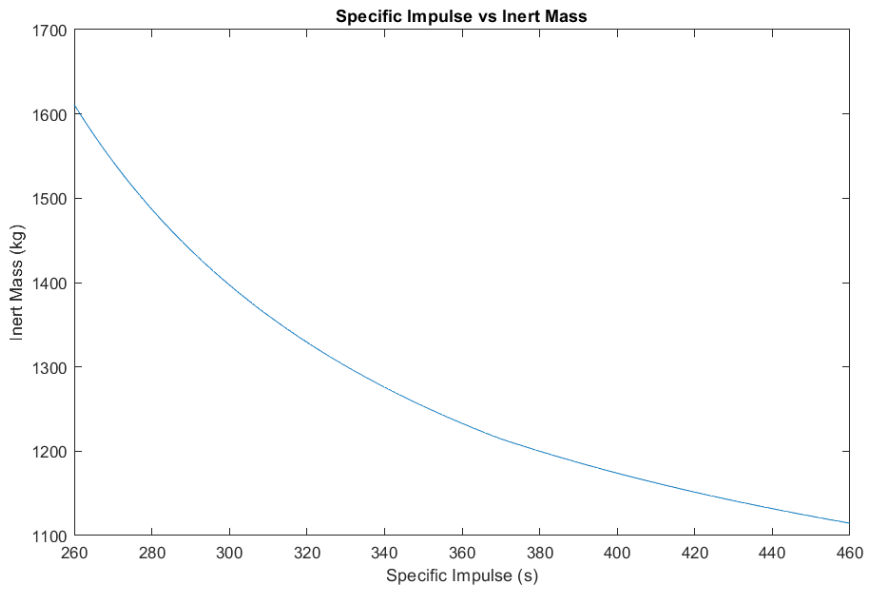


Figure 42: Plot of I_{sp} vs Inert Mass for Methalox Engine for Moon Mission

7.3.5.9 Specific Impulse Trend for Hydrolox Engine for Mars Mission

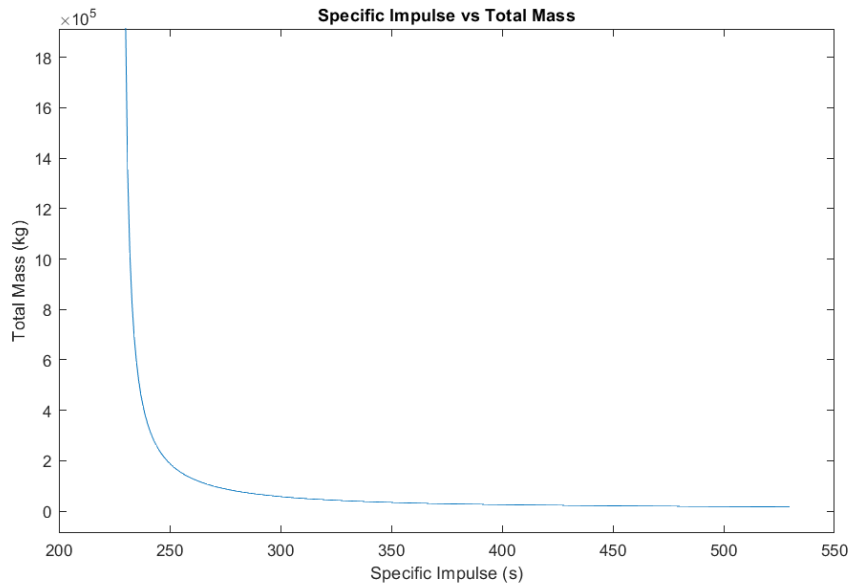


Figure 43: Plot of I_{sp} vs Total Mass for Hydrolox Engine for Mars Mission

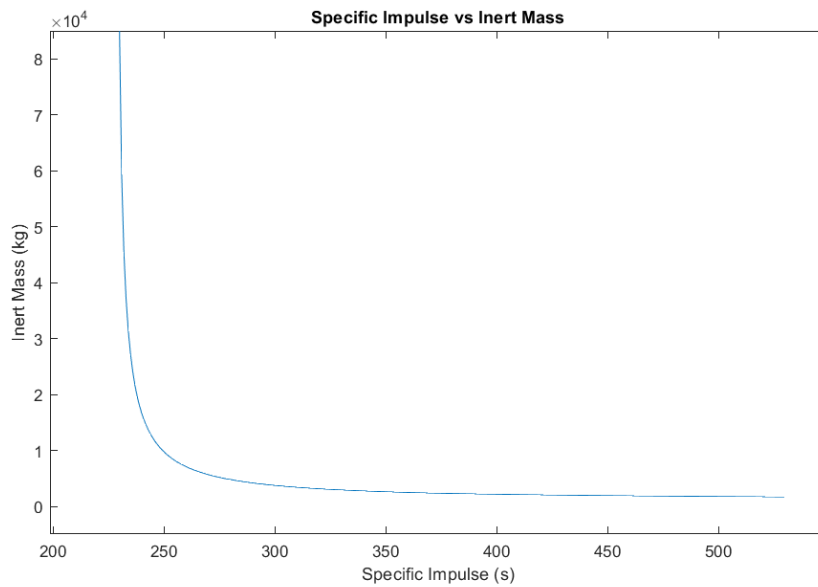


Figure 44: Plot of I_{sp} vs Inert Mass for Hydrolox Engine for Mars Mission

7.3.5.10 Specific Impulse Trend for Methalox Engine for Mars Mission

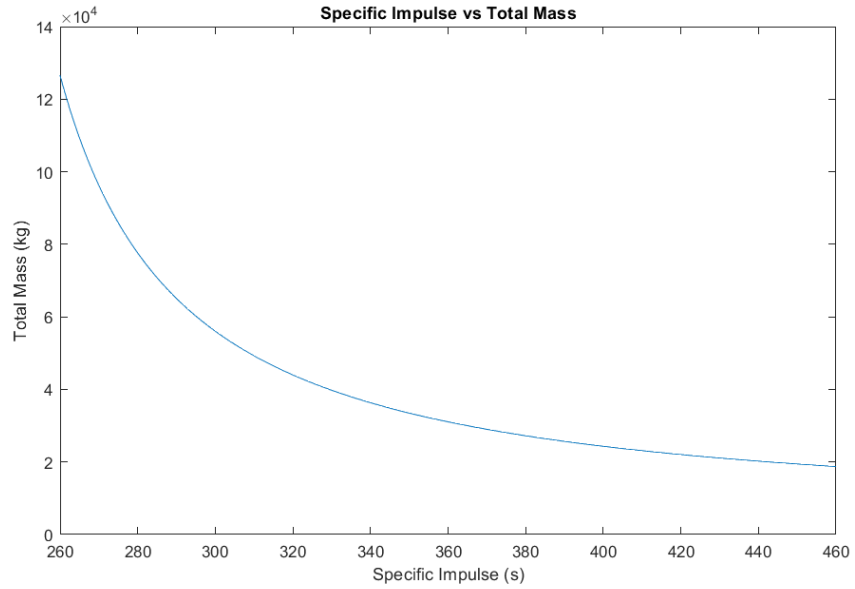


Figure 45: Plot of I_{sp} vs Total Mass for Methalox Engine for Mars Mission

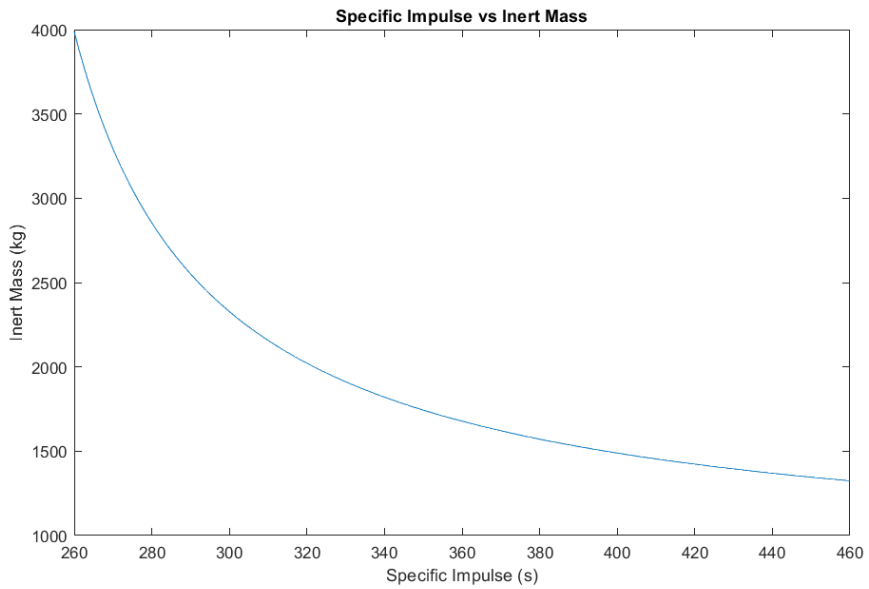


Figure 46: Plot of I_{sp} vs Inert Mass for Methalox Engine for Mars Mission

7.3.6. Summary

Below is the summary of the results of the Matlab Mass Estimation Tool.¹

Input	Unit	Moon- Hydrolox	Moon- Methalox	Mars- Hydrolox	Mars- Methalox
ΔV	m/s	3946.9	3946.9	5646.5	5646.5
Thrust	N	50000	50000	50000	50000
Combustion Chamber Pressure	Pa	2000000	2000000	2000000	2000000
Oxidiser to Fuel Ratio	-	5.0	3.6	5.0	3.6
Fuel	-	Hydrogen	Methane	Hydrogen	Methane
Initial Mass Fraction Assumption	-	0.08	0.08	0.08	0.08
Specific Impulse	s	427.50	346.54	427.50	346.54
Payload Mass	kg	3900	3900	3900	3900
Engine Mass	kg	546.3	425.1	546.3	425.1
Oxidiser Tank Diameter	m	3.5	3.5	3.5	3.5
Fuel Tank Diameter	m	3.5	3.5	3.5	3.5
Interstage Height	m	1.0	1.0	1.0	1.0

Table 6: Inputs for the Mass Estimation tool

¹See Appendix A for the Matlab code

Output	Unit	Moon- Hydrolox	Moon- Methalox	Mars- Hydrolox	Mars- Methalox
Total Mass	kg	13962.4	16648.7	22752.3	34399.3
Inert Mass	kg	1548.3	1260.9	2019.7	1768.8
Fuel Mass	kg	1419	2497.4	2805.4	6245.8
Oxidiser Mass	kg	7095.1	8990.5	14027.2	22484.8
Fuel Tank Height	m	2.2435	0.6627	4.4355	1.6575
Oxidiser Tank Height	m	0.6986	0.8853	1.3812	2.2140

Table 7: Outputs of the Mass Estimation tool

7.4. Conclusion and Scoring

Some of the main takeaways from this analysis are as follows:

- Irrespective of the mission destination, i.e. regardless of the required ΔV , the Inert Mass of the spacecraft with the Methalox Engine was always smaller as compared to the mass of the spacecraft with the Hydrolox Engine.
- But similarly, irrespective of the required DeltaV, the Total Mass of the spacecraft with the Methalox Engine was always larger as compared to the mass of the spacecraft with the Hydrolox Engine.
- The fuel tank dimensions for the Hydrolox spacecraft were always greatly larger than the Methalox spacecraft. This means, the hydrogen tanks will have a very large surface area, and therefore, face even more significant thermal management and boil off problems.

Chapter 7 System Mass and Fuel Budget

Below is a visual representation of the tank sizes for the two engine types.

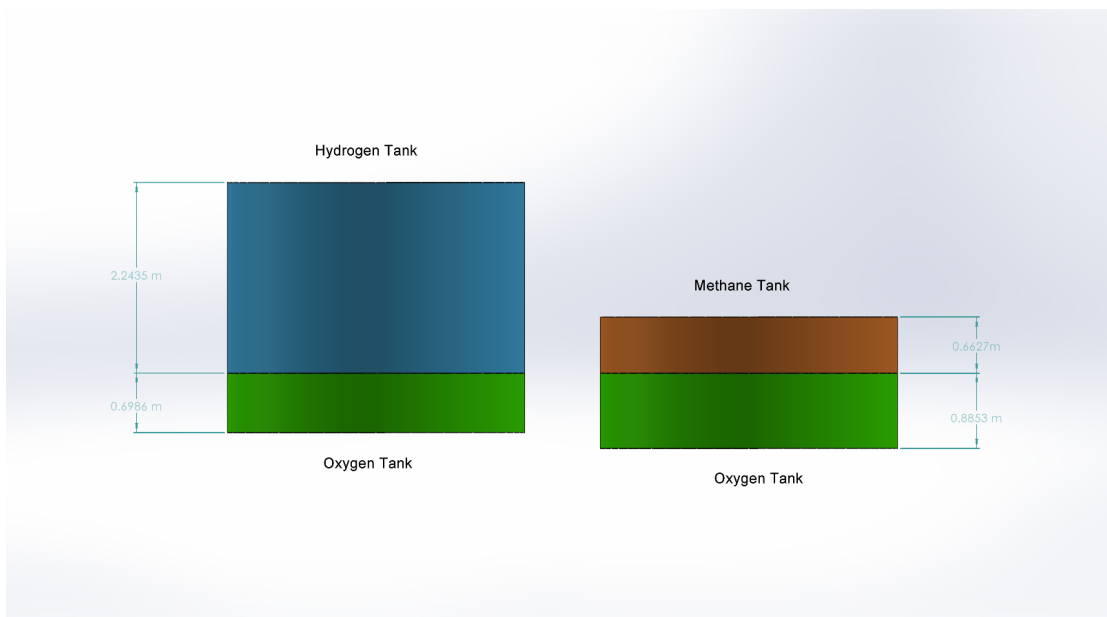


Figure 47: Tank sizes for Hydrolox Engine (Left) and Methalox Engine (Right) for the Moon mission

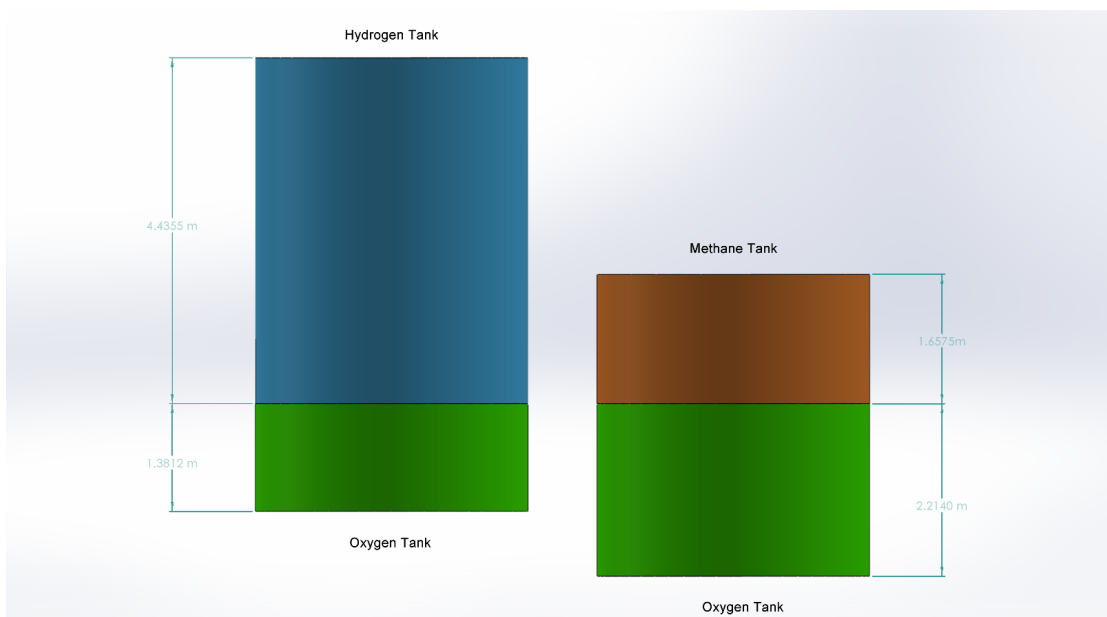


Figure 48: Tank sizes for Hydrolox Engine (Left) and Methalox Engine (Right) for the Mars Mission

Aspects considered when scoring:

- The Methalox version's inert mass can be even further reduced by improving the tank architecture using non-conventional methods, such as having a common bulkhead.
- The propellant mass of the Hydrolox system is significantly lower than the Methalox system. This is due to the higher efficiency of the Hydrolox Osiris Engine. Due to this, for the same amount of propellant, the Hydrolox engine can provide more ΔV compared to the Methalox engine, and therefore, less propellant is needed in total.
- Due to this advantage because of efficiency being scored in the previous section, here, that advantage can be ignored.
- One major aspect that is not considered in these total system mass numbers is the problem of extreme boil off which takes place with liquid hydrogen. This will be separately addressed in chapter 10.
- This means that, even though in the current analysis the propellant mass of the Hydrolox system is lower than the Methalox system, in reality, when the boil off will have to be compensated, the Hydrolox spacecraft might have to be loaded with additional propellant; and therefore might end up having a much heavier propellant mass and therefore system mass.

Therefore, for the sake of scoring, only the differences in the inert mass of the system will be considered.

To really compare the two versions of the engine, the difference in inert mass for the specific mission needs to be inspected. To do this, the lighter engine will be given a score of 10 on a scale of 0 to 10, and then scale the score of the other engine accordingly.

$$\begin{aligned} \text{Difference between the inert mass for the Moon mission} &= 1548.3 - 1260.9 \\ &= 287.4kg \end{aligned}$$

$$\begin{aligned} \text{Difference between the inert mass for the Mars mission} &= 2019.7 - 1768.8 \\ &= 250.9kg \end{aligned}$$

$$\begin{aligned} \text{Difference percentage for Moon mission} &= 287.4kg/1548.3 \times 100 \\ &= 18.562\% \end{aligned}$$

Chapter 7 System Mass and Fuel Budget

$$\begin{aligned} \text{Difference percentage for Mars mission} &= 250.9/2019.7 \times 100 \\ &= 12.422 \% \end{aligned}$$

Therefore, hydrogen can be scored 18.562 % lower score for the Moon mission, and 12.422 % lower score for the Mars mission.

The score for Hydrogen for the Moon mission is 8.14.

The score for Hydrogen for the Mars mission is 8.75.

Part	Moon-Hydrolox	Moon-Methalox	Mars-Hydrolox	Mars-Methalox
Score	8.14	10	8.75	10

Table 8: Scoring for System Mass

8. Pump Power Requirements

For a pump fed engine, one of the most important elements is the fuel and oxidiser pumps. As discussed in the overview of the liquid rocket engines 2, the pumps are driven by a different source according to engine cycle type. For the Gas Generator cycle and the Staged Combustion cycles, the pre-burner combustion products are what power the motors, for the Expander cycle it is the heated fuel expanded in the turbine and for the Electric Pump cycle, it is simply the electric motor that powers the pump for the entire duration of engine burn. But for the Electrically Augmented Expander cycle, the motor is responsible for powering the pumps during startup and low thrust phases, and the turbine with the expanding fuel for the rest.

Therefore, it is important to understand how the power requirements for the pumps are different for the two fuel options, hydrogen and methane. The pump design and analysis were carried out during the Masters Project work on the Osiris engine, and here, the pump design will be overviewed. After this, the impact of the different fuels on the power requirement will be discussed [4].

8.1. Osiris Hydrogen and Methane Pump Overview

First, let's look at the overview of steps that were taken to design the fuel pump for the Hydrolox version of the Osiris Engine [4].

The mass flow of the fuel for the engine is known to be 1.79 kg/s.

In the beginning, the pressure losses are listed due to the fuel flowing from the pump through the cooling channels, through the turbine, and then the injector before reaching the combustion chamber.

$$\begin{aligned}
 \delta P_{injector} &= 3.5bar \\
 \delta P_{line\ losses} &= 0.5bar \\
 \delta P_{turbine} &= 24bar \\
 \delta P_{cooling\ channels} &= 15bar \\
 \delta P_{line\ losses\ to\ cooling\ channels} &= 7bar \\
 \delta P_{total} &= 50bar \\
 P_{cc} &= 20bar \\
 P_{hy\ pump\ outlet} &= 70bar \\
 P_{hy\ pump\ inlet} &= 4bar \\
 P_{hy\ head} &= 66bar
 \end{aligned}$$

The RL-10A 3-3 was used as a reference for the losses [40].

Chapter 8 Pump Power Requirements

Since the pump head was so large, a two-stage pump design was chosen so as to not have a very large or very fast pump.

Stage 1: 4 bar - 38 bar

Stage 2: 36 bar - 70 bar

These inputs were then used to generate a pump design by using a modified version of a Matlab tool created by Jonas Bishoff for his Masters Thesis [41].

The following were the output parameters for the pump design:

Parameter	Value
Pump Flow (Q)	$0.02526m^3/s$
rotational speed	$30000rpm$
Optimal Pump Power (P_u)	$155.5kW$
Optimal Head (H)	$5597m$

Table 9: Hydrogen Pump (Stage 1) Key Parameters [4]

Parameter	Value
Pump Flow (Q)	$0.02526m^3/s$
rotational speed	$30000rpm$
Optimal Pump Power (P_u)	$155.5kW$
Optimal Head (H)	$5597m$

Table 10: Hydrogen Pump (Stage 2) Key Parameters [4]

And the following were the physical output parameters. These parameters are for one stage of the hydrogen pump, but they are the same vales for both stages.

Parameter	Value
Minimum Shaft Diameter	9.5mm
Pump Outer Diameter	196.1mm
Circumferential speed	307.99m/s
Inlet Hub Diameter	23.68mm
Inlet Diameter	54.0mm
Impeller Inlet Angle	26.43°
Impeller Outlet Angle	23.51°
Impeller Blade Thickness	1.2mm

Table 11: Hydrogen Pump Design Parameters [4]

Below is the performance of the pump and the streamlines in the impeller.

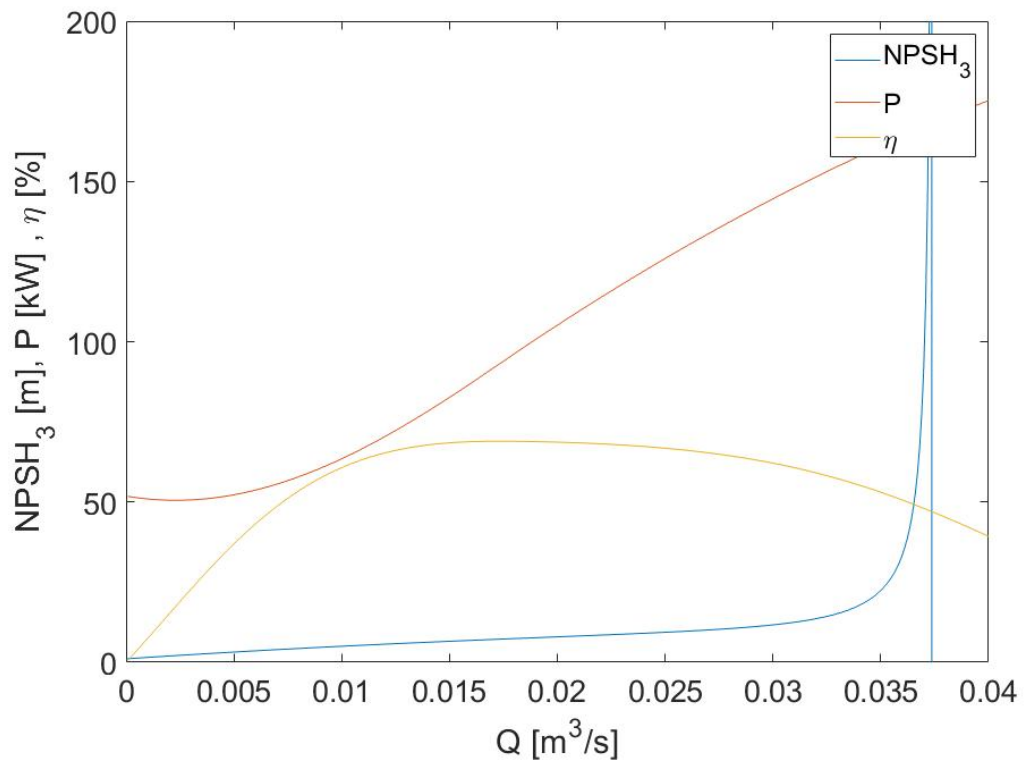


Figure 49: Performance of the Hydrogen Pump (Stage 1) at 30000 rpm [4]

Now, for the design of the methane pump, the same procedure was followed.

The mass flow of the methane for the engine is 2.88 kg/s.

Unlike the hydrogen fuel pump, just a single-stage pump can be used for methane since there is around five times less volume of methane to be pumped due to methane having a higher density.

The same method was employed to design the methane fuel pump using the Matlab tool, and the following were the output parameters for the pump design:

Parameter	Value
Pump Flow (Q)	$0.0044m^3/s$
rotational speed	$20000rpm$
Optimal Head (H)	$1555m$
Power (P)	$83.000kW$
Torque (T)	$39.65N * m$

Table 12: Methane Pump Key Parameters [4]

The following were the physical output parameters:

Parameter	Value
Minimum Shaft Diameter	$9.5mm$
Pump Outer Diameter	$153.7mm$
Circumferential speed	$160.99m/s$
Inlet Hub Diameter	$23.75mm$
Inlet Diameter	$40.0mm$

Table 13: Methane Pump Design Parameters [4]

Below is the performance of the pump and the streamlines in the impeller.

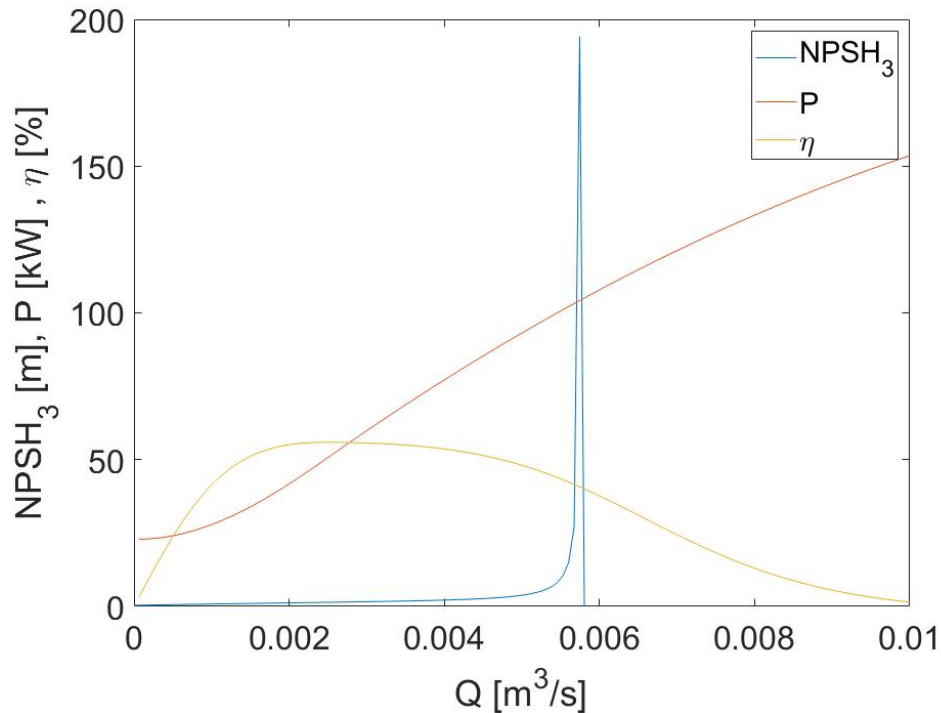


Figure 50: Performance of the Methane Pump at 20000 rpm [4]

8.2. Start Up Power

Based on the pump design, it can be seen that the peak power requirement of the hydrogen fuel pump is 311 kW. For the Hydrolox version of the Osiris Engine, the power requirement for the oxygen pump is 38.5 kW. Therefore, at peak thrust, the power required to run both pumps would be 349.5 kW.

Likewise, the peak power requirement of the methane fuel pump is 83 kW. And for the Methalox version, the power requirement for the oxygen pump is 38.5 kW. Thus, the combined power requirement at peak thrust is 121.5 kW.

In the Electrically Augmented Expander Cycle engine, the electrical motor is used to start the engine, therefore, it is important to understand the requirements of this motor and what will be demanded of it at startup.

Now, the power requirement of the pump is not the same throughout the throttle range. This is because the change in mass flow of the propellant changes the thrust of the engine, and this, therefore, changes the power required by the pump.

Additionally, the power that can be extracted from the turbine also decreases with a decrease in thrust as there is less heat to extract from the cooling channels.

Therefore the Power vs Thrust curve of the Osiris engine looks as follows:

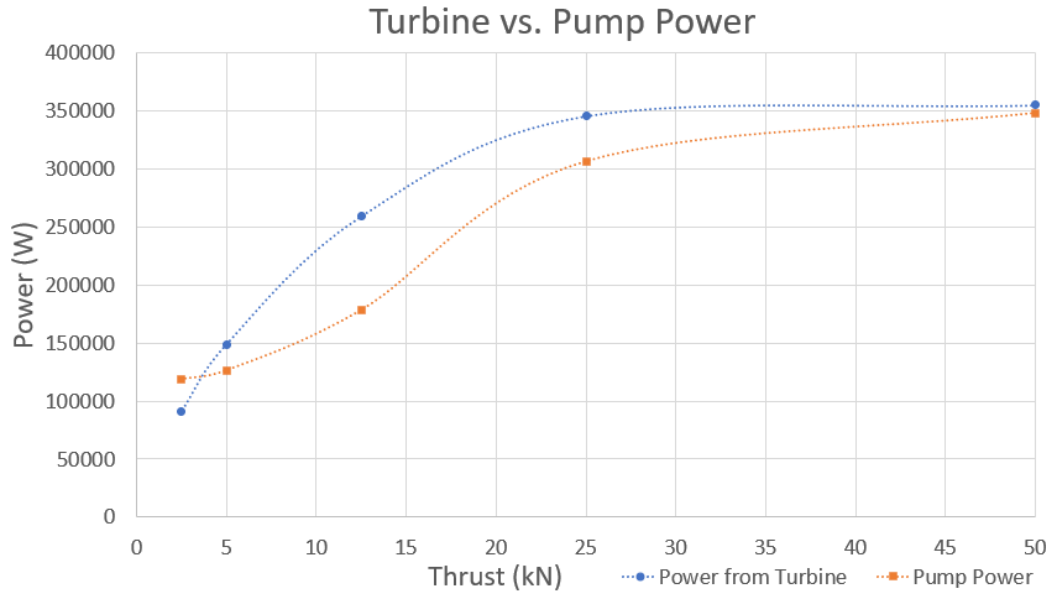


Figure 51: Thrust vs Power Curve for the Hydrolox Osiris Engine [4]

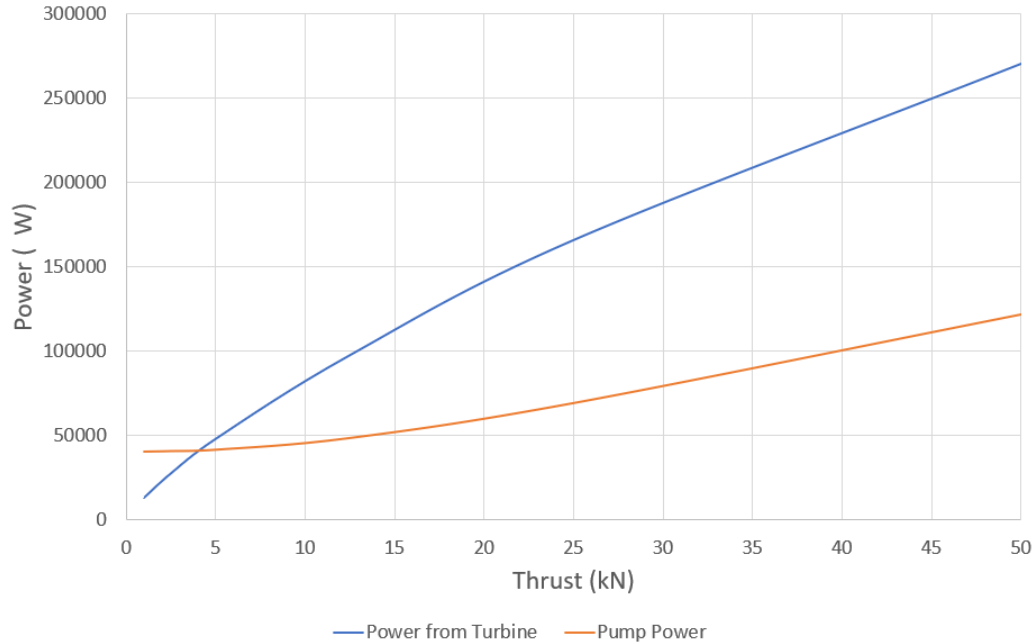


Figure 52: Thrust vs Power Curve for the Methalox Osiris Engine [4]

As can be observed, in both cases, the turbine is not able to provide enough power to the pumps to start the engine. Therefore, the electric motor will be used to supply this start up power.

The motor would then have to further support powering the pumps at least until the point when the Power from Turbine curve crosses the Pump Power curve in figures 51 & 52. Here, the turbine would then be able to supply enough power to the pumps. Therefore, for the Hydrolox version, the electric motor would have to supply at least 120 kW, and for the Methalox version, the electric motor would have to supply at least 41.5 kW.

And herein lies the biggest problem. The power requirements for the Hydrolox version are extremely high compared to the Methalox version. Therefore, the size of this motor would be very large.

8.3. Conclusion and Scoring

To satisfy the requirement of the Hydrolox version of the engine, the P400R manufactured by YASA was suggested in the Osiris Project report [4]. It weighs 28.2 kg and has a maximum power output of 160 kW.

For the Methalox version, the REB 50 manufactured by ROTEX Electric was selected. It weighs 12 kg and has a working power output of 50 kW [4].

What can be clearly understood here, is that higher power demand from the motor for the Hydrolox version is the biggest drawback of using hydrogen as a fuel for the Osiris engine. The Methalox version only requires 41.5 kW, compared to the 120 kW required by the Hydrolox version, which is almost three times the power demand. This directly translates to a much heavier electrical motor and higher cooling demands due to a higher wattage motor. This is, of course, additionally to the fact that the two-stage pump of the Hydrolox version leads to not just a heavier design but also a more complicated design. The startup for the Methalox engine will also be much easier.

Another major factor that is directly affected by the change in motor power usage is the size of the batteries. The battery plus controller for the Methalox engine would be around 45 kg. On the other hand, the battery plus the controller for the Hydrolox engine would be around 143 kg. This alone is responsible for more than 1/4th of the entire engine mass! (From Table 1 & 2)

Therefore, it can unequivocally be said that having a Hydrolox system for the Osiris Electrically Augmented expander cycle system has tremendous mass and complexity penalties.

Chapter 8 Pump Power Requirements

Hence, if it is broken down to the masses of these two systems, the distribution is as follows:

For Hydrolox Osiris Engine:

$$\begin{aligned} \text{Mass of the Electric Motor} &= 28.2 \text{ kg} \\ \text{Mass of Battery and Controller} &= 143 \text{ kg} \\ \text{Mass of 2 Stage Fuel Pump and Housing} &= 50 \text{ kg} \\ \text{Total Mass} &= 221.2 \text{ kg} \end{aligned}$$

For Methalox Osiris Engine:

$$\begin{aligned} \text{Mass of the Electric Motor} &= 12 \text{ kg} \\ \text{Mass of Battery and Controller} &= 45 \text{ kg} \\ \text{Mass of 2 Stage Fuel Pump and Housing} &= 20 \text{ kg} \\ \text{Total Mass} &= 77 \text{ kg} \end{aligned}$$

Therefore, the difference in mass is 144.2 kg.

Using a similar philosophy as in the previous section, the lighter power system can be scored as a 10. Therefore, the Methalox version is scored a 10 on a scale of 0 to 10.

$$\begin{aligned} \text{Difference percentage} &= 144.2/221.2 \times 100 \\ &= 65.19 \% \end{aligned}$$

Therefore, hydrogen can be given a 65.19% lower score.

The score for hydrogen is then 3.481.

Part	Moon-Hydrolox	Moon-Methalox	Mars-Hydrolox	Mars-Methalox
Score	3.481	10	3.481	10

Table 14: Scoring for Pump Power Requirements

9. Storability and Long-Term Use

9.1. Introduction

One of the most important factors for propellant selection is its intended duration of storage and use. And this is why it is imperative to consider the storability of the propellants for use in longer duration missions as this becomes a critical factor. Therefore, this is what will be discussed in this section.

9.2. Factors affecting storability and long-term use

9.2.1. Molecule Size

One of the most infamous drawbacks of hydrogen is its small molecular size. This is an important consideration when evaluating its use as a fuel for spacecrafts. While the small size of hydrogen molecules allows for high specific impulse and clean exhaust, it also presents challenges in terms of containment and leakage. The small size of hydrogen molecules can make it difficult to contain hydrogen within fuel tanks, as they can easily escape through tiny gaps and fissures in the tank walls. This can increase the risk of leaks and safety hazards during fuel storage and transport, which can be particularly problematic for spacecraft due to the need for high reliability and safety. This is also a big problem for all of the piping and tubing in the spacecraft. As a result, the design and construction of hydrogen storage and transport systems for spacecraft must take into account the small molecular size of hydrogen and the need for effective containment and leak prevention measures [42].

One approach to addressing the challenges posed by the small molecular size of hydrogen is the use of advanced materials and designs for fuel storage and transport systems. However, the development and implementation of such systems can be complex and costly, which can pose challenges to the widespread adoption of spacecraft systems if the rate of space exploration keeps growing at its current pace.

The molecular size of methane is significantly larger than hydrogen. The diameter of a hydrogen molecule is about 289 picometers, while the diameter of a methane molecule is about 380 picometers [43]. This means that methane molecules are about 1.3 times larger than hydrogen molecules.

The larger molecular size of methane makes it less prone to leakage than hydrogen, reducing the risk of safety hazards during fuel storage and transport. This can make methane a more attractive option for long-duration space missions, where reliable and safe fuel storage is critical.

9.2.2. Cryogenic Temperature

Liquid hydrogen is a cryogenic fluid that must be stored and transported at extremely low temperatures, typically below -253°C . In the context of space missions, the challenges of storing and handling liquid hydrogen are further compounded. The harsh conditions of space can cause insulation materials to degrade, leading to heat transfer and fuel boil off. Additionally, the need for specialised equipment and insulation materials can add complexity, cost, and mass to the design, making liquid hydrogen less practical. However, even with these measures, liquid hydrogen can still boil off and evaporate over time due to its low boiling point. This can lead to the loss of valuable fuel. In a Hydrolox system, additional measures need to be taken to insulate the hydrogen tank from the oxygen tank to prevent heat from being transferred from the oxygen tank, which is usually at a higher temperature [44].

In contrast to liquid hydrogen, liquid methane can be stored and transported at higher cryogenic temperatures, typically below -162°C . This is due to the higher boiling point of methane compared to hydrogen, which means that it requires less extreme thermal management to remain in a liquid state. The higher temperature requirements for liquid methane storage and transport can simplify the design and construction of equipment, as well as reduce material degradation. Additionally, the higher boiling point of methane means that it is less prone to boil off and evaporate compared to liquid hydrogen, reducing the risk of fuel loss and safety hazards [45].

The boiling point of liquid oxygen is around -183°C , which is much closer to liquid methane. This provides two main advantages. One is that the thermal management between the tanks is much more simplified, and the second is the possibility of using a common bulkhead. Due to the similar temperatures, it is possible to use a common structure between the methane and oxygen tanks, and this can prove to give a significant mass reduction of the overall system. However, like hydrogen, methane also requires cryogenic storage at extremely low temperatures, which can pose challenges in terms of insulation and containment to a certain extent.

9.2.3. Interaction with Materials

Hydrogen is known to cause hydrogen embrittlement, a phenomenon in which hydrogen atoms can diffuse into a material and weaken its structure, making it brittle and susceptible to cracking or failure. This is a significant concern in the context of spacecraft materials, as hydrogen can potentially react with many commonly used materials, including metals, polymers, and composites, and cause hydrogen embrittlement. One example of hydrogen embrittlement in spacecraft with the use of titanium alloys, which are commonly used in fuel tanks and structural components

due to their strength and lightweight properties. When exposed to hydrogen, titanium can become brittle and susceptible to cracking, which can compromise the structural integrity of the spacecraft. To mitigate the risk of hydrogen embrittlement, special coatings or surface treatments may be applied to prevent hydrogen diffusion and minimise the risk of failure. In addition to titanium, hydrogen can also cause embrittlement in other materials commonly used in spacecraft, such as aluminium alloys and composites. Therefore, it is important to consider this aspect when comparing fuels [46].

In contrast, methane does not pose as significant a risk of embrittlement as hydrogen. While it can potentially react with some materials, such as certain types of polymers and elastomers, its effects on structural materials, such as metals, are relatively limited. This makes methane a more attractive option as a fuel in comparison.

9.2.4. Handling on Earth and other Planetary bodies

Another important aspect to consider is the handling, storage and transportation of these cryogenic fuels on ground. Because of the factors discussed above, it is extremely difficult to handle liquid hydrogen. Both, liquid hydrogen and liquid methane, have boil off on Earth, but the quantity of boil off for hydrogen is significantly larger, and this is a loss of valuable resources but also, the evaporated hydrogen forms an explosive mixture with air. The lower temperatures of liquid hydrogen also make transportation and storage bulky and cumbersome, and handling challenging. But these difficulties are compounded when it comes to other planetary bodies. Not only is handling by humans restricted in spacesuits in an alien environment, but storage and transportation are also hindered due to limited resources [47].

9.2.5. Toxicity

The toxicity factor for these two fuels has a limited effect on the choice between them as handling on ground and on the spacecraft is done with a high safety factor but it is important to have an overview of their possible dangers.

Hydrogen is not considered toxic, as it is not harmful to humans or the environment in its natural state. However, it can pose certain safety risks if not handled properly. For example, if released in a confined space, hydrogen gas can displace oxygen and create an oxygen-deficient atmosphere, leading to asphyxiation [48].

On the other hand, methane is considered mildly toxic in high concentrations. Inhalation of methane gas can lead to dizziness, headaches, and nausea. Methane can also displace oxygen in a confined space, creating an oxygen-deficient atmosphere. Methane is also highly flammable and can ignite if exposed to a spark or flame. However, it is less reactive than hydrogen and does not pose as much risk in terms of explosion or combustion [49].

9.2.6. Boil Off

The consequence of boil off on long-term space missions cannot be understated. For liquid hydrogen and liquid methane, this difference is especially huge. Due to its significant impact on evaluating the fuels, the next chapter has been dedicated to analysing this phenomenon 10.

9.3. Conclusion and Scoring

In conclusion, the storability and long-term use of propellants are critical factors to consider when selecting a fuel for an engine, especially if its intended use is interplanetary missions. The small molecular size of hydrogen can present challenges in terms of containment and leakage, while the need for cryogenic storage and handling can add complexity and cost to the design. Methane, on the other hand, has a larger molecular size and can be stored and transported at higher cryogenic temperatures, making it a more attractive option for long-duration space missions where reliable and safe fuel storage is critical.

For this, the concept of storability can be approached from a relative point of view. Some common fuels can be considered that could be used in space travel, and put it on a scale of 0 to 10 for perspective.

Water would be a 10, as it is very easy to handle and store and requires very little maintenance.

RP 1 would be an 8, as it is a relatively stable fuel.

Liquid Methane would be a 6, as it is easier to contain and does not react with storage materials as much, but it is still a cryogenic fluid.

Liquid hydrogen would be a 3 due to containment problems, hydrogen embrittlement, and handling problems.

Therefore, the score is as follows:

Part	Moon-Hydrolox	Moon-Methalox	Mars-Hydrolox	Mars-Methalox
Score	3	6	3	6

Table 15: Scoring for Storability and Long-Term Use

10. Boil Off Behaviour

10.1. Introduction

One of the most important differences between liquid hydrogen and liquid methane are its thermal properties and, more importantly, its liquefaction point. This is especially important for longer-duration missions, such as interplanetary missions. The major source of heat in a spacecraft is the solar heat flux. This means that for missions towards the inner solar system, the boil off problem gets even more exacerbated [50].

Hydrolox engines have always been one of the most efficient propellant combinations, but there is one main reason why currently it is limited to use in Low Earth Orbit. It is due to liquid hydrogen boil off. Liquid hydrogen very rapidly boils off into gaseous hydrogen, and to maintain a certain pressure in the tank, the excess hydrogen gas has to be thrown out of the spacecraft. For shorter mission durations, such as low Earth missions, the total amount of time the propellant would have to be stored, is much less. So, the propellant can be consumed by the engine before there is enough loss of propellant. But for longer-duration missions, this becomes much more challenging. This, of course, also occurs with liquid methane, but at a much lower rate [53].

Therefore, it is important to understand the boil off behaviour of the two fuels that are being compared. Thus, in this section, that aspect of the two fuels will be looked at.

10.2. Boil Off Estimate with Heat Flux Input Estimation Tool

10.2.1. Approach

The goal of this Matlab tool is to provide an estimate of the heat input into the spacecraft tank, using which boil off can be estimated. Just like the approach of the previous tool, the aim is to provide a simplified understanding of the main heat sources and inputs, and therefore, this is a really simple approach to that and is useful for making a comparison of the fuels.²

The assumptions made are as follows:

- A simplified thermal model is assumed, with the Sun as the primary source of heat.

²The approach for the entire boil off estimation was verified by Daniel Just from the Thermal Department at ArianeGroup Bremen.

- One Astronomical Unit (AU) is 149,597,870,700 m [51].
- Variations due to the Solar cycle are ignored.
- Seasonal variations in solar activity are ignored.
- Distance of Mars from the Sun is 1.52366231 AU [52].
- Distance of the Moon from Earth is 384400 km [54].
- Radius of Earth is 6371 km [54].
- Radius of the Moon is 1737 km [54].
- Radius of Mars is 3389 km [52].
- View factor is always 1.
- Solar zenith angle is always 0.
- Albedo of Earth is 0.31 [55].
- Albedo of the Moon is 0.12 [56].
- Albedo of Mars is 0.25 [52].
- For the journey from Earth to Moon, the spacecraft is assumed to be flying towards the Sun in the direction of the Moon.
- The boil off calculated will be with the average incoming heat flux and not as it varies over time.
- The path considered for the journey from Earth to Mars is a two-dimensional linear journey (not considering transfer between orbits). This is because a simplified heat flux distribution is the goal, and since only the average heat flux is being used, the actual distribution of the path travelled by the spacecraft is not considered.
- Black Body temperature of Earth is 253.72 K [57].
- Black Body temperature of the Moon is 270.4 K [54].
- Black Body temperature of Mars is 209.8 K [52].
- Assume absorptivity as 0.25 due to white colour paint [59].
- Spacecraft is assumed to be inside fairings during launch.

- Tank architecture plays a major role in the thermodynamics surrounding it. Since the study is only looking at a simplified thermal model, the effect of different tank architectures will not be explored, and therefore, different heat dissipation mechanisms will not be considered. Hence, both fuels would be compared with the same assumptions.

Any further assumptions will be mentioned where applicable.

Steps followed to get a heat flux input estimate:

1. Calculate the Solar Flux distribution across the Solar System.
2. Display the Solar Flux distribution between Earth and the target body.
3. Calculate the Heat Flux input due to Earth's Albedo.
4. Calculate the Heat Flux input due to Earth's IR radiation.
5. Calculate the Heat Flux input due to the target body's Albedo.
6. Calculate the Heat Flux input due to the target body's IR radiation.
7. Calculate the Net Heat Flux across the Journey between Earth and the target body.
8. Find the Average Heat Flux over the entire journey and multiply this by absorptivity and the tank surface area exposed to the heat flux to get the power input to the tank.
9. Use this as input for BoilFast Software and get boil off estimate.

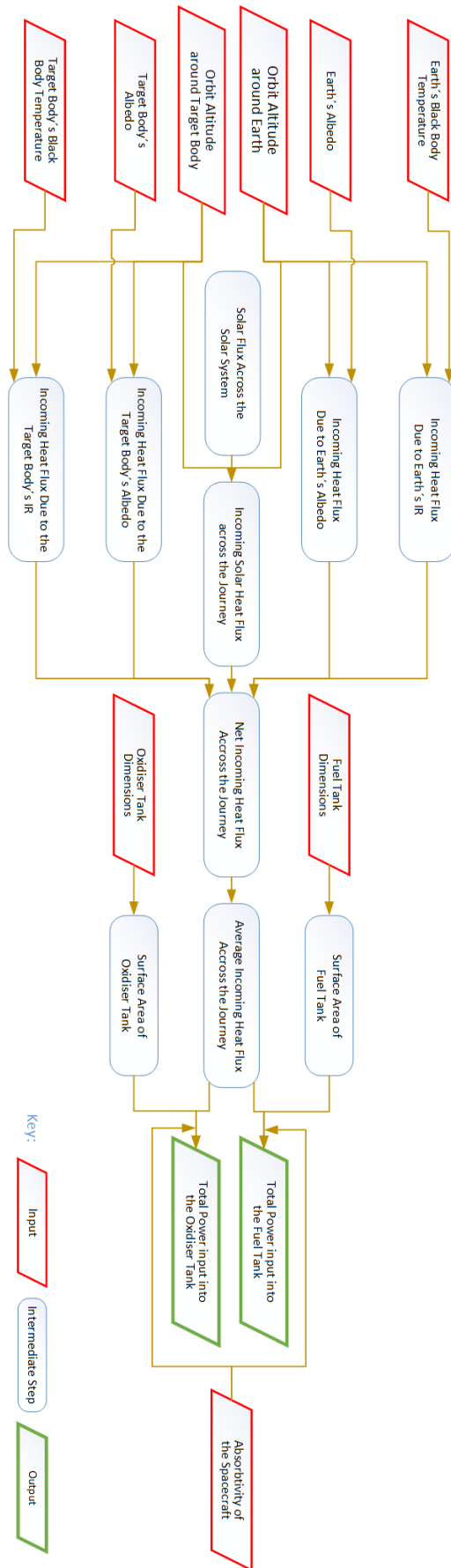


Figure 53: Matlab Heat Flux Estimation Tool Logic Flow

Input	Unit
Altitude of Orbit around Earth	km
Altitude of Orbit around Target Body	km
Earth's Black Body Temperature	K
Earth's Albedo	-
Target Body's Black Body Temperature	K
Target Body's Albedo	-
Fuel Tank Surface Area	m ²
Oxidiser Tank Surface Area	m ²

Table 16: Inputs for the Heat Flux Estimation Tool

Output	Unit
Total Power Input into the Fuel Tank	W
Total Power Input into the Oxidiser Tank	W

Table 17: Outputs of the Heat Flux Estimation Tool

After this, the Tool BoilFAST is used to estimate the boil off. This is a tool developed at the University of Western Australia by the Fluid Science & Resources research group [61].

The main inputs for this software are:

- Type of Fluid
- Liquid surface condition
- Vapour temperature
- Tank type
- Tank dimensions
- Vapour relief pressure
- Ambient temperature
- Heat transfer coefficients
- Heat flows

- Simulation length
- Simulation step interval

The main outputs of this software are the following values within the tank for liquid and vapour across the simulation time:

- Temperature
- Pressure
- Volume
- Quantity
- Density
- Enthalpy
- Boil off rate
- Relief Rate
- Heat transfer rate

10.3. Results

10.3.1. Power inputs to the Spacecraft Tanks using Matlab Tool

10.3.1.1 Solar Heat Flux Distribution Graph

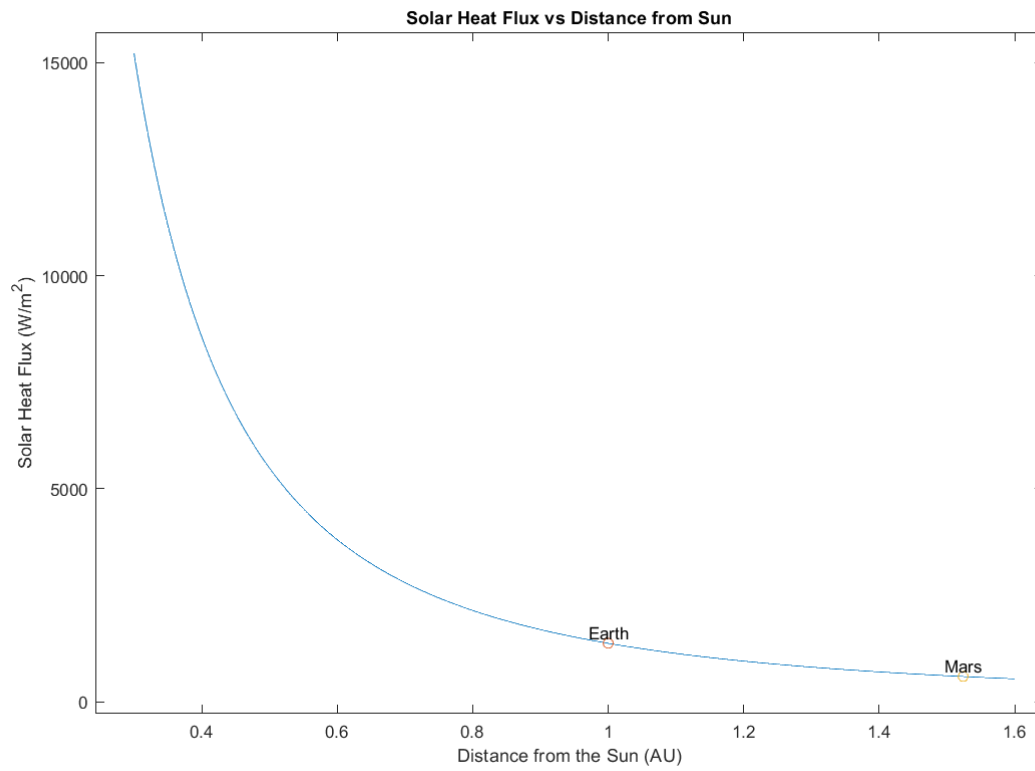


Figure 54: Solar Heat Flux Distribution Graph

10.3.1.2 For Moon mission

From 170 km Low Earth Orbit to 110 km Lunar Orbit as described in chapter 5.

Solar Heat Flux between Earth and Moon vs Distance from Earth's Surface

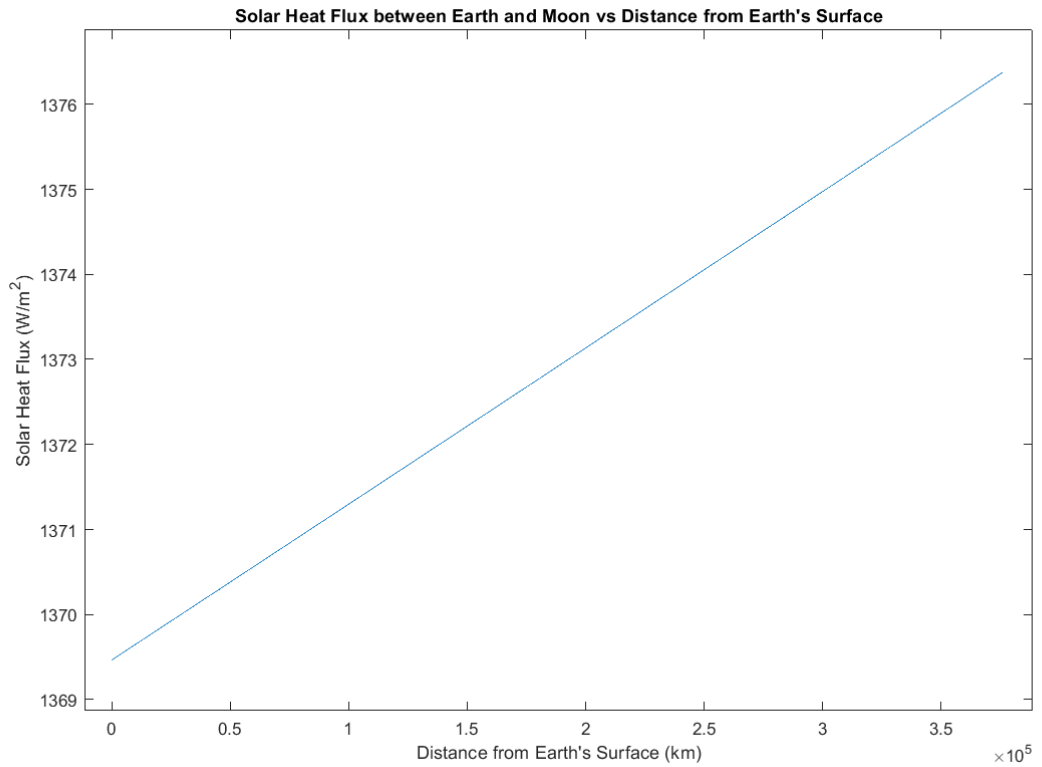


Figure 55: Solar Heat Flux between Earth and Moon vs Distance from Earth's Surface

Incident Heat Flux due to Earth's Albedo vs Distance from Earth's Surface

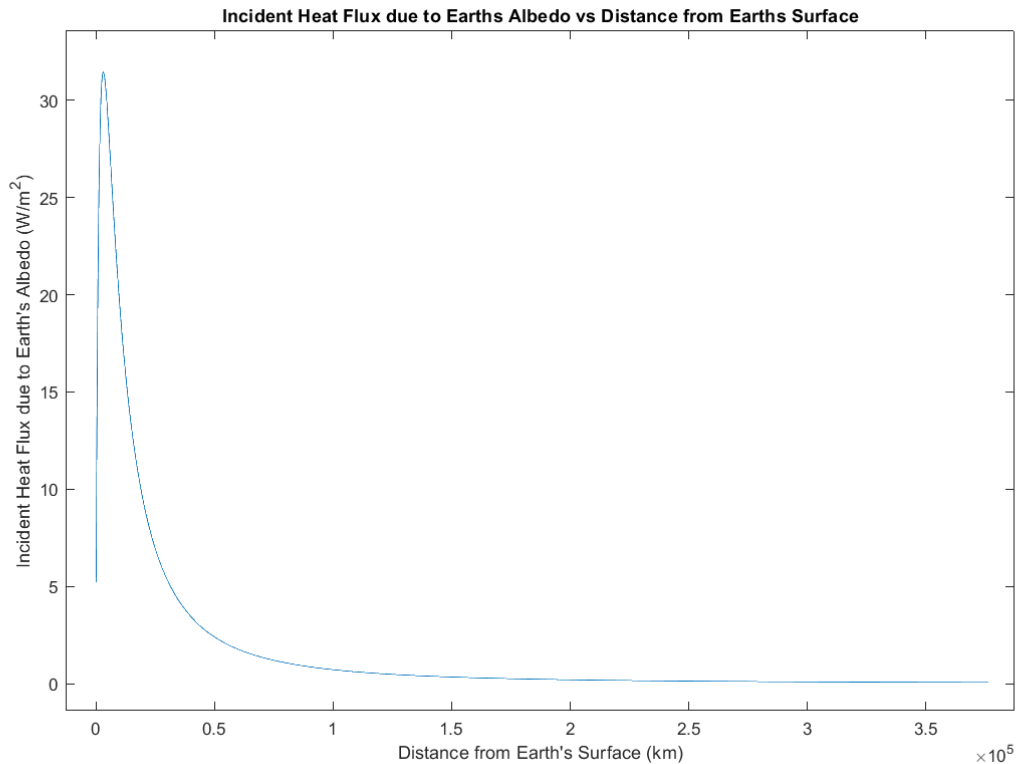


Figure 56: Incident Heat Flux due to Earth's Albedo vs Distance from Earth's Surface

It is interesting to note here that, as the spacecraft moves away from Earth, the heat flux due to Earth's Albedo first increases and then decreases. This is because there are two variable factors that are changing.

Firstly, it is the area of the Earth that is in the view of the spacecraft. In the simplified illustration of this, shown below in figure 57, it can be seen that compared to an altitude closer to Earth (Red), the area of the Earth visible at a higher altitude (Blue) is larger. Therefore, there is a larger surface that the reflected light can reach the spacecraft from, as the spacecraft moves further away from Earth. Secondly, as the spacecraft moves further away from the Earth, the intensity of the heat flux reduces by the square of the distance from Earth. As seen in the graph above, in the beginning, the increase in surface area dominates the direction

of the heat flux curve, but after a certain point, the effect of reducing heat flux due to distance takes dominance. This effect also takes place as the spacecraft approaches the target body.

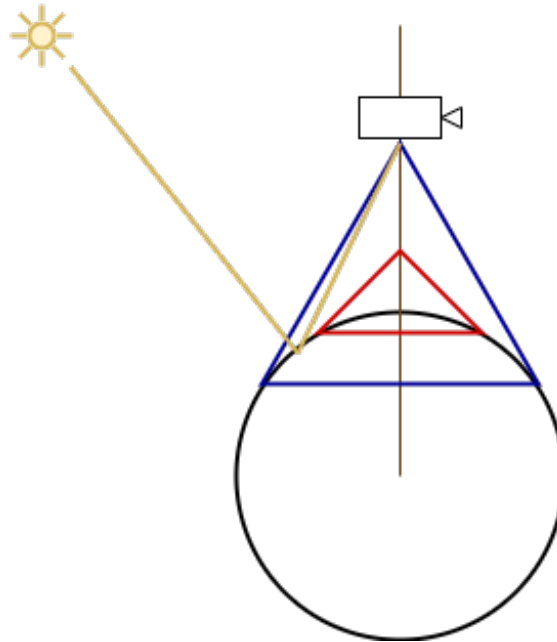


Figure 57: Change in Incident Heat Flux due to Earth's Albedo

Incident Heat Flux due to Earth's IR Radiation vs Distance from Earth's Surface

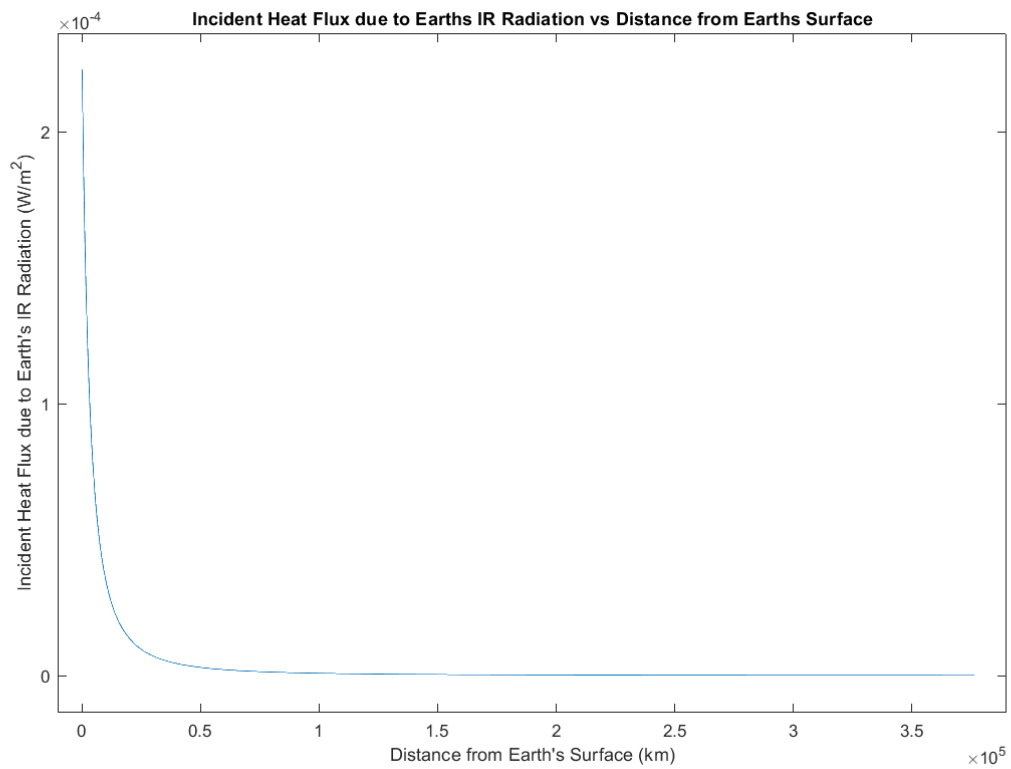


Figure 58: Incident Heat Flux due to Earth's IR Radiation vs Distance from Earth's Surface

Incident Heat Flux due to the Moon's Albedo vs Distance from Earth's Surface

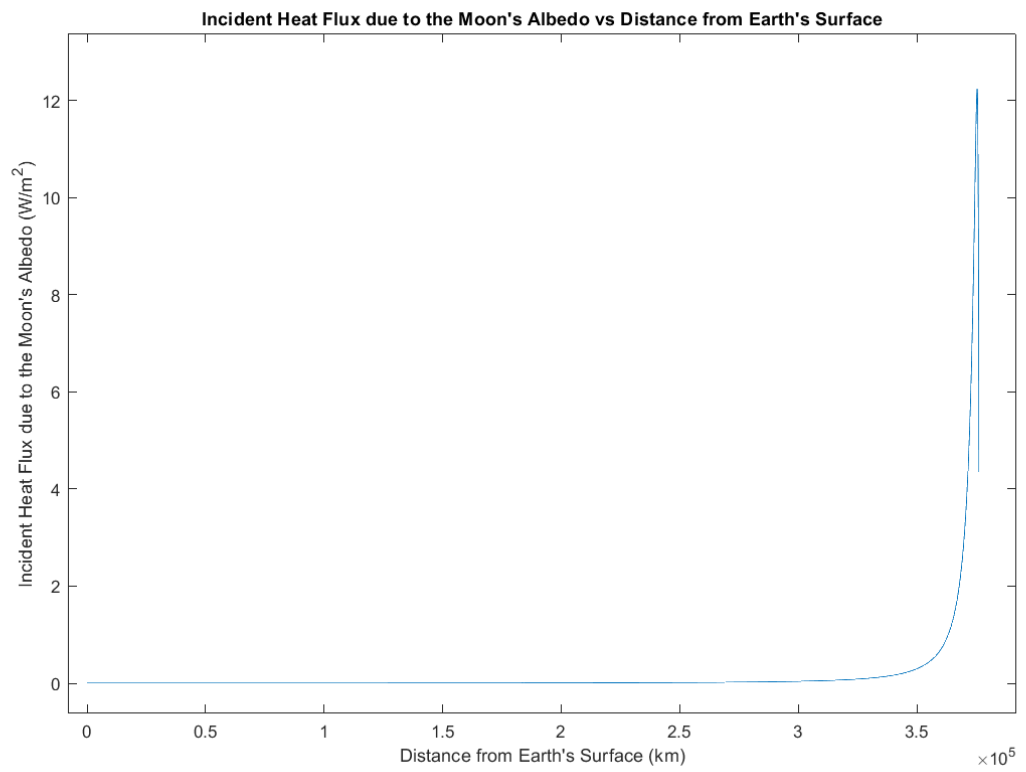


Figure 59: Incident Heat Flux due to the Moon's Albedo vs Distance from Earth's Surface

Incident Heat Flux due to the Moon's IR Radiation vs Distance from Earth's Surface

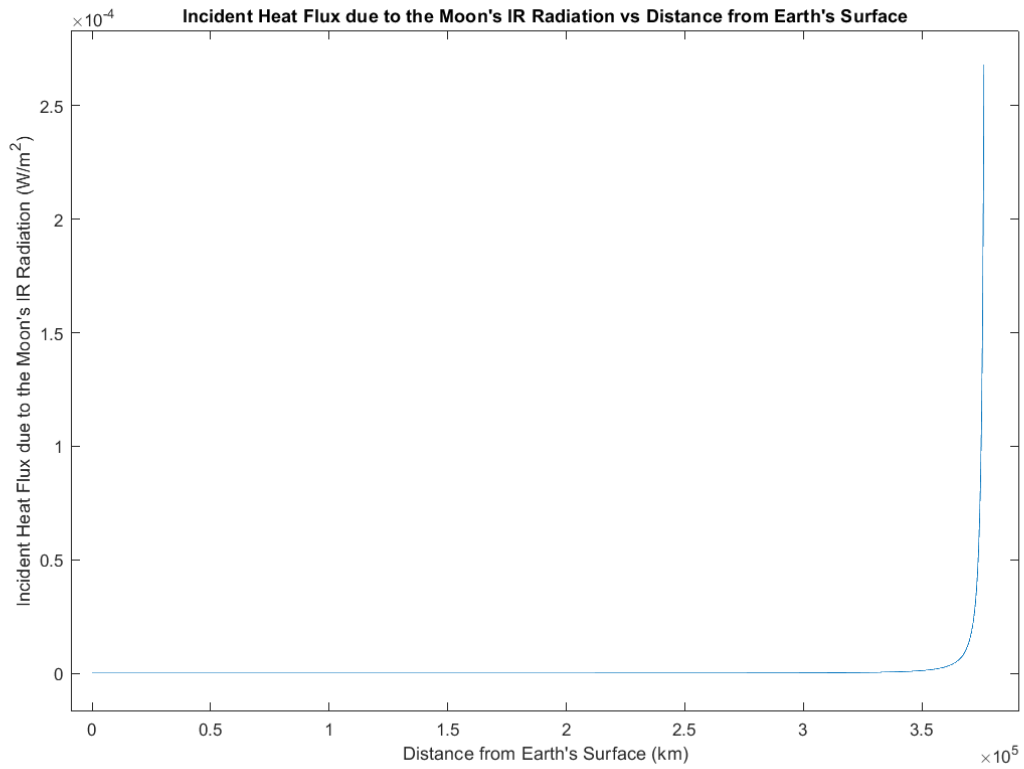


Figure 60: Incident Heat Flux due to the Moon's IR Radiation vs Distance from Earth's Surface

Net Heat Flux across the Journey vs Distance from Earth's Surface

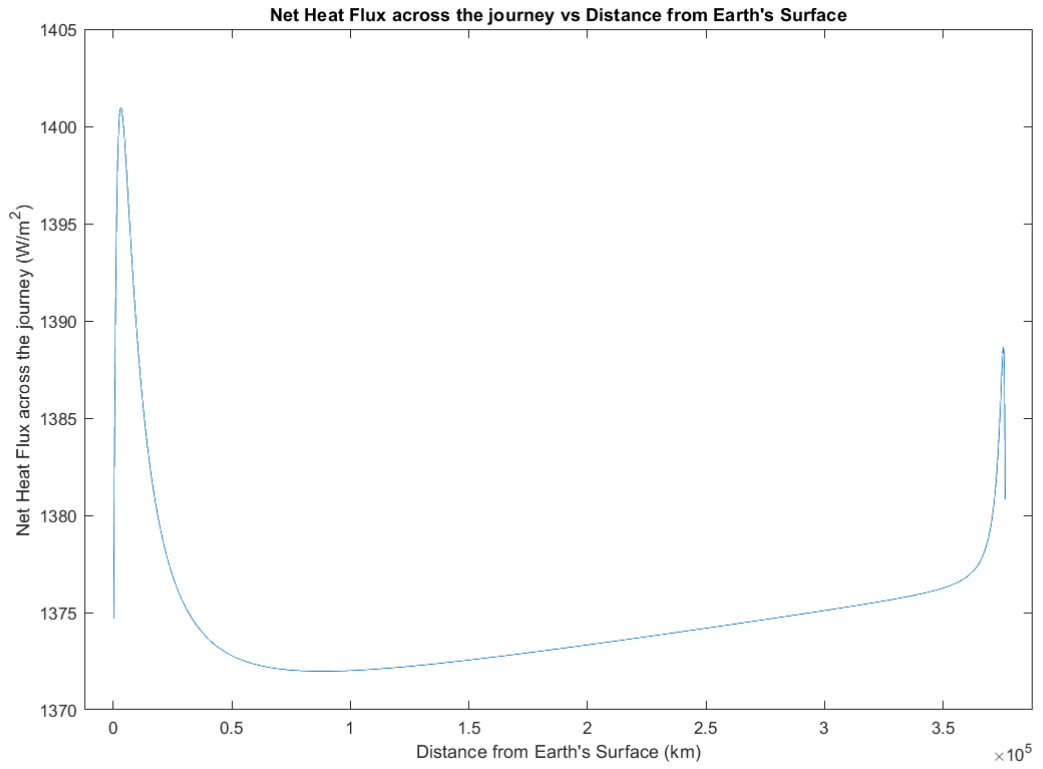


Figure 61: Net Heat Flux across the Journey vs Distance from Earth's Surface

Hydrolox Engine

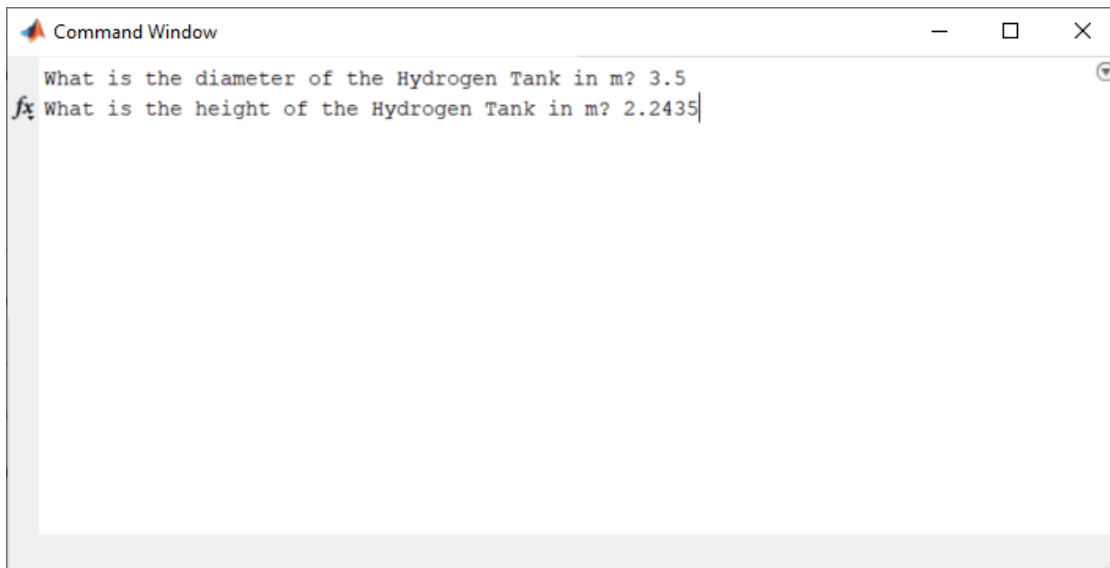


Figure 62: Input of the Tank Size for Hydrolox Engine for Moon Mission

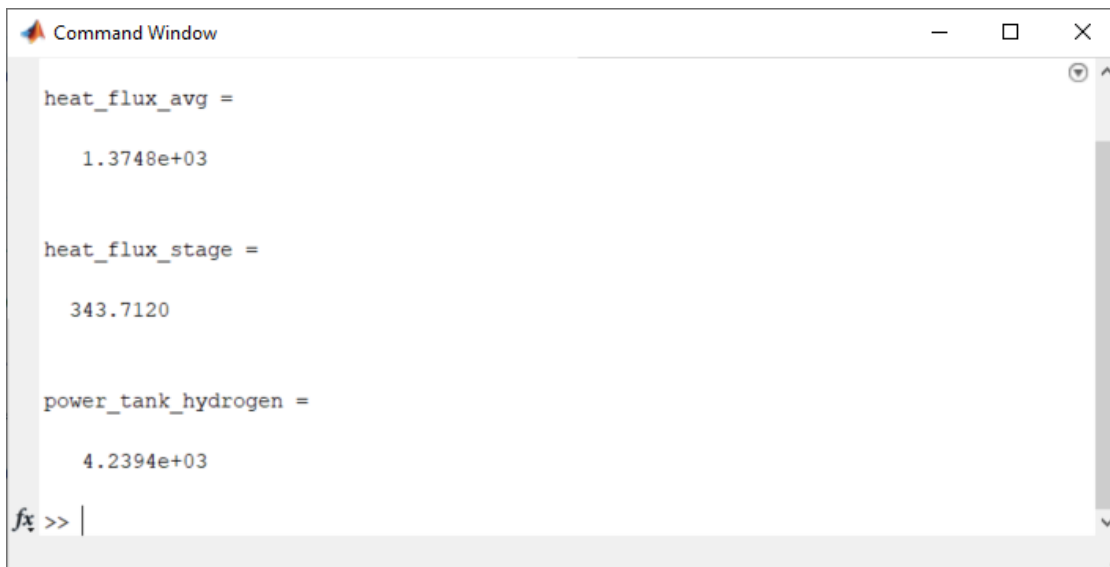


Figure 63: Output of the Heat Flux and Power for Hydrolox Engine for Moon Mission

Methalox Engine

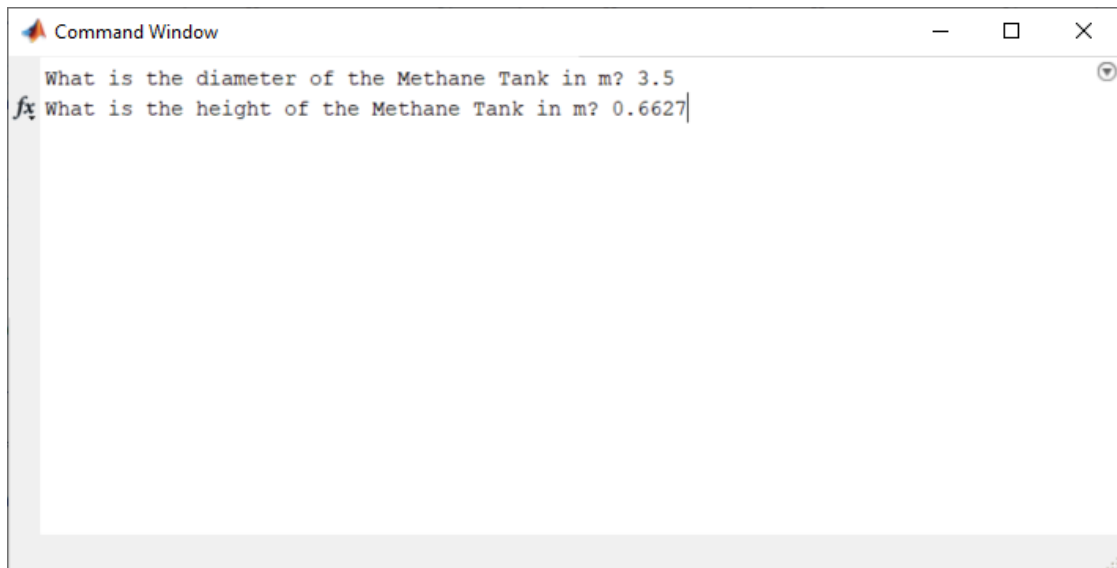


Figure 64: Input of the Tank Size for Methalox Engine for Moon Mission

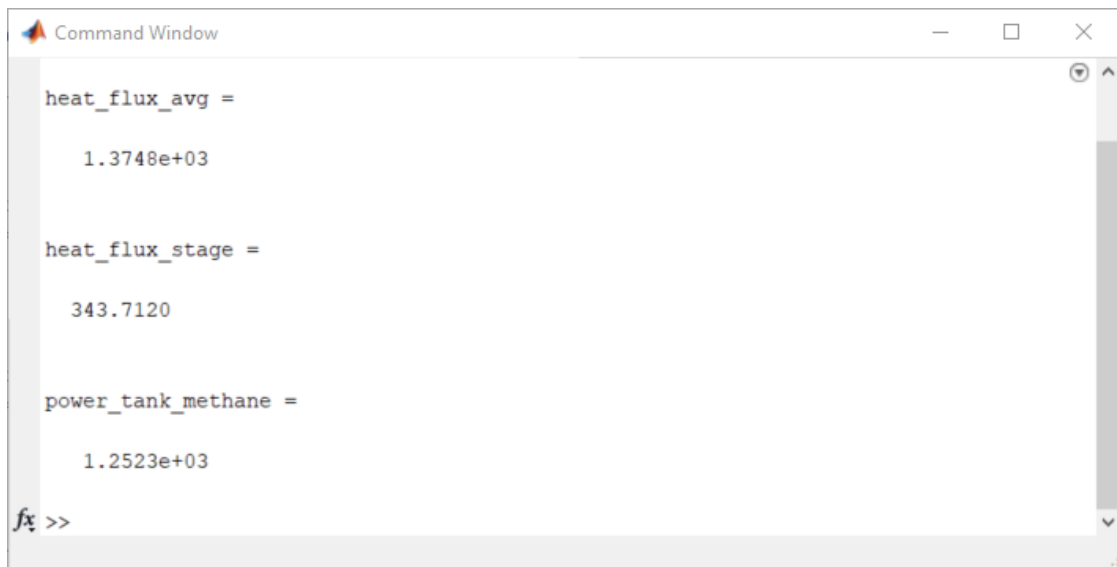


Figure 65: Output of the Heat Flux and Power for Methalox Engine for Moon Mission

10.3.1.3 For Mars mission

From 500 km Low Earth Orbit to 250 km Mars Orbit as described in chapter 5.

Solar Heat Flux between Earth and Mars vs Distance from Earth's Surface

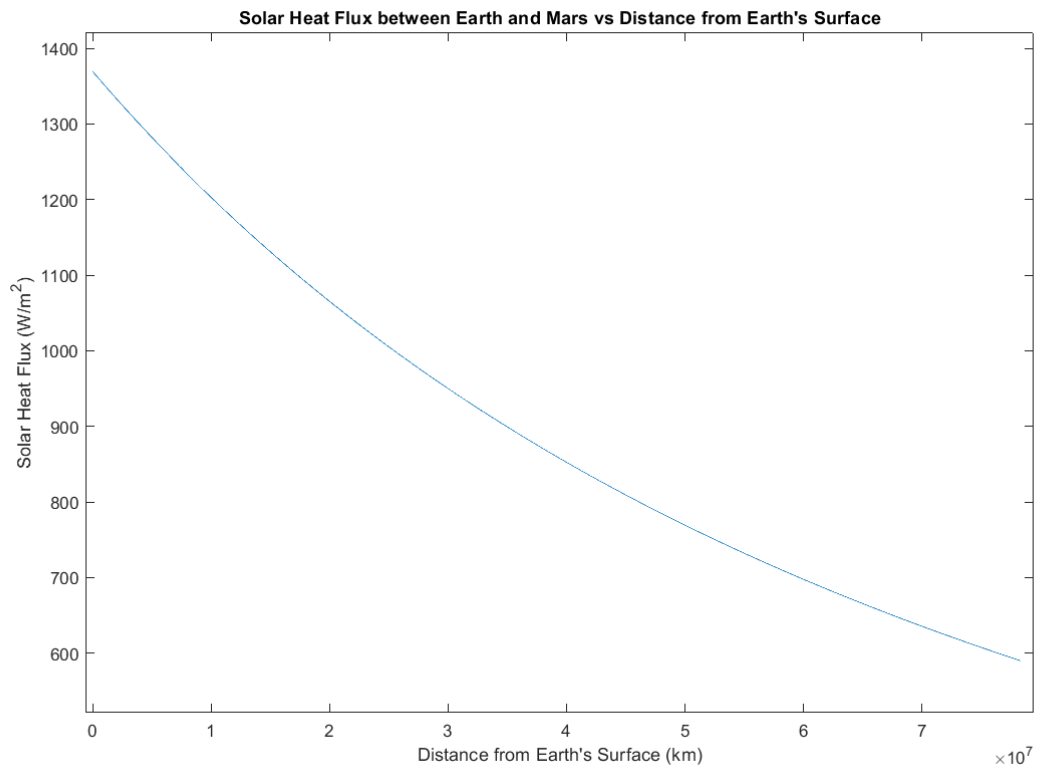


Figure 66: Solar Heat Flux between Earth and Mars vs Distance from Earth's Surface

Incident Heat Flux due to Earth's Albedo vs Distance from Earth's Surface

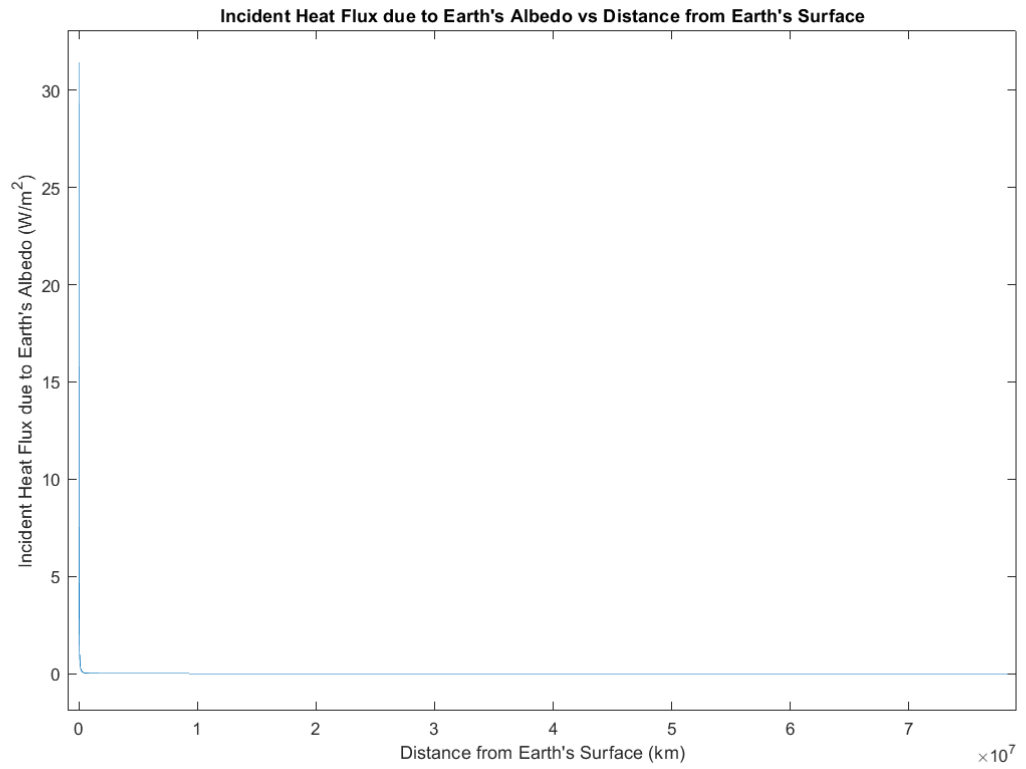


Figure 67: Incident Heat Flux due to Earth's Albedo vs Distance from Earth's Surface

Incident Heat Flux due to Earth's IR Radiation vs Distance from Earth's Surface

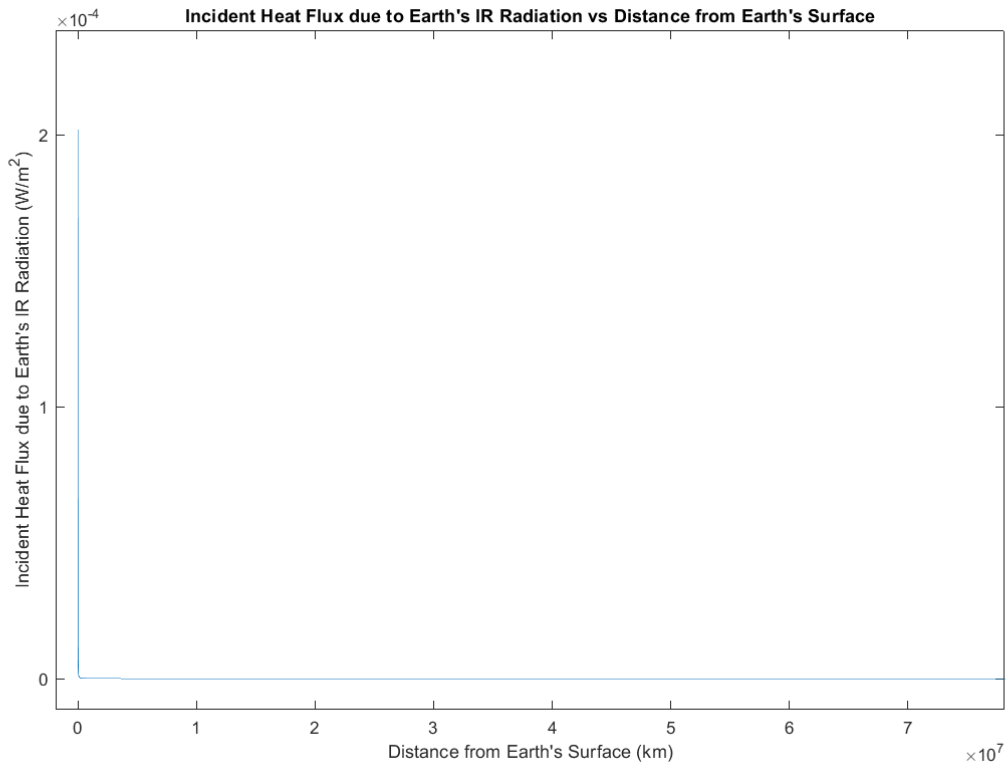


Figure 68: Incident Heat Flux due to Earth's IR Radiation vs Distance from Earth's Surface

Incident Heat Flux due to Mars' Albedo vs Distance from Earth's Surface

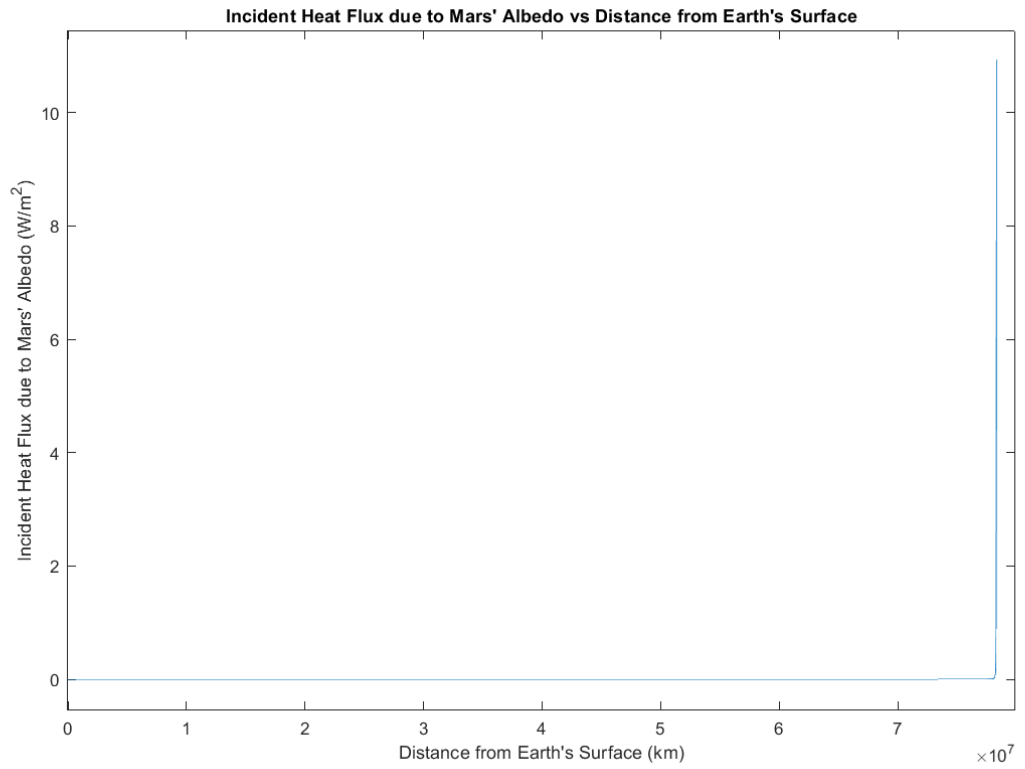


Figure 69: Incident Heat Flux due to Mars' Albedo vs Distance from Earth's Surface

Incident Heat Flux due to Mars' IR Radiation vs Distance from Earth's Surface

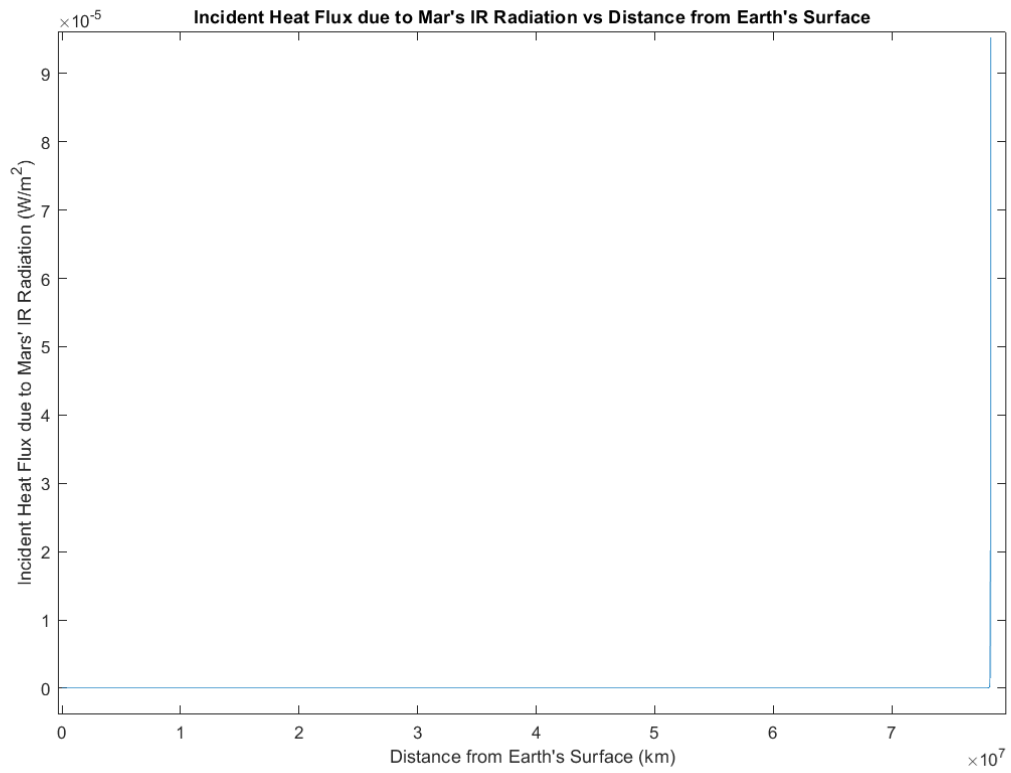


Figure 70: Incident Heat Flux due to Mars' IR Radiation vs Distance from Earth's Surface

Net Heat Flux across the Journey vs Distance from Earth's Surface

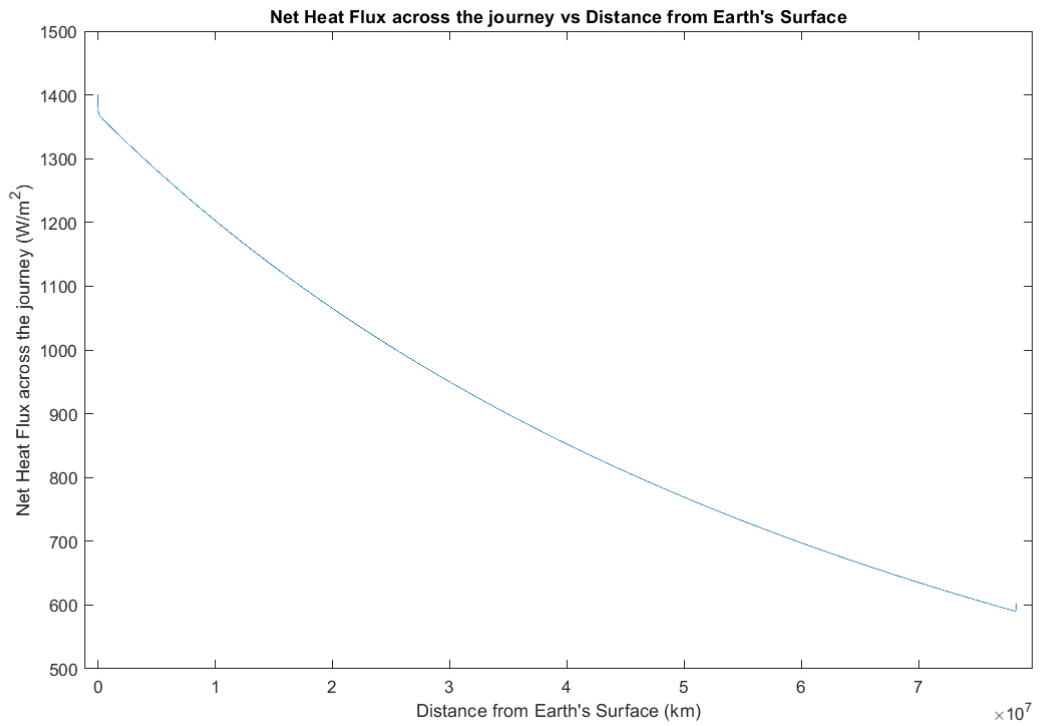


Figure 71: Net Heat Flux across the Journey vs Distance from Earth's Surface

Hydrolox Engine

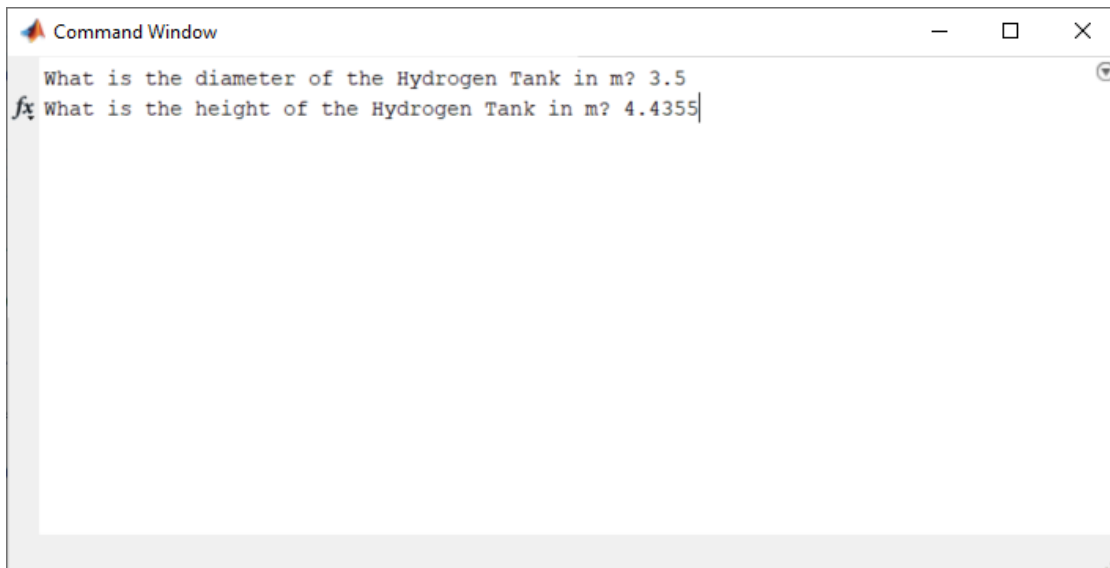


Figure 72: Input of the Tank Size for Hydrolox Engine for Mars Mission

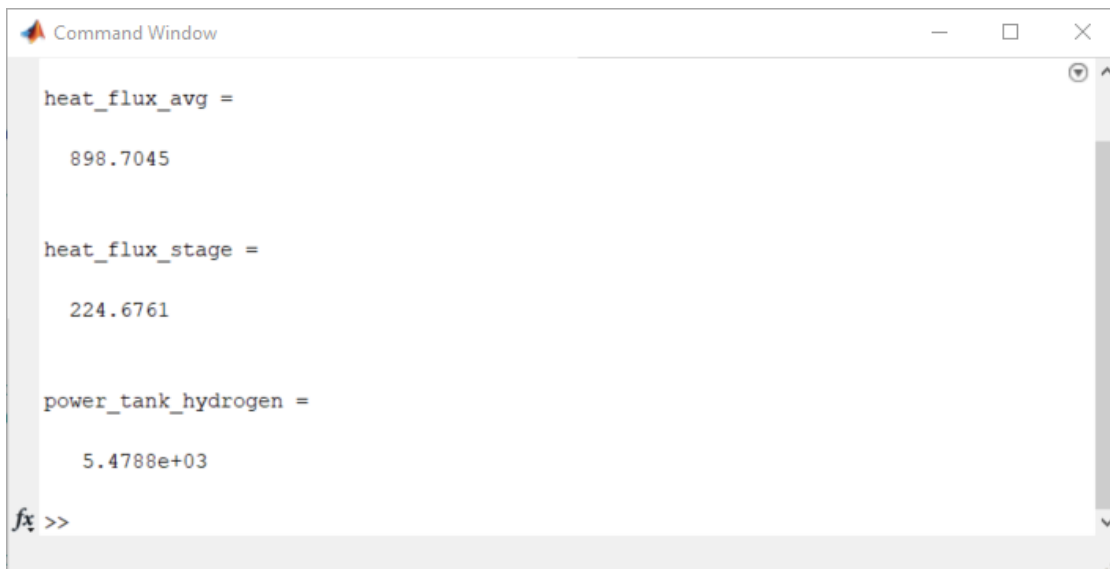


Figure 73: Output of the Heat Flux and Power for Hydrolox Engine for Mars Mission

Methalox Engine

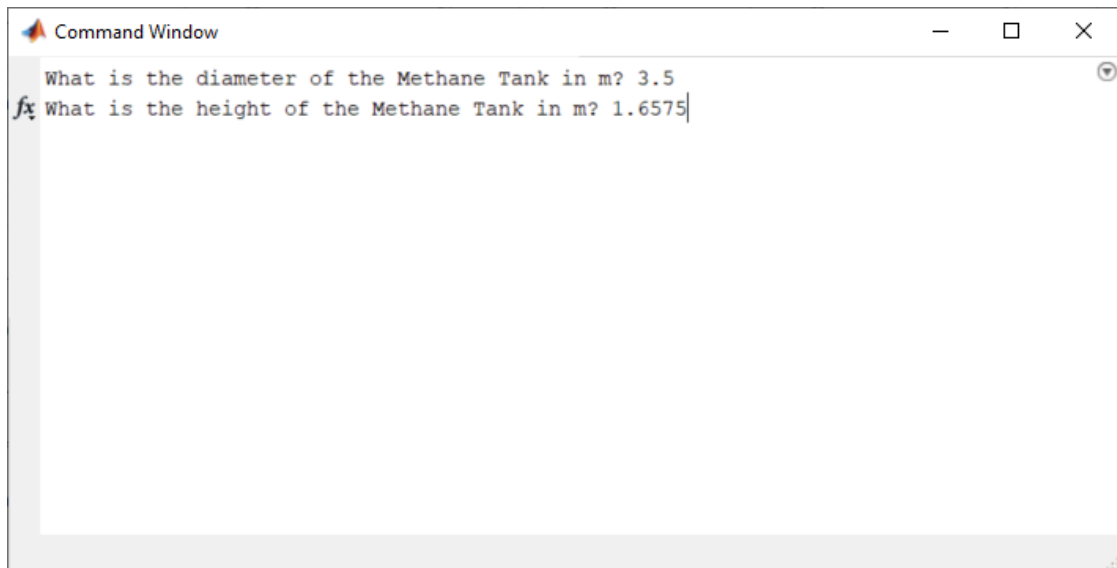


Figure 74: Input of the Tank Size for Methalox Engine for Mars Mission

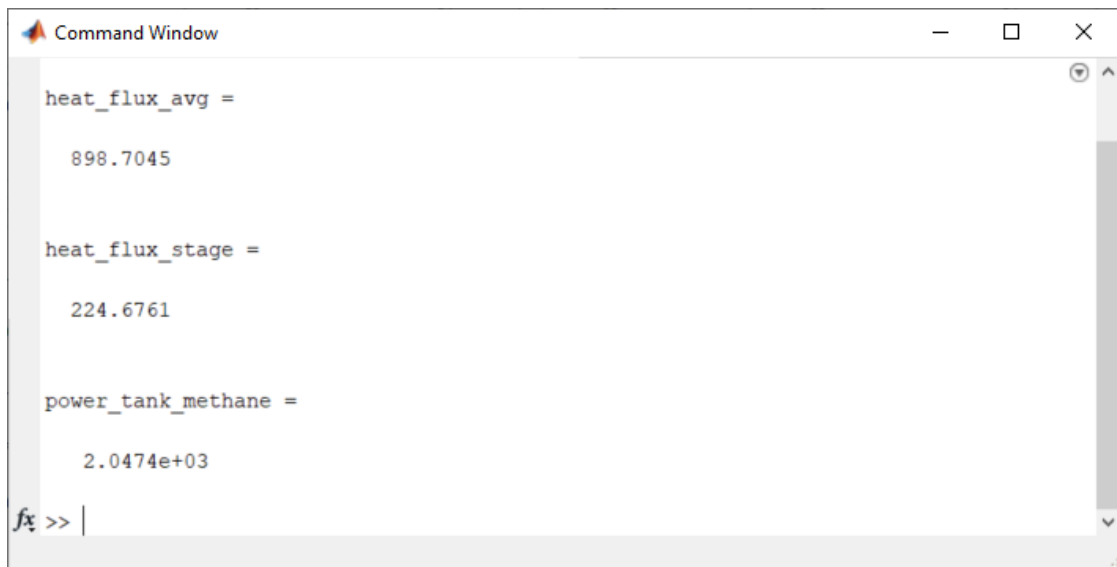


Figure 75: Output of the Heat Flux and Power for Methalox Engine for Mars Mission

10.3.2. Boil Off calculation using BoilFAST

Using this tool, the boil off of the cryogenic fuels during their coasting phase towards the target body can be obtained. To really observe the boil off behaviour more properly, one assumption has been made for this section. The fuel tank will be considered as full during the coasting phase. In reality, during this segment of the mission, there would be much less propellant due to it being consumed during the transfer burn. However, having a full tank gives us more room to observe and understand the boil off behaviour, and therefore, a good indicator of reality.

10.3.2.1 For Liquid Hydrogen Tank for Moon Mission

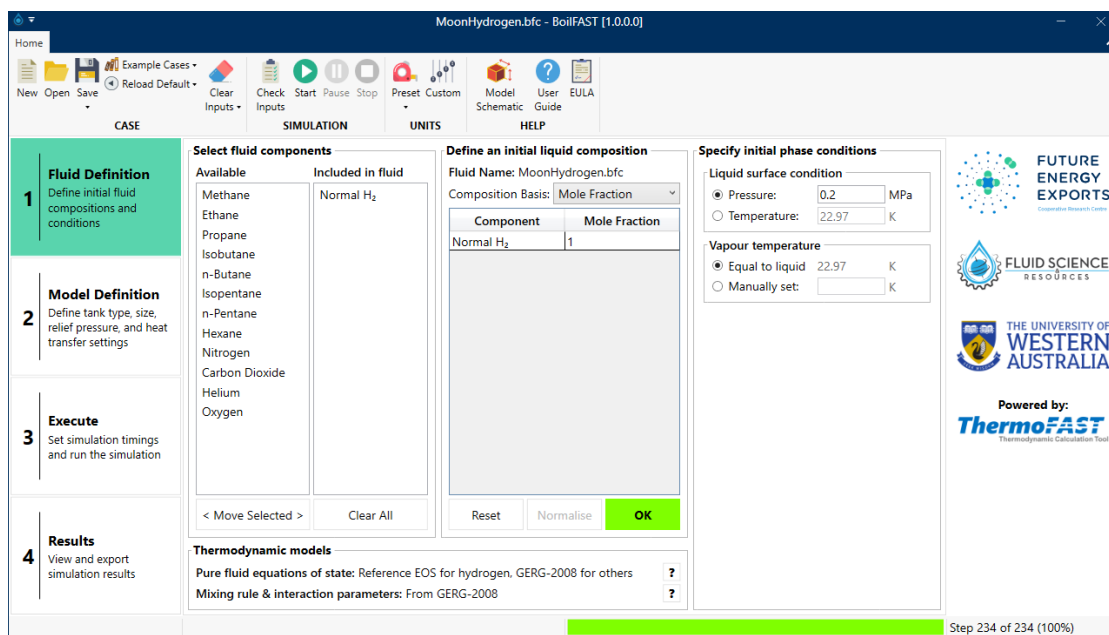


Figure 76: First Input page for BoilFAST for LH₂ Tank for Moon Mission

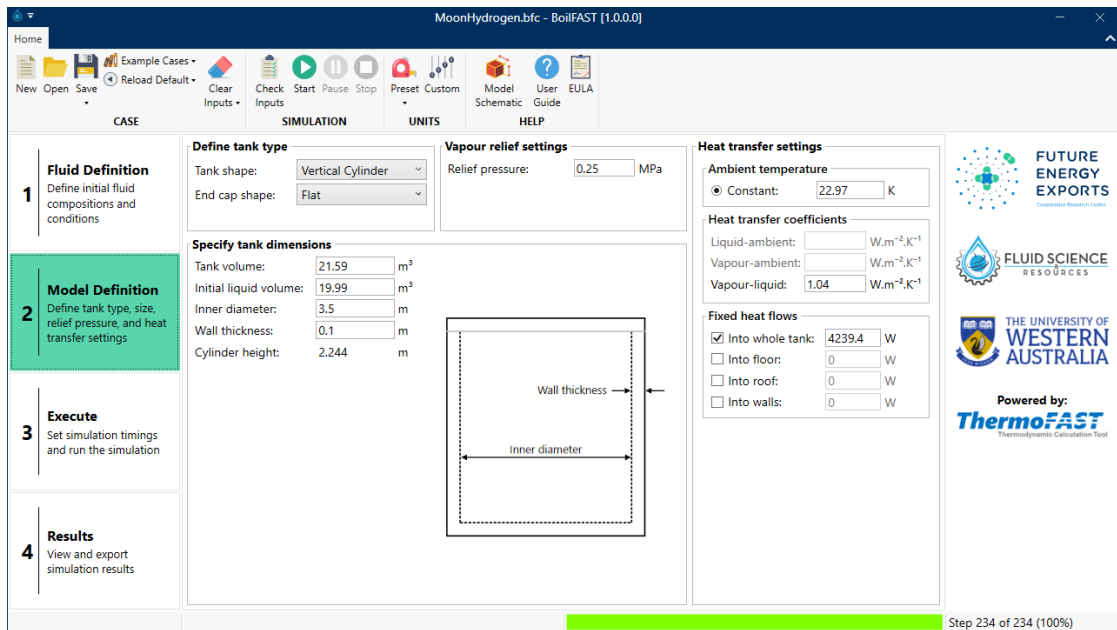


Figure 77: Second Input page for BoilFAST for LH₂ Tank for Moon Mission

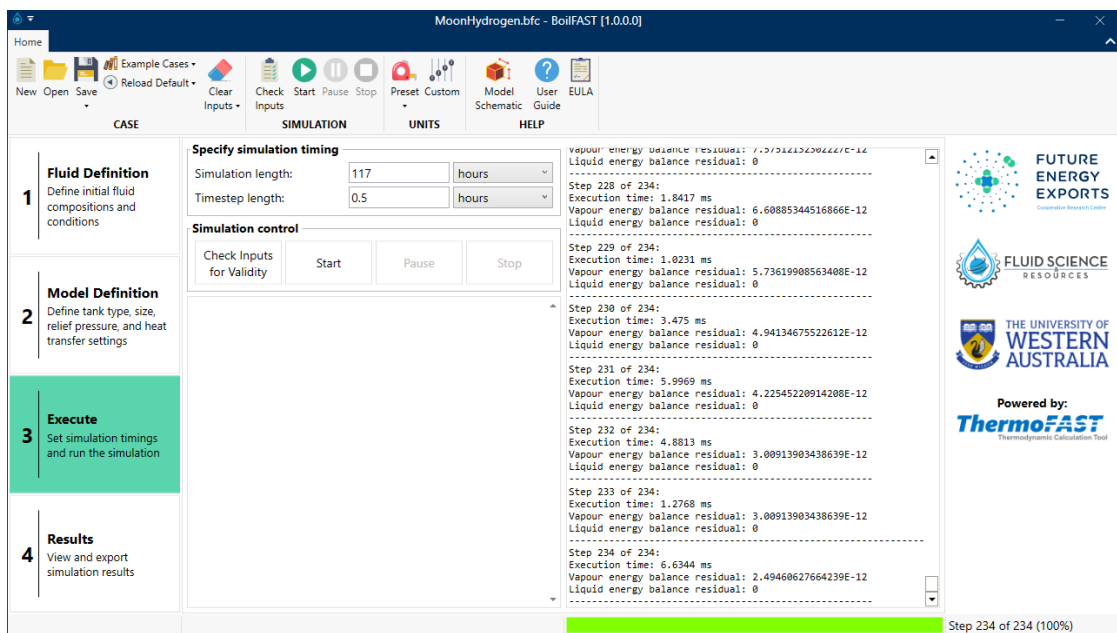


Figure 78: Third Input page for BoilFAST for LH₂ Tank for Moon Mission

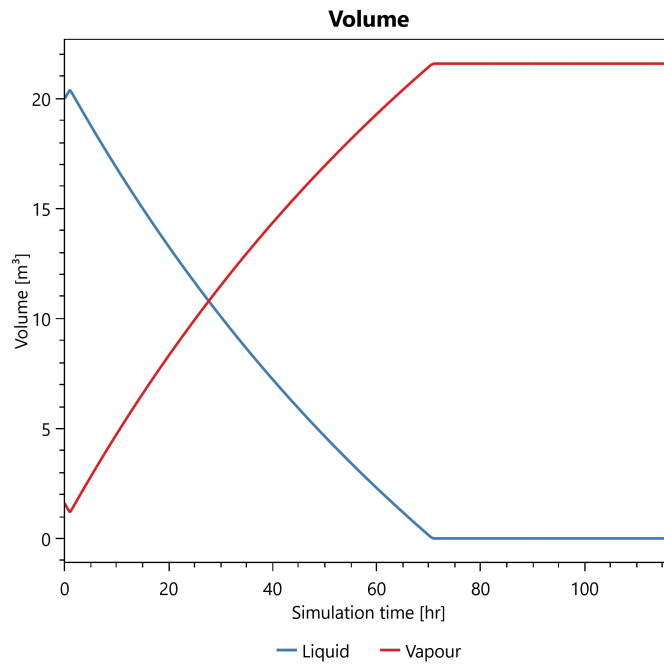


Figure 79: Volume of Fuel vs Time for LH₂ Tank for Moon Mission

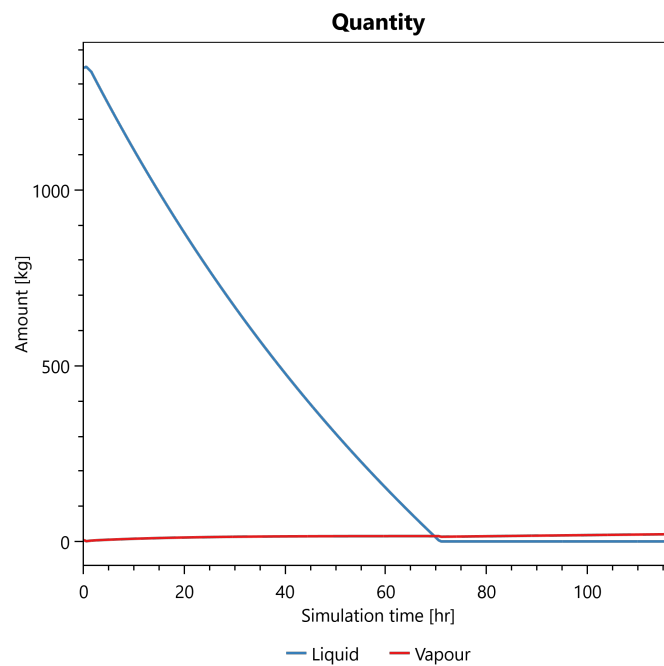


Figure 80: Quantity of Fuel vs Time for LH₂ Tank for Moon Mission

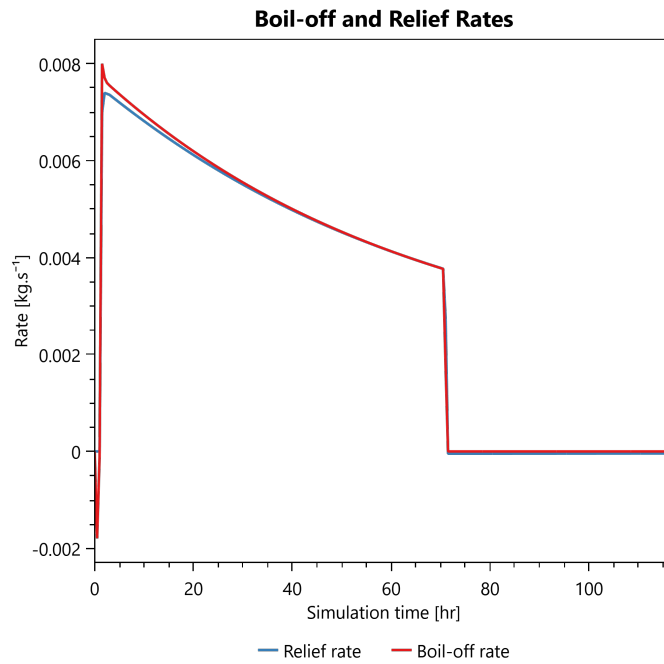


Figure 81: Boil Off Rates of Fuel vs Time for LH₂ Tank for Moon Mission

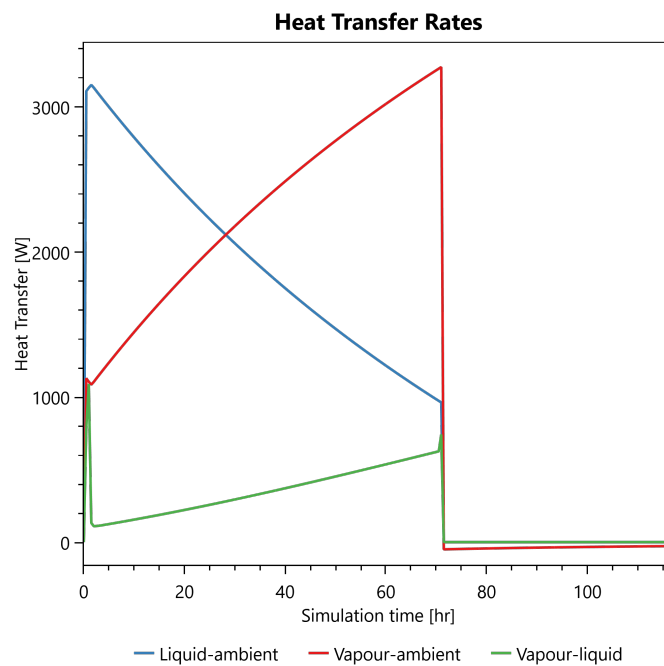


Figure 82: Heat Transfer Rates of Fuel vs Time for LH₂ Tank for Moon Mission

10.3.2.2 For Liquid Methane Tank for Moon Mission

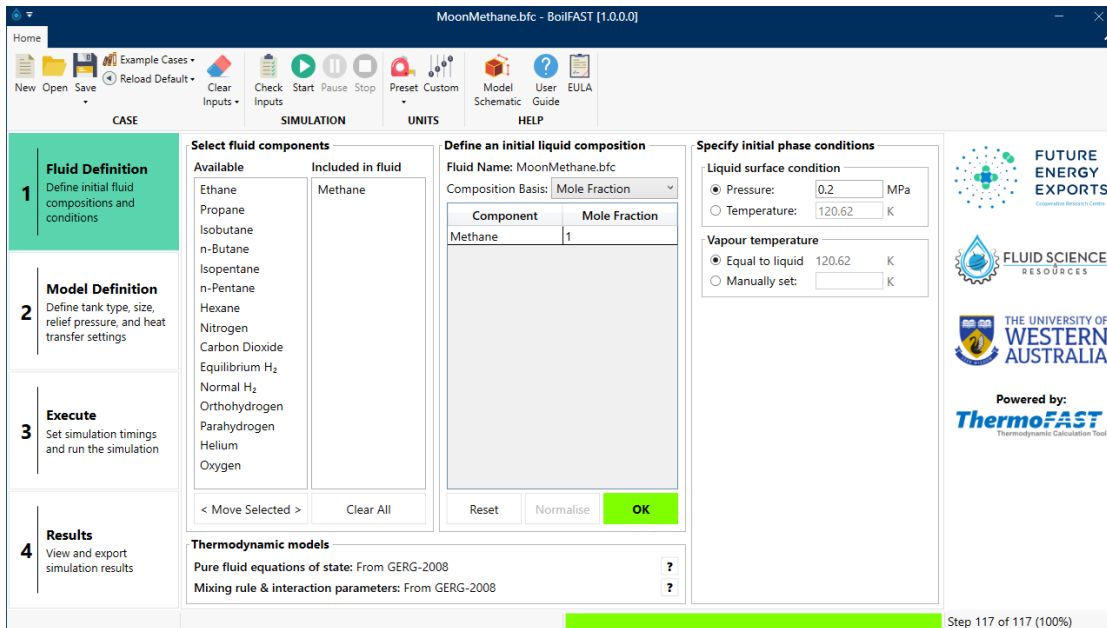


Figure 83: First Input page for BoilFAST for LCH₄ Tank for Moon Mission

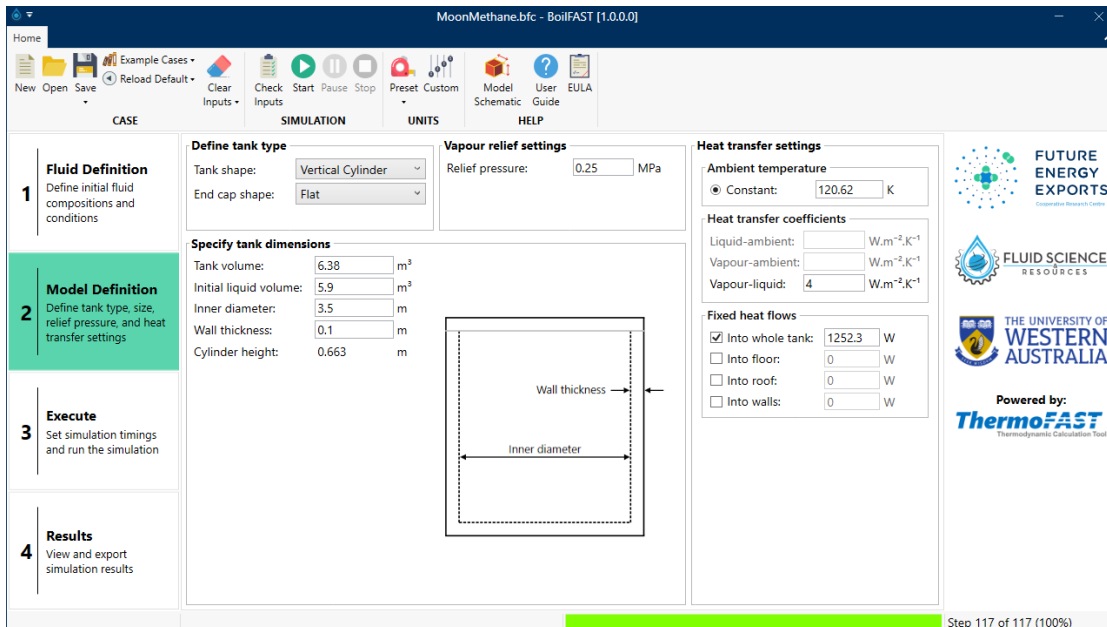


Figure 84: Second Input page for BoilFAST for LCH₄ Tank for Moon Mission

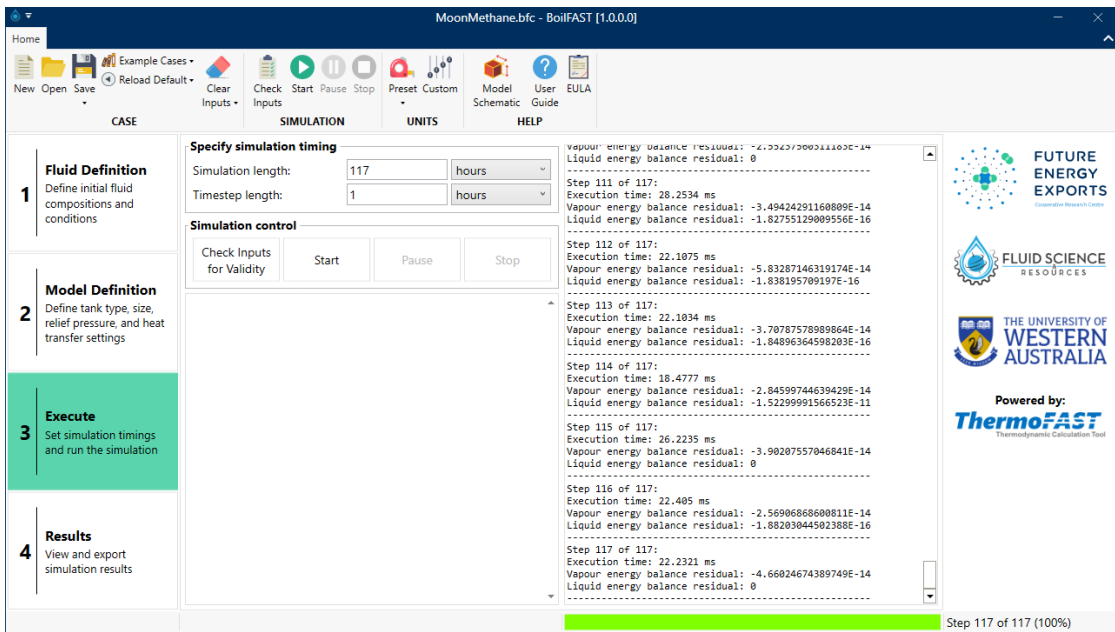


Figure 85: Third Input page for BoilFAST for LCH₄ Tank for Moon Mission

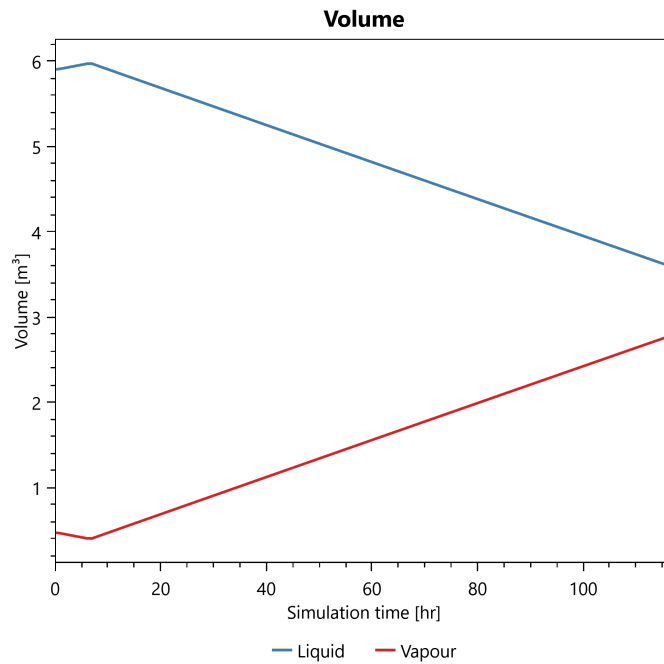


Figure 86: Volume of Fuel vs Time for LCH₄ Tank for Moon Mission

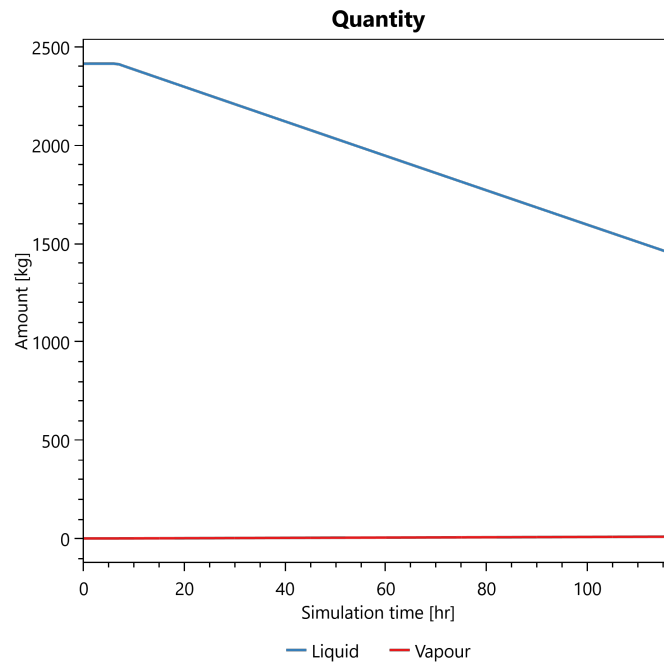


Figure 87: Quantity of Fuel vs Time for LCH₄ Tank for Moon Mission

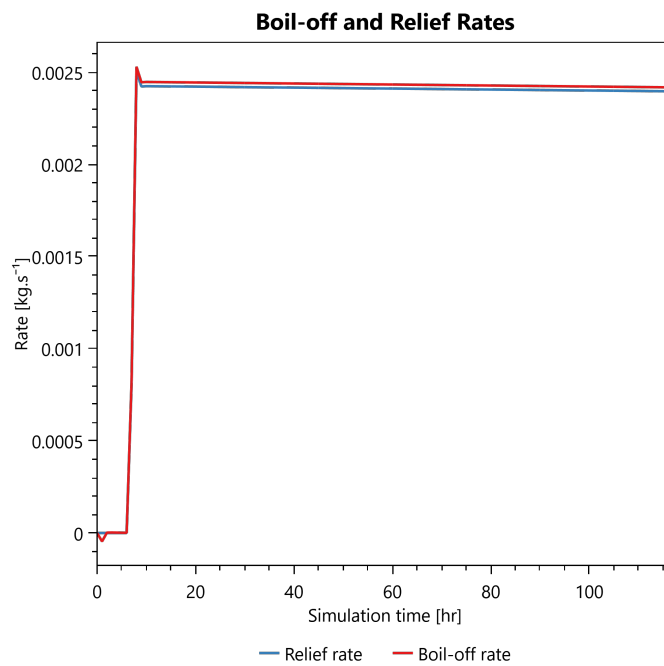


Figure 88: Boil Off Rates of Fuel vs Time for LCH₄ Tank for Moon Mission

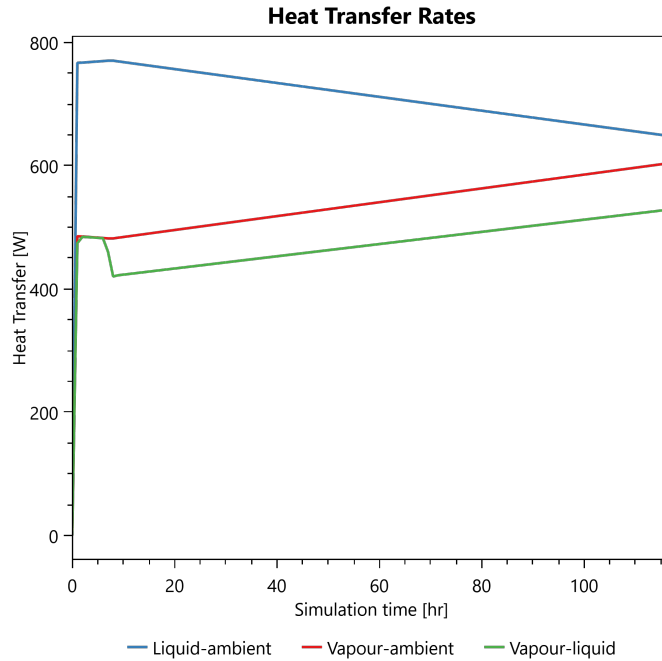


Figure 89: Heat Transfer Rates of Fuel vs Time for LCH₄ Tank for Moon Mission

10.3.2.3 For Liquid Hydrogen Tank for Mars Mission

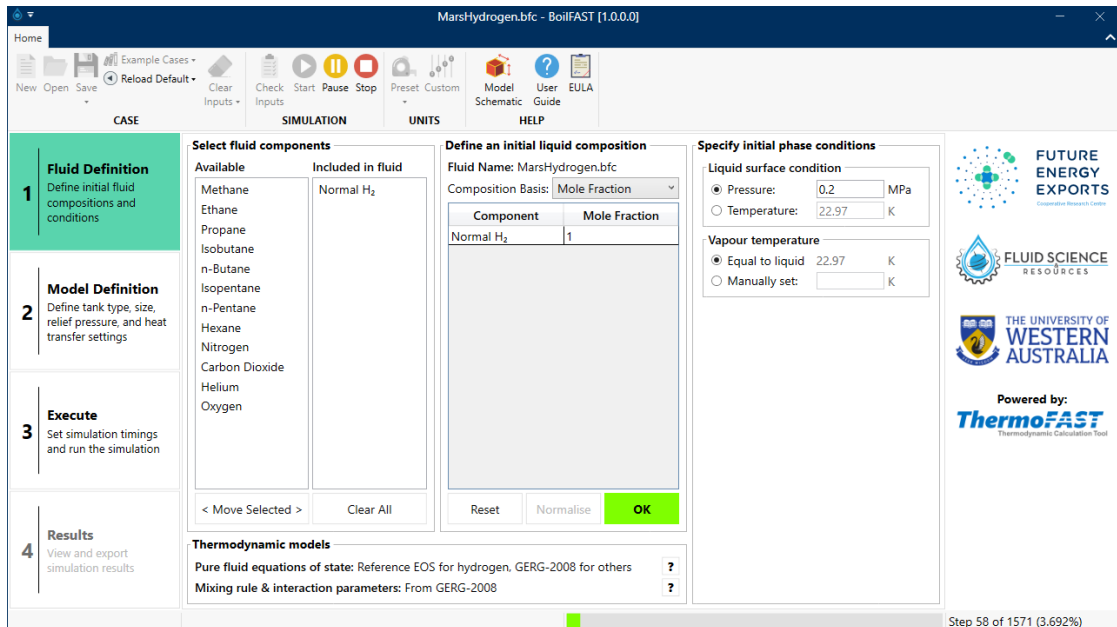


Figure 90: First Input page for BoilFAST for LH₂ Tank for Mars Mission

Chapter 10 Boil Off Behaviour

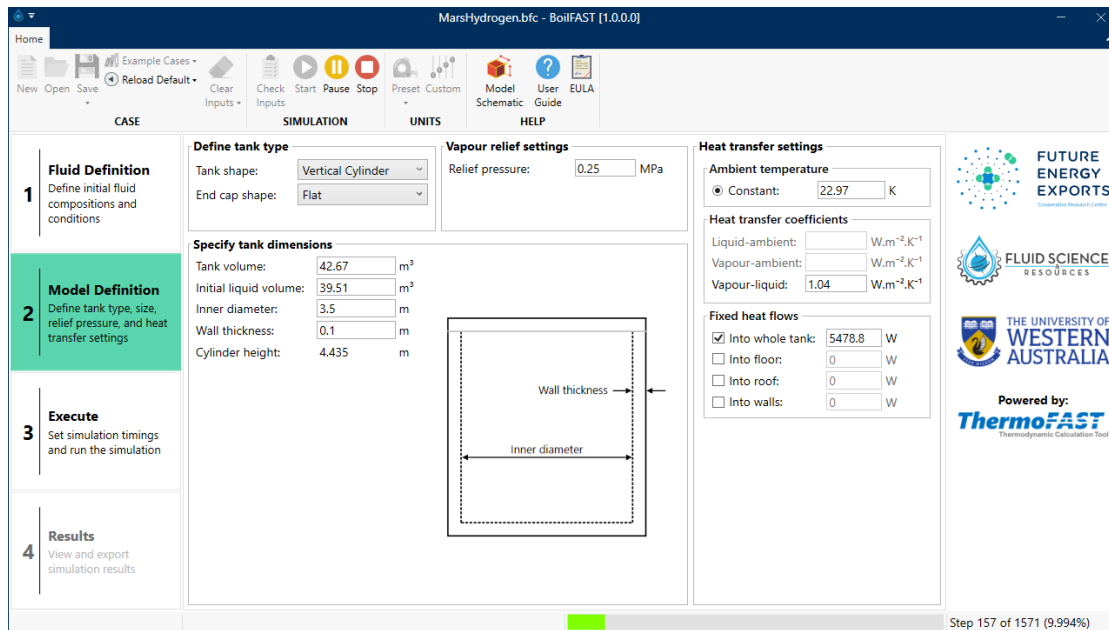


Figure 91: Second Input page for BoilFAST for LH₂ Tank for Mars Mission

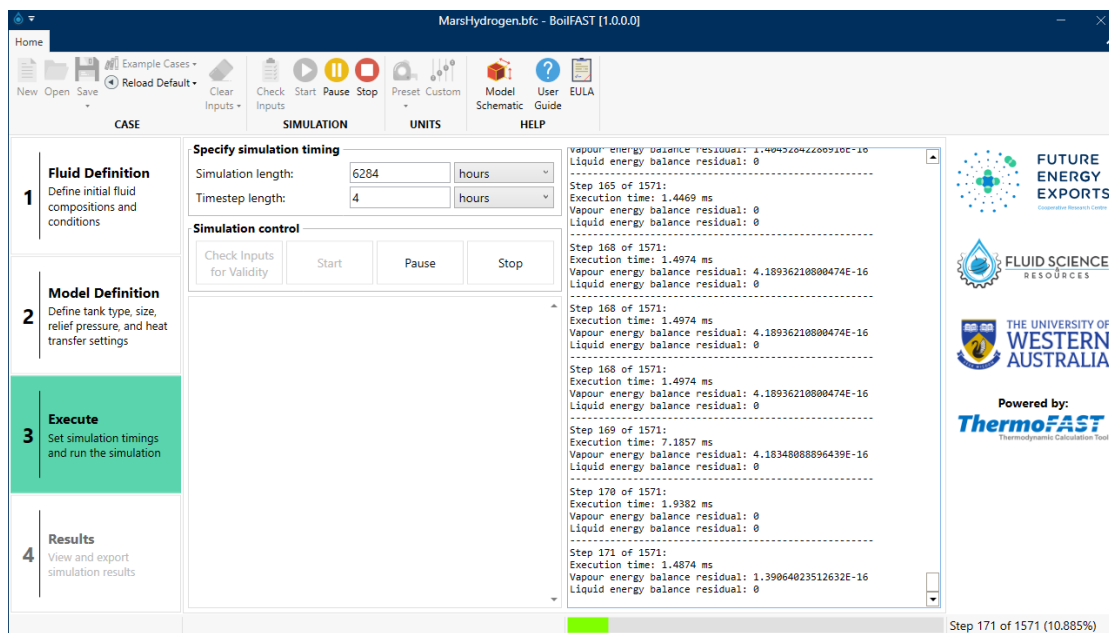


Figure 92: Third Input page for BoilFAST for LH₂ Tank for Mars Mission

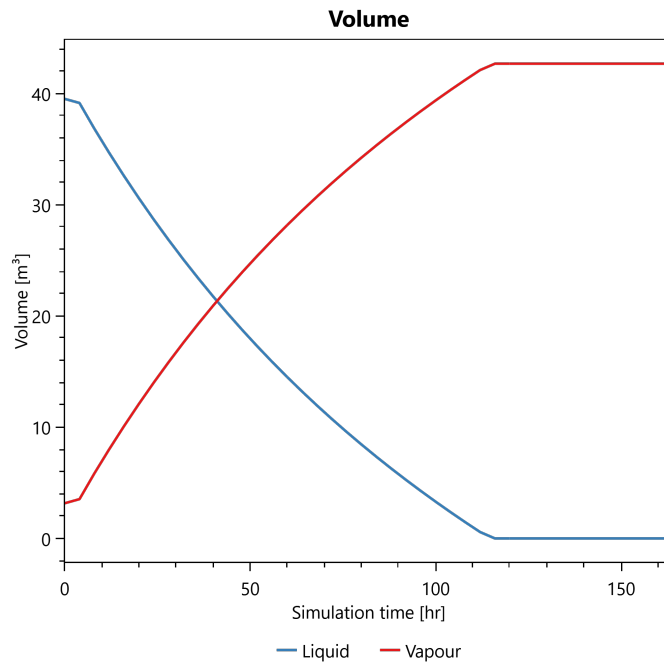


Figure 93: Volume of Fuel vs Time for LH₂ Tank for Mars Mission

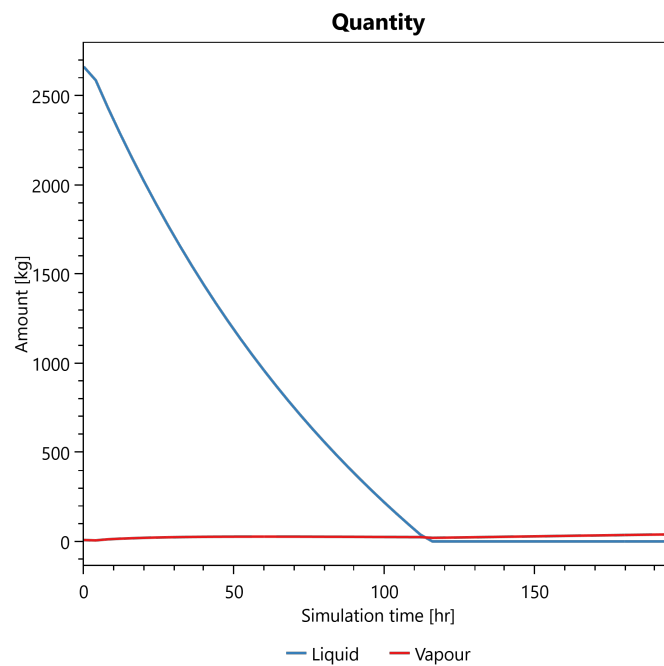


Figure 94: Quantity of Fuel vs Time for LH₂ Tank for Mars Mission

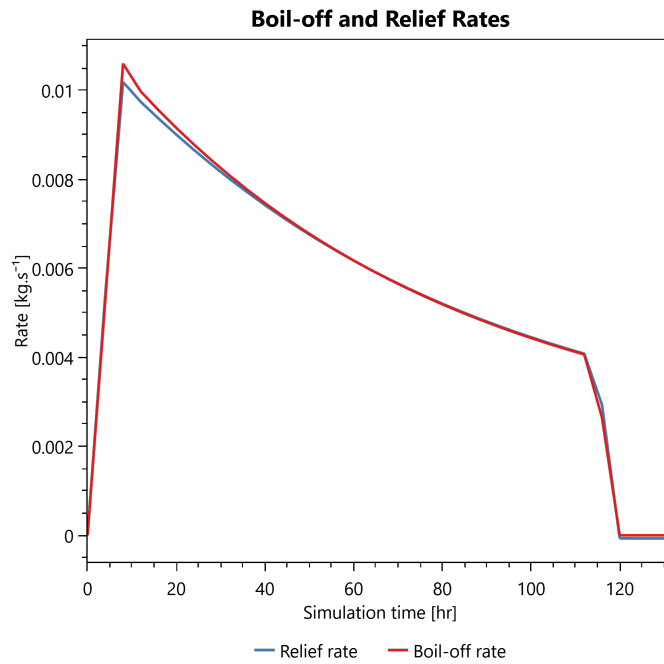


Figure 95: Boil Off Rates of Fuel vs Time for LH₂ Tank for Mars Mission

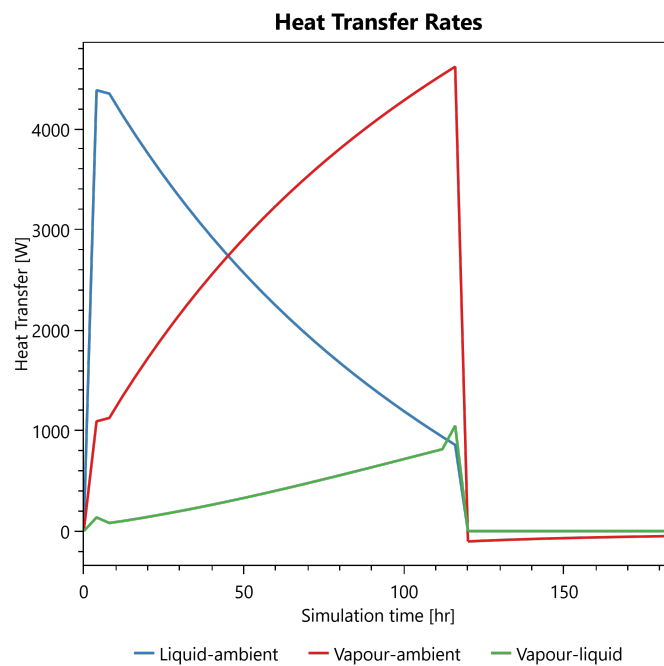


Figure 96: Heat Transfer Rates of Fuel vs Time for LH₂ Tank for Mars Mission

10.3.2.4 For Liquid Methane Tank for Mars Mission

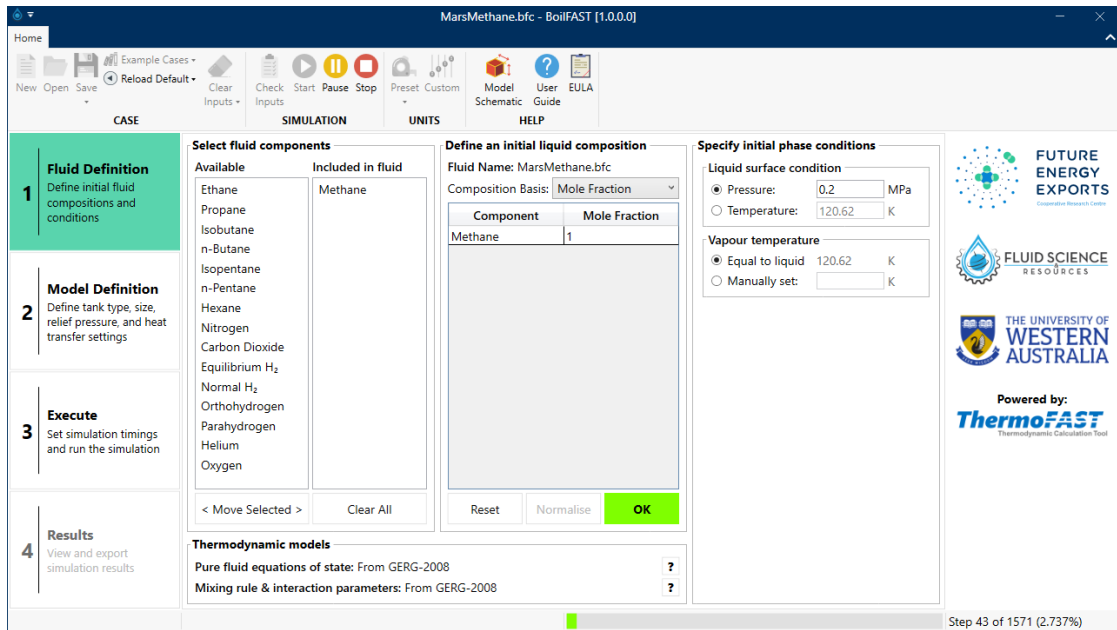


Figure 97: First Input page for BoilFAST for LCH₄ Tank for Mars Mission

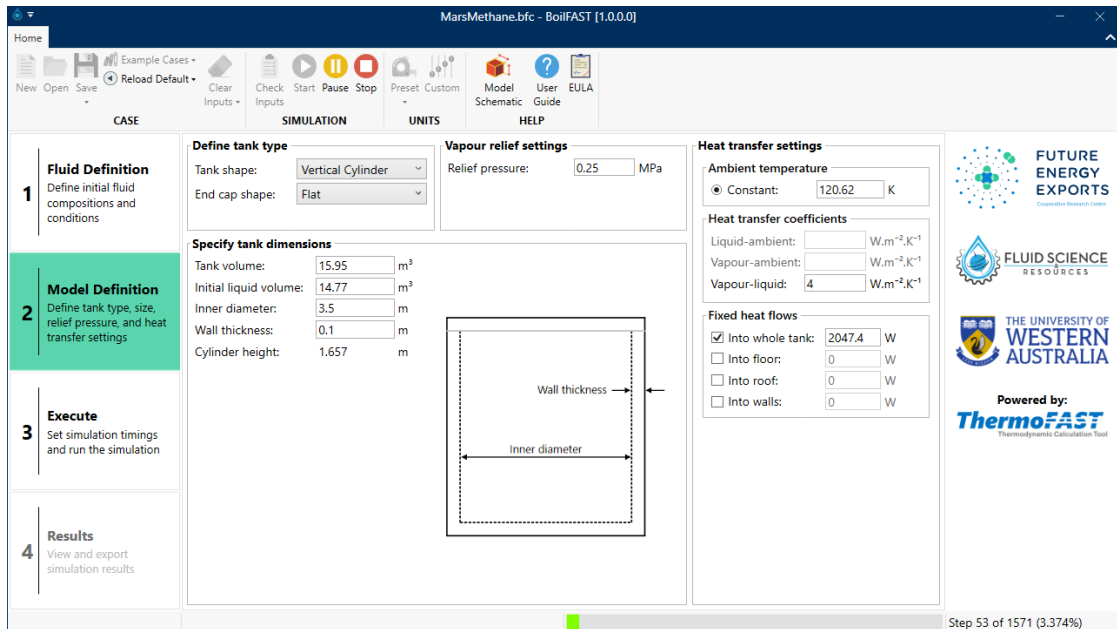


Figure 98: Second Input page for BoilFAST for LCH₄ Tank for Mars Mission

Chapter 10 Boil Off Behaviour

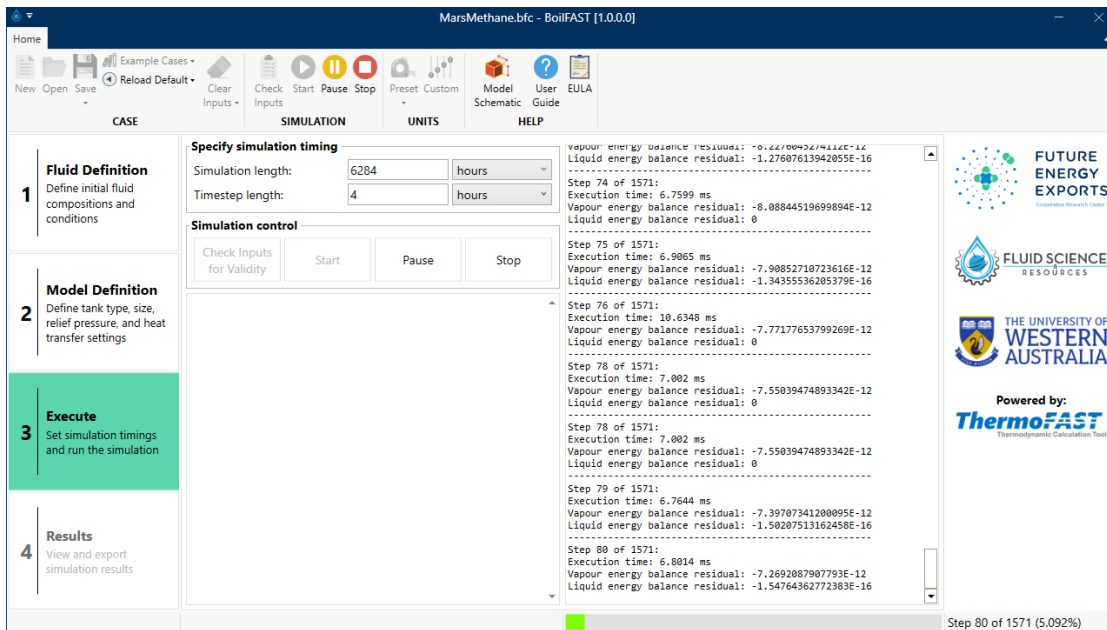


Figure 99: Third Input page for BoilFAST for LCH₄ Tank for Mars Mission

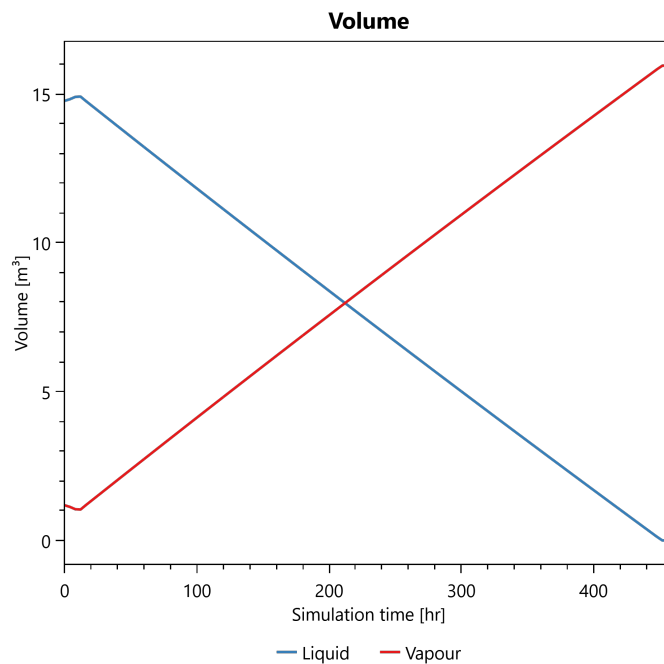


Figure 100: Volume of Fuel vs for LCH₄ Tank for Mars Mission

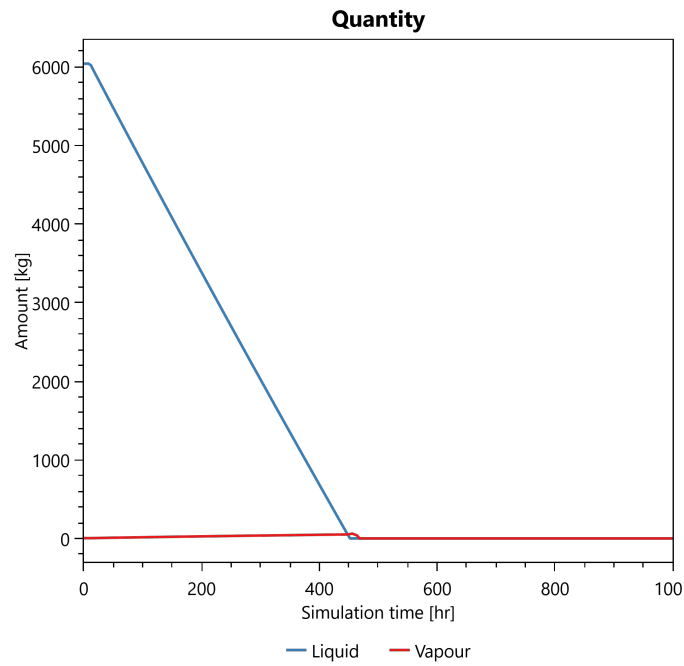


Figure 101: Quantity of Fuel vs Time for LCH₄ Tank for Mars Mission

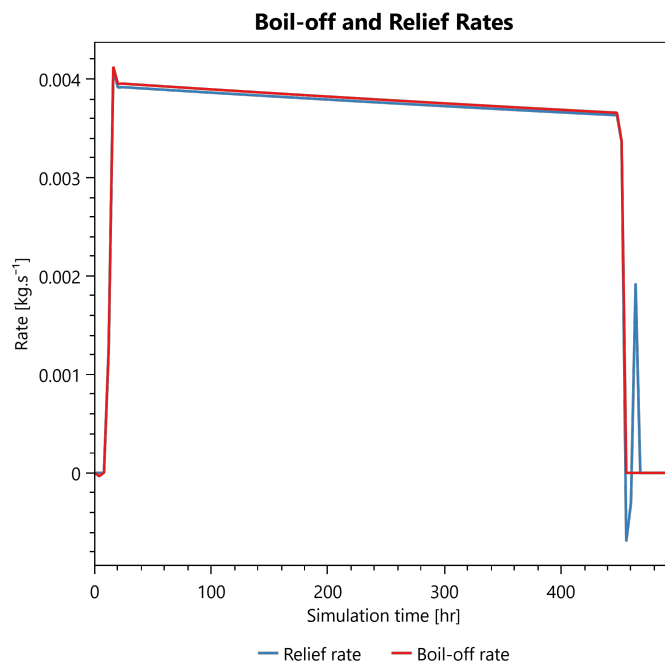


Figure 102: Boil Off Rates of Fuel vs Time for LCH₄ Tank for Mars Mission

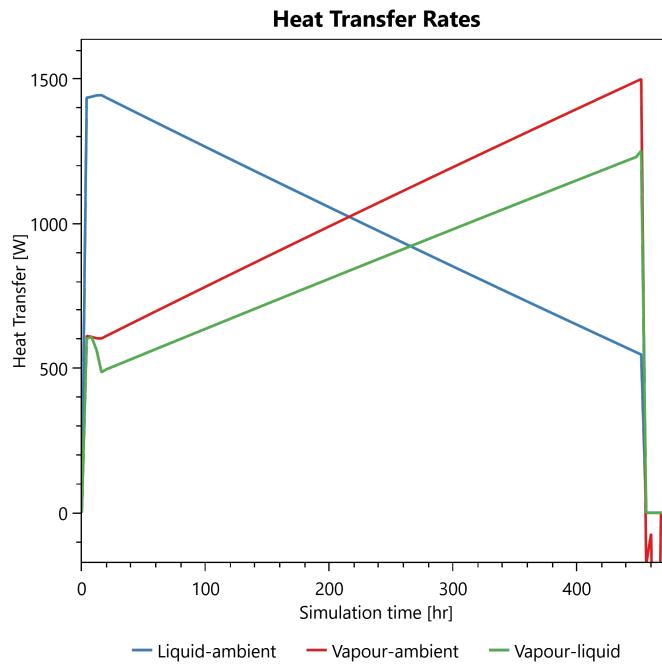


Figure 103: Heat Transfer Rates of Fuel vs Time for LCH₄ Tank for Mars Mission

10.4. Summary

Below is the summary of the results of the Matlab Heat Flux Estimation Tool and BoilFAST Tool.³

10.4.1. Heat Flux Estimation using Matlab Tool

Input	Unit	Moon-Hydrolox	Moon-Methalox	Mars-Hydrolox	Mars-Methalox
Fuel Tank Diameter	m	3.5	3.5	3.5	3.5
Fuel Tank Height	m	2.2435	0.6627	4.4355	1.6575

Table 18: Inputs to the Heat Flux Estimation tool

³See Appendix B and C for the Matlab code

Output	Unit	Moon-Hydrolox	Moon-Methalox	Mars-Hydrolox	Mars-Methalox
Average Heat Flux Incident	W/m ²	1374.8	1374.8	898.7	898.7
Average Heat Flux Absorbed	W/m ²	343.71	343.71	224.67	224.67
Power Input to Fuel Tank	W	4239.4	1252.3	5478.8	2047.4

Table 19: Outputs of the Heat Flux Estimation tool

10.4.2. Boil Off Estimation using BoilFAST

Output	Unit	Moon-Hydrolox	Moon-Methalox	Mars-Hydrolox	Mars-Methalox
Average Boil Off Rate	kg/s	0.00523	0.00227	0.00616	0.00367
Approximate time till fuel is completely boiled off	hours	71	-	116	452

Table 20: Outputs of the BoilFAST tool

10.5. Conclusion and Scoring

Boil off of cryogenic fuels is one of the main reasons why they are not currently being used for longer-term missions. But with upcoming momentum towards exploration missions and sustained human presence on the Moon and Mars, it will be important to use fuels that could be produced in situ, for which hydrogen and methane are currently the best options. This is why it is important to understand their behaviour and select the fuel that best withstands the effect of boil off.

It is important to note that the thermal condition in an actual spacecraft will be much better managed. There is a scope for better thermal management by having a better tank architecture, using better insulation material and so on. But the goal of this study was to demonstrate the boil off behaviour of both these fuels on an equivalent platform and then understand how they behave, and that was achieved.

It is very clear that the boil off behaviour of liquid methane is far superior to that of liquid hydrogen. Apart from this, the cryogenic temperature of liquid methane being higher at -162°C , makes it easier to thermally manage. For long-term missions, hydrogen becomes a near-impossible option due to the fuel completely disappearing. Unless more advanced thermal management capabilities and architecture are used.

For scoring, the difference in their boil off rates will now be looked at.

$$\begin{aligned} \text{Difference between boil off rates for the Moon mission} &= 0.00523 - 0.00227 \\ &= 0.00296 \text{ kg/s} \end{aligned}$$

$$\begin{aligned} \text{Difference between boil off rates for the Mars mission} &= 0.00616 - 0.00367 \\ &= 0.00249 \text{ kg/s} \end{aligned}$$

Since methane has a lower boil off rate, it can be given a score of 10 on a scale of 0 to 10. This will help understand how significantly more the boil off of hydrogen is and then score it in relation.

$$\begin{aligned} \text{Difference percentage for Moon mission} &= 0.00296/0.00523 \times 100 \\ &= 56.59\% \end{aligned}$$

$$\begin{aligned} \text{Difference percentage for Mars mission} &= 0.00249/0.00616 \times 100 \\ &= 40.422\% \end{aligned}$$

Therefore, hydrogen can be scored a 56.59% lower score for the Moon mission and a 40.422% lower score for the Mars mission.

The score for Hydrogen for the Moon mission is then 4.341.

The score for Hydrogen for the Mars mission is then 5.957.

Part	Moon-Hydrolox	Moon-Methalox	Mars-Hydrolox	Mars-Methalox
Score	4.341	10	5.957	10

Table 21: Scoring for Boil Off Behaviour

11. In Situ Production

11.1. Introduction

“In situ resource utilisation (ISRU) is a concept for increasing the efficiency of space missions by utilising indigenous resources on a planet or moon in order to reduce the amount of material that must be brought from Earth” [62].

But before discussing ISRU and its importance, it is essential to weigh the cost of ISRU and understand if it is significantly beneficial for the given goals. For plans and missions to the Moon and Mars, ISRU is definitely a worthy endeavour. This is because of plausible ways to extract hydrogen and methane, and therefore, use them as fuel as well as the goal of long-term human presence on these bodies. For this comparison, ISRU on the destination bodies is an especially important factor, as the feasibility of ISRU of propellants could mean the difference between an occasional exploration mission and a fully sustainable colony and research base. ISRU will be the foundation for continuous space exploration. Research around the world is being carried out to figure out the most effective way to utilise these planetary bodies and their resources to build sustained human presence by being less reliant on Earth.

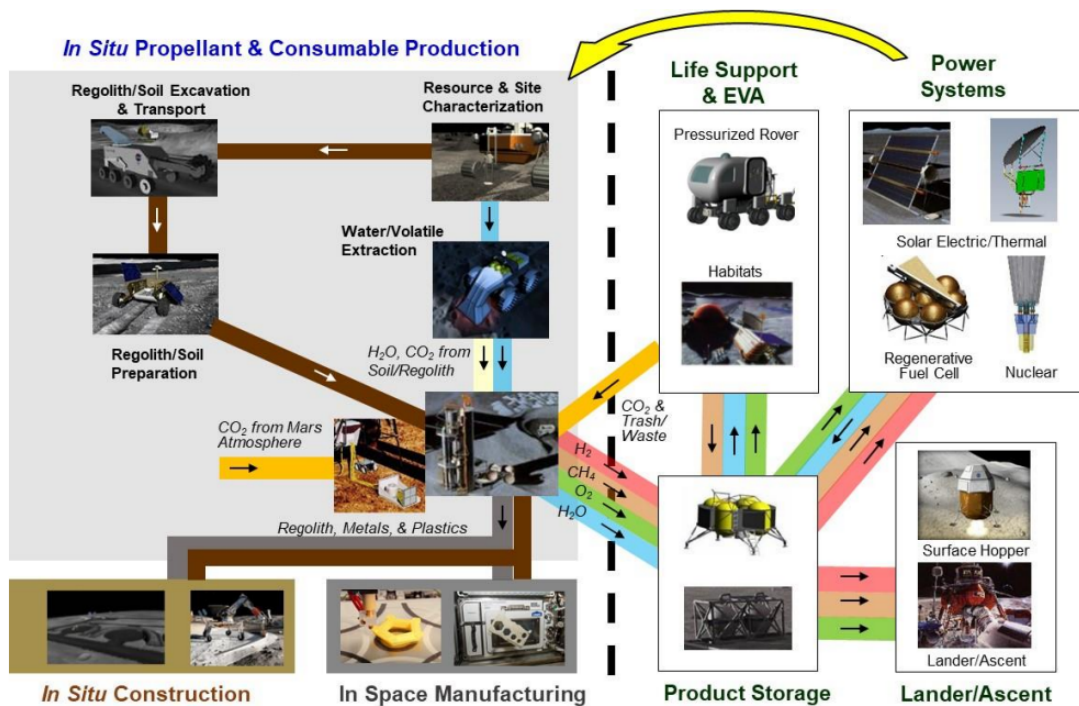


Figure 104: Example of an ecosystem with In Situ Resource Utilization [63]

It is important to discuss ISRU from the earliest phase, which here would be engine development. This is because ISRU requires an approach that is integrated on a system level and ingrained in the mission architecture, which also includes spacecraft design. This makes the goal of ISRU streamlined.

This is especially important for the Osiris engine as the domain in which it truly shines with its capabilities is at interplanetary and medium-to-long-term missions. The goal of the Osiris Engine is to be the workhorse of exploration missions in the near future, and ISRU will play an important choice in propellant selection and, therefore, the engine.

For this comparison, only the propellant production using In Situ Resource Utilisation will be looked at and specifically the fuels hydrogen and methane.

11.2. Mars

11.2.1. Resources

On Mars, one of the most abundant resource available is its atmosphere. It is composed of (by volume) 96% CO_2 , 1.9% N_2 , and 1.9% Ar , along with gases such as O_2 , CO , H_2O , NO and CH_4 in minor amounts [64].

Recently, the Mars Rover Curiosity detected an increase in atmospheric methane of more than 30 times the previously known background peak. While the source of this methane is not known, it can potentially be from a subsurface methane accumulation [65]. Therefore, it may be possible to benefit from this and extract methane directly as well.

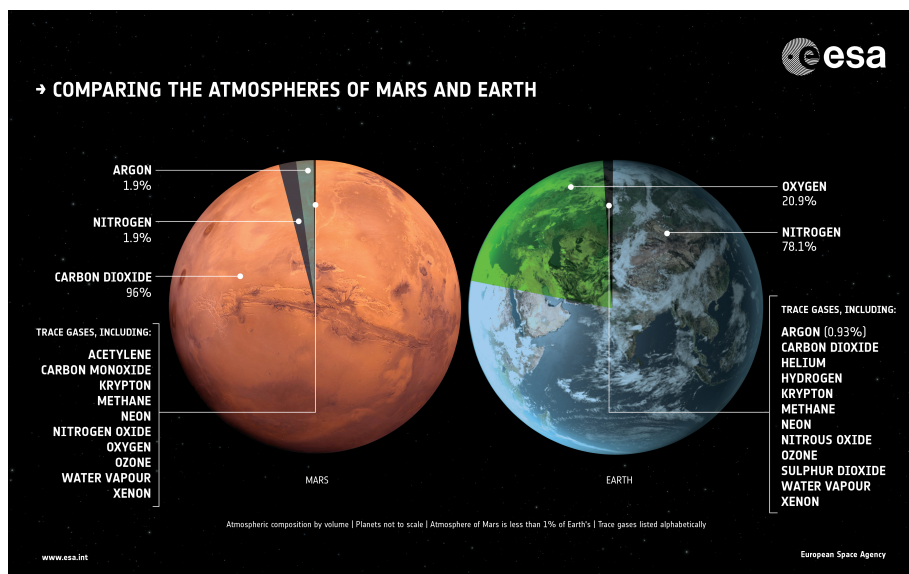


Figure 105: Mars' Atmosphere as compared to Earth [64]

The notion of water on Mars had existed since the time of Cassini in the 1600s when the observable polar ice was believed to be water ice. Over the last century, mankind has gained a tremendous wealth of information about the environment on Mars and now has a better understanding of water on Mars. Water on Mars is mostly found underground and in the form of ice. Therefore, it is difficult to simply use water on Mars, and instead, it needs to be mined and extracted first. There is estimated to be around $5 \times 10^6 \text{ km}^3$ of water ice available on Mars [66]. There is a water content of around 1 to 10 % by weight around the middle latitude region of Mars, i.e. between the 30 degrees North and South latitudes in the upper 1 metre of Mars regolith. This is distributed within mineral deposits of phyllosilicates, carbonates, sulphates, and silica, and usually, the water content around these deposits goes slightly up, on average around 8% by weight. Additionally, around 1 to 3 % by weight of water is expected in the loose surface regolith based on data from Viking I, Viking II and Curiosity rover's Sample Analysis onboard instrument. Several Mars orbiters carry radar and imaging instruments, and with that, evidence of large subsurface ice sheets was found using a very interesting approach. Very young craters on Mars were observed, and it was found that the recently exposed subsurface, due to the impact, had ice formation in approximately the 10-metre range of subsurface depth in the latitude ranging from 35 to 60 degrees North and South [63].

Therefore, summarising the types of ice resources on Mars:

1. Loose surface regolith with a water content of around 1 to 3 % by weight, found in most regions of Mars
2. Dense hydrated minerals with a water content of around 6 to 10 % by weight, found in the top 1 metre of the Martian surface in the mid-latitudes between 30 degrees North and South.
3. And subterranean ice sheets with large ice accumulation, found in the 10-metre range of subsurface depth around 35 to 60 degrees North and South latitudes and many craters.

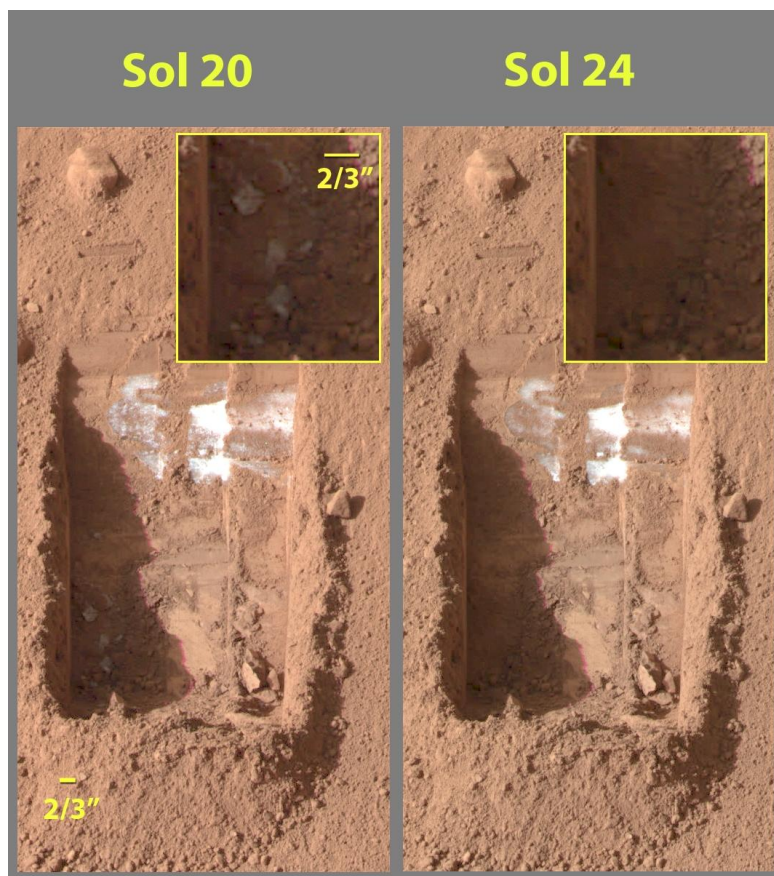


Figure 106: Subsurface ice detected by NASA's Phoenix Mars Lander's Surface Stereo Imager. Here the ice is shown sublimating between the interval of 4 Martian Days [68]

In terms of resource extraction and planning, for earlier missions with small crews and simpler goals such as scientific research, smaller glacial deposits covered with regolith scattered around the planet should be adequate. The water ice should be enough for the purpose of life support and a small production plant.

But for more permanent settlements and Mars colonies, a central mining location should be established with transportation logistics to the habitats. There are currently 18 identified craters in the northern polar region with large quantities of water ice accumulation. The Korolev and Dokka craters are the largest among these, with the Korolev Crater alone boasting a build-up of around 3000 km³ of ice [67].

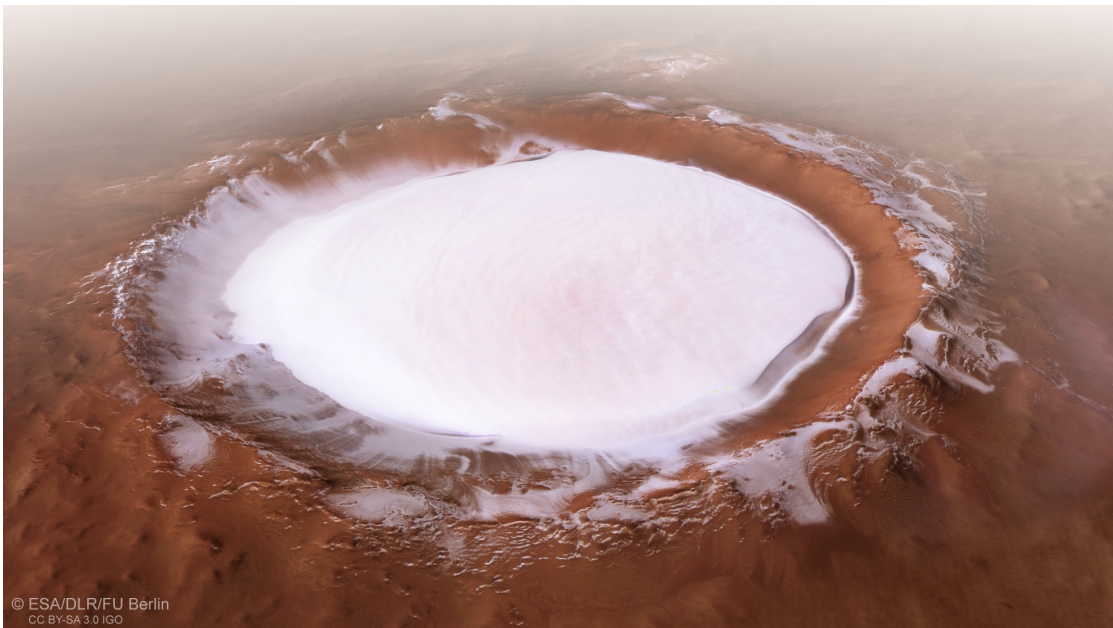


Figure 107: The Korolov Crater captured by ESA's Mars Express [69]

11.2.2. ISRU for Hydrogen on Mars

To consider the production of hydrogen as a fuel, the main source on Mars is most definitely water. There is essentially no molecular hydrogen in the Martian atmosphere due to its low density and Mars' lower gravity. So practically, the only way to extract hydrogen from in situ supplies would be from Mars' water ice [70].

There are currently three methods of extracting hydrogen from water:

1. Electrolysis
2. Magnetite / Wustite Redox Cycle Method
3. Water Gas Shift Reaction

11.2.2.1 Electrolysis

Water Electrolysis was discovered by Jan Rudolph Deiman and Adriaan Paets van Troostwijk in the Netherlands in 1789. This was done by observing the electrostatic discharge between two gold electrodes dipped in water [71].

Water Electrolysis is essentially the process of passing electricity through water, and the water then, using this energy, dissociates into its constituents, hydrogen

and oxygen. At standard temperature and pressure (1 bar and 298 K), the reaction is as follows [72]:



The electrochemistry of this reaction is as follows [71]:

At 298 K, the standard enthalpy of formation is 286.03 /kJmol, and the ideal gas entropy is 0.163 /kJmol/K of gaseous water.

According to Gibbs Free Energy Equation:

$$\Delta G^\circ = \Delta H^\circ - T\Delta S^\circ \quad (40)$$

$$\Delta G^\circ = 286.03 - (298 \times 0.163)$$

$$\Delta G^\circ = 237.46 \text{ /kJmol}$$

Therefore, to make a single molecule of hydrogen ($n = 2$),

$$V_{rev} = -\frac{\Delta G^\circ}{nF} \quad (41)$$

Where F is Faradays Constant,

$$V_{rev} = -\frac{237,460}{2 \times 96,485}$$

$$V_{rev} = -1.23 \text{ V}$$

But to first change the liquid water to gas, now more energy is needed.

$$\Delta H^\circ + \text{Energy Required to Vaporise Liquid Water} = 286.030 \text{ /kJmol}$$

$$V_{rev} = -\frac{286,030}{2 \times 96,485}$$

$$V_{rev} = -1.48 \text{ V}$$

This is the minimum required voltage to dissociate water into hydrogen and oxygen. If the voltage is further increased, the rate of reaction increases and this is known as overpotential.

Effect of Impurities in Martian Water and Subzero Temperatures

The process of electrolysis requires a certain level of electrical conductivity within the water and a certain temperature to maintain the kinetics of the electrodes. On Mars, these conditions don't exist. Electrolysis doesn't work on the brackish water that is available on Mars, which contains elevated perchlorate content. Normally for electrolysis, an electrolyte is needed in the water to conduct the discharge from the electrodes further than just the local area, and for this, a small concentration of non-interfering salts does the trick. But unlike this, the brine water on Mars has a high concentration of perchlorate salts. This salt needs to be removed first if the standard electrolysis process is to be performed, as is done on Earth [73]. Additionally, the temperature of the water on Mars can be below $-36\text{ }^{\circ}\text{C}$. This cuts down the molecular activity of the water, and therefore, reduces the effectivity of the electrolysis process.

But these hostile conditions of Martian water are not completely hostile to certain specialised methods to perform electrolysis. Pralay Gayen and a group of researchers from the Department of Environmental & Chemical Engineering at Washington State University in St. Louis, USA, have come up with an innovative method to perform electrolysis on Martian Brine [73].

The researchers attempted to counteract the drawbacks of the salts in the water by changing the material of the electrodes and therefore targeting the solution at the location of the biggest challenge, i.e. the electrodes.

The setup attempted to imitate the Martian conditions. The simulated Martian brine was composed of water with 2.8 molar Magnesium Perchlorate ($\text{Mg}(\text{ClO}_4)_2$) purged with CO_2 so as to saturate it. This was kept at $-36\text{ }^{\circ}\text{C}$ to simulate Martian conditions by surrounding the setup with a solution of ethylene glycol and ethanol with dry ice in it. The electrolysis setup consisted of an anode made of $\text{Pb}_2\text{Ru}_2\text{O}_{7-\delta}$ and supported by glassy carbon (GC), and a platinum cathode also supported by glassy carbon. These electrodes are separated by a generic anion-exchange membrane (AEM) [73].

The results of this experiment were very promising. The energy efficiency of the setup was estimated to be around 60% compared to around 60-80% efficiency for water electrolyzers in Earth Conditions. The output of this system is also very good. Compared to Mars Oxygen In-Situ Resource Utilization Experiment (MOXIE) aboard NASA's Perseverance Mars Rovers, the oxygen production from this water electrolysis method is 25 times for the same amount of power input [73].

Therefore even with these hostile conditions of Martian water and environment, water electrolysis is possible.

Effect of Martian Gravity on Electrolysis

The effect of gravity on water electrolysis is unknown, and more specifically, the effect of lower gravity. What is known, is that the formation of bubbles at the electrodes during electrolysis is governed by the 3 phases interfacial phenomena, and this is definitely greatly reliant on gravity. The nature of the bubble evolution directly impacts the electrochemical efficiency of the dissociation of the water molecules. Therefore, it is extremely important to understand and overcome this gap in knowledge, as this will lead to a more informed stance in designing systems for the electrolysis of water specifically for interplanetary use [74].

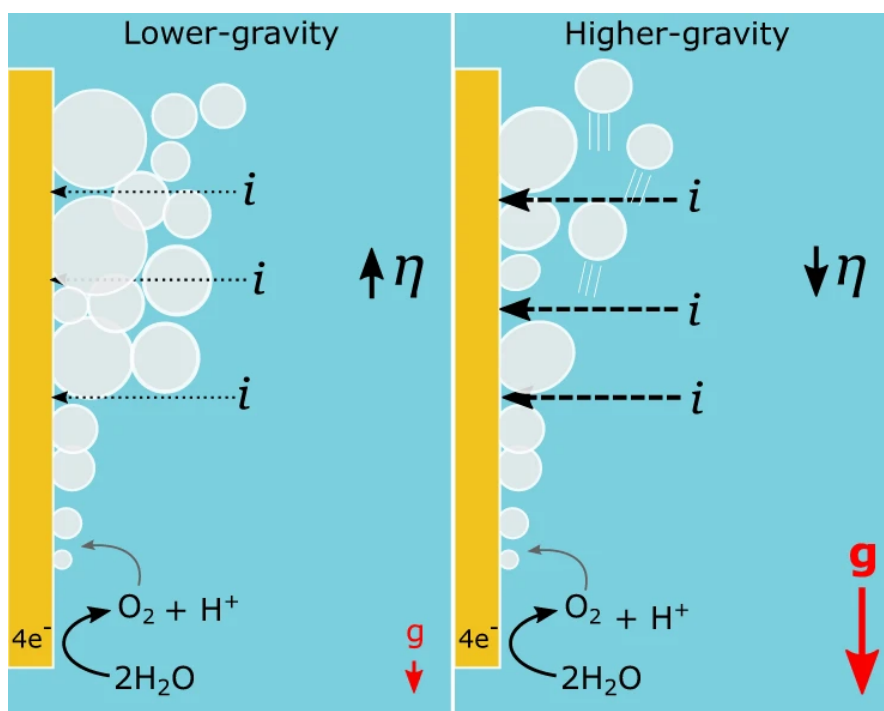


Figure 108: Comparison between the formation of gas bubbles in a lower and higher gravity environment [74]

Very recently, a research team from the University of Glasgow and the University of Manchester set out to answer this question. The team performed the electrolysis experiment at different gravity levels, all the way from 0.01 g (microgravity) to 8 g [74].

The experiment for the reduced gravity electrolysis was conducted by putting electrolysis cells on a centrifuge, and these were then operated on microgravity-inducing parabolic flights. During the microgravity periods, the centrifuge was

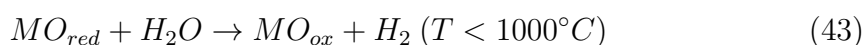
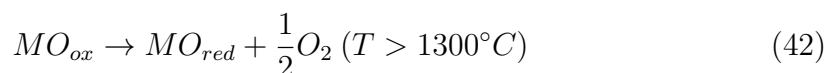
spun at different speeds to simulate different levels of reduced gravity.

What was found, was that a layer of froth of small bubbles at the electrode surface was more prevalent as the gravity levels went down. The size of the bubbles were identified into three groups; large, medium and small. On average, the size of the large bubbles remained the same. On the other hand, at reduced gravity, the number of small-sized fizz increased with a decrease in gravity. The number of medium-sized bubbles also increased. For Mars, where the gravity is 1/3rd that of Earth, it was found that for the same amount of power supplied, there is a 6% decrease in the products obtained as compared to on Earth [74].

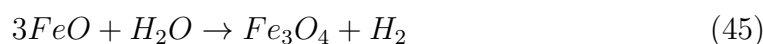
Hence, it can be concluded that the effect of the lower gravity on Mars does not have a constraining effect on the use of electrolysis of water on Mars.

11.2.2.2 Magnetite / Wustite Redox Cycle Method to Produce Hydrogen

Another method that can be used to produce hydrogen on Mars is the Magnetite / Wustite Redox Cycle. This process is the two-step reaction of a metal oxide at a high temperature with steam, and results in an endothermic reaction. The reaction is as follows [76]:



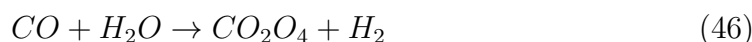
It is known that oxides of Iron, including Magnetite and Wustite, can be found on Mars [75]. Therefore, potentially this metal oxide redox reaction can be performed with Magnetite to get Wustite, and then react it with steam to get hydrogen or directly react with Wustite to get hydrogen. The reaction would look as follows [76]:



This can be an additional source of hydrogen but definitely would not be able to sustain the high demands of hydrogen as a fuel.

11.2.2.3 Water Gas Shift Reaction

In this method of hydrogen production, carbon monoxide is reacted with steam. This can prove to be an excellent alternative to hydrogen production as compared to water electrolysis, since carbon monoxide is present in Mars' atmosphere. The reaction for Water Gas Shift is as follows [77]:



11.2.2.4 Liquid Hydrogen Storage

If the hydrogen generated is to be used as a fuel, it needs to be stored. The most efficient way of storing hydrogen is in its liquid form at high pressures. For this, large tanks are needed that hold between 350 to 700 bars of pressure and can maintain cryogenic temperatures.

Therefore, energy would be required for liquefaction, pressurisation, as well as maintaining the storing conditions. This is one major disadvantage of hydrogen as a fuel compared to methane. Even though water would have to be used to supply the hydrogen required for the Sabatier process to obtain methane, the hydrogen doesn't need to be liquified, pressurised, and stored.

11.2.3. ISRU for Methane on Mars

To obtain methane from in situ resources on Mars, the two components of the methane molecule are required, carbon and hydrogen. To obtain hydrogen, the same resource strategy is followed as used to obtain hydrogen as the main rocket fuel, i.e. obtain it from water. To obtain carbon, the most abundant resource available on Mars is used, the carbon dioxide in its atmosphere. This is, of course, apart from the other obvious source, which could be the molecular methane directly available on Mars'.

Therefore, the two ways of obtaining methane in situ on Mars are:

1. From molecular methane
2. From carbon dioxide through the Sabatier Reaction

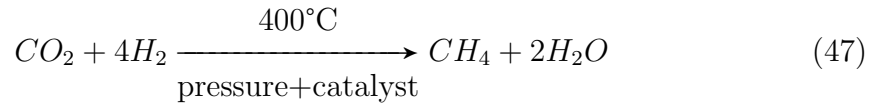
11.2.3.1 Natural Methane

Atmospheric methane is very rare on Mars and is available in very trace quantities ranging between 0 to 30 parts per billion volume with seasonal peaks of up to 60 ppbv [78]. Molecular methane is extremely unstable in the atmosphere of Mars due to its oxidising nature and due to its breakdown by the Sun's UV radiation. At 1 bar, the boiling point of methane is -161.5°C ; therefore, if this atmospheric methane can be pressurised and then cooled, it can be condensed and stored as liquid methane. Nonetheless, molecular methane remains an unviable source for large requirements for methane as a fuel.

11.2.3.2 Sabatier Process

The Sabatier process is essential to a settlement on Mars if methane is to be used as fuel. The Sabatier process was discovered by Paul Sabatier and Jean-Baptiste Senderens in France in 1897. It is the process by which carbon dioxide and hydrogen, under high temperatures and in the presence of a catalyst, form methane and water.

The reaction for this is as follows [79]:



This is usually performed with a metal catalyst like Nickel, Rubidium, Rhodium, and Zinc and is performed at temperatures between 250-400°C.

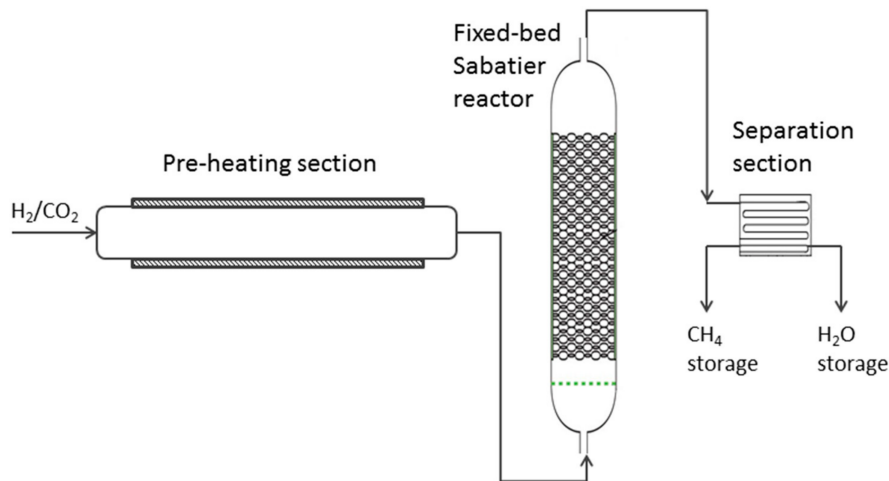


Figure 109: The Sabatier Process Setup [80]

On Mars, the dust from the atmosphere needs to be first filtered out. Then, the carbon dioxide is separated from the rest of the components of the atmosphere, and this is done by condensing and storing the carbon dioxide in a liquid form. Parallely, water is electrolysed as described in section 11.2.2.1. From the products, the oxygen is liquified and then stored for use as propellant and for other purposes. The carbon dioxide and the hydrogen are then reacted in the Sabatier reactor. The main products of this reaction are methane and water vapour, but along with the main reaction products, are also unreacted carbon dioxide and hydrogen. First, this mixture is passed through a condenser which collects the water, and it is used again for electrolysis. The remaining components are then passed through a chamber where Pressure Swing Adsorption takes place, and the carbon dioxide

and hydrogen gases are channelled back to the Sabatier reactor. The remaining methane then passes on to be liquified and stored as propellant [81].

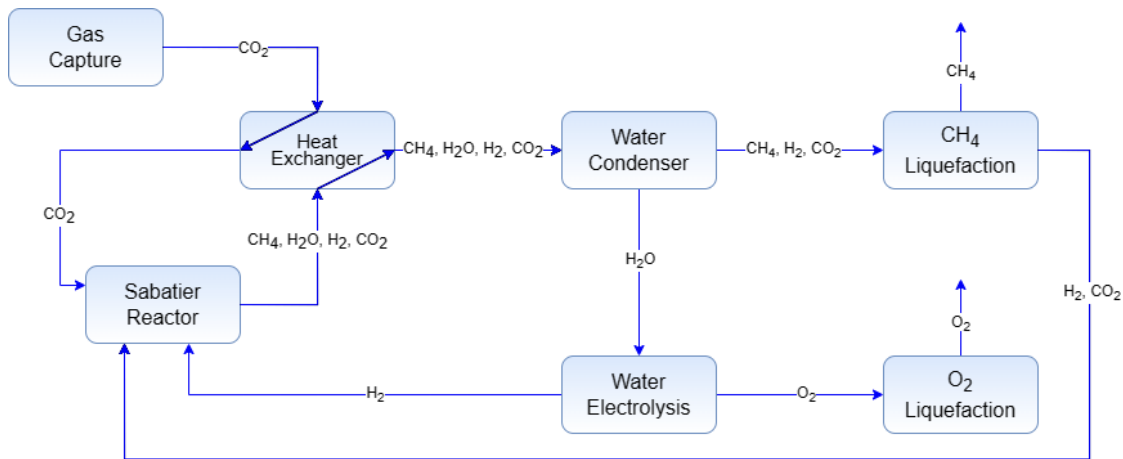


Figure 110: Flowchart representing the flow of resources for an ecosystem on Mars where methane is the fuel [82]

11.2.3.3 Liquid Methane Storage

Liquid methane can be stored with relative ease as compared to hydrogen due to it having a much higher boiling point. Additionally, the hydrogen produced by the electrolysis does not need to be stored and is directly used in the Sabatier process. Therefore, the energy required for liquefaction and storage is also saved as compared to storing it as liquid hydrogen as fuel.

11.3. The Moon

11.3.1. Resources

The resources on the Moon are much more limited as compared to Mars due to its smaller size.

They can be categorised into two main categories:

1. Lunar Regolith based
2. Polar Water / Volatile based

The Lunar Regolith can be an important resource for long-term settlement and exploration for civil engineering applications. Within the scope of propellant resource utilisation, it is worth noting that Lunar regolith is composed of 40% oxygen

by mass, mostly as oxides. This can be extracted as oxygen for the oxidiser for the engines. But in terms of fuel, there is not as much of worth to extract from the Lunar regolith.



Figure 111: Lunar Regolith [86]

Water can be the most game-changing resource on the Moon. One of the first samples of Lunar regolith came with the Apollo program in the 1970s, but no evidence of water was found in those samples. In 1978, hope in Lunar water was rekindled when the Soviet Luna 24 probe returned with Lunar samples, and it was found that these samples contained 0.01% water by mass [83]. In 2009, India's Chandrayaan 1 orbiter identified absorption features resembling water or water-bearing minerals with its Moon Mineralogy Mapper. The Chandrayaan then released the Moon Impact Probe into a crater in the Lunar south pole and further displayed evidence of water ice. Later missions on the Lunar Crater Observation and Sensing Satellite (LCROSS) and the Lunar Reconnaissance Orbiter (LRO) have further discovered evidence of water ice. One of the more interesting observations was when a used Centaur upper stage crashed in the crater Cabeus at the Lunar south pole and ejected a plume. This plume was then measured by the LCROSS satellite and

found to be 5.5% water by weight [84]. The Research team led by Shuai Li from the University of Hawaii analysed the data from the Moon Mineralogy Mapper and found that in some regions of the Lunar craters, there could be water ice up to 30% by weight [85].

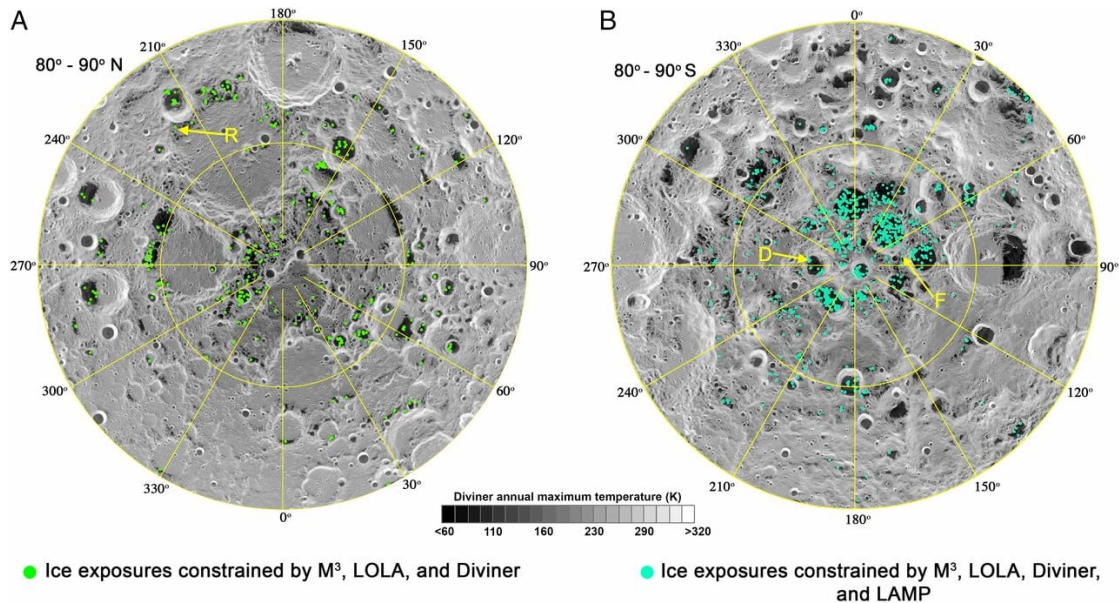


Figure 112: (A) Lunar North Pole and (B) Lunar South Pole. Green and Blue dots indicate detected surface water ice. [85]

But in terms of the exact form in which the water is stored, the concentration of ice reserves, and its distribution, especially in the shadowed craters, not much is known yet. Therefore, it will be imperative that more is found out about water reserves on the Moon with expedition missions.

What is known, is that most of the water ice that can be observed, is located on the poles and, more specifically, in the craters, where the temperatures are colder. In the short term, landing sites would have to be chosen near the poles, such as the Artemis mission, which will land near the south pole, so that more exploration can be done to learn more about Lunar water ice. This will also make it logistically easier to utilise this ice for ISRU. Later, mining areas would probably have to be set up near the poles and habitation in another area of the Moon with transportation lines in between.

11.3.2. ISRU for Hydrogen on the Moon

For the Moon as well, water will be the de facto source of hydrogen. The Moon does receive some Solar Wind Volatiles, and it includes some hydrogen. But there is no chance of this staying anywhere on the Moon due to low gravity. Electrolysis with water still remains the best option for large-scale hydrogen production. There is no known source of iron oxides that are in reasonable quantities, and carbon monoxide is not found in ambient conditions and would require mining to utilise small deposits. Therefore, the Magnetite / Wustite Redox Cycle method and the Water Gas Shift Reaction method can't really be used in a practical way.

Electrolysis and the effect of Lunar gravity on Electrolysis

Similar to the discussion about the process of electrolysis on Mars and the effect of gravity on bubble formation, due to the Moon having a lower gravity, the rate of electrolysis here is also hindered. But according to Lomax et al's experiments, it was proved that even in the Moon's gravity, which is 1/6th of the Earth, the reduction in the electrolysis product is just 11% as compared to the Earth with the same power input [29].

The hydrogen harnessed on the Moon would also have to be stored in liquid form. This entails all the same energy requirements as on Mars.

11.3.3. ISRU for Methane on the Moon

In situ production of methane has always been an elusive ordeal since there was never a source of carbon that was known of on the Moon. But this view has been changing recently.

When data from the LCROSS satellite was received about the plume created when the spent Centaur stage impacted the Moon, some interesting observations were made. According to the study published in the Science Journal by Anthony Colaprete and his team, the plume created by the impact contained considerable quantities of carbon monoxide and water along with small quantities of C_2H_4 , carbon dioxide, methane and CH_3OH [84].

This could mean that the electrolysis of water could be performed, and oxygen and hydrogen could be obtained as products. From these products, the carbon monoxide can be reacted on the Moon with some of the oxygen, and the rest can be used as propellant. The product of this reaction would be carbon dioxide which can then be reacted with the hydrogen produced from the electrolysis, which can then be used in the Sabatier process to get methane as a propellant.

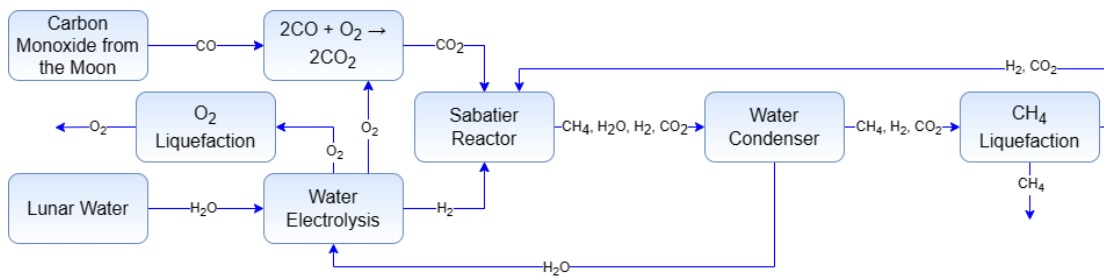


Figure 113: Manufacturing of methane as a Fuel from carbon monoxide and water

That being said, the source of carbon on the Moon will always be limited as compared to the demand for making methane to be used as a propellant. In the long term, this might be a problem if a large settlement of humans is envisioned. In that case, there will be a large amount that will be readily available as human waste in the form of carbon dioxide as respiration waste and bio waste.

11.4. Conclusion and Scoring

In conclusion, it is important to look at the in situ propellant development aspects in the early development phase as it can help make essential decisions, such as fuel selection for engine development. ISRU is an especially important factor to look at because of two reasons. One is that the development and momentum from the public and private sectors have grown exponentially in the space sector, and more specifically, Lunar and Martian exploration. This makes it especially important to consider the resources already available at the destinations for the development of the vehicles that will be used to get there and back. The second reason why this aspect is important for this discussion is that the Osiris engine is exactly designed to fill a role in that interplanetary exploration ecosystem. Therefore, ISRU consideration during its development seems imperative.

For Mars, its most important resource for propellant production is the water ice and its atmosphere. To obtain both, methane and hydrogen, on Mars, water ice will have to be utilised. Therefore, comparing it just on the basis of water extraction would not make sense. But what can be considered, is the difference between liquefying and storing the hydrogen produced when it is supposed to be used as a fuel, as compared to it directly being utilised in the Sabatier process. The important difference would be the cost, difficulty, and energy that would be required as compared to storing methane as fuel. On top of that, with the abundance of CO₂ on Mars that is freely available in the atmosphere, as well as a neatly connecting ecosystem of all the resources used in the process, as shown in figure 110, methane seems the most compelling choice.

For the Moon, its most important resource for propellant production is the water ice and its regolith. Similar to Mars, on the Moon as well, water would have to be electrolysed regardless of which fuel is chosen. But one aspect that is different on the Moon is that carbon is not as abundant. The same disadvantages of liquifying and storing hydrogen apply on the Moon as well, but there is a difference in one aspect here. It is cooler in the shaded regions on the Moon, and therefore, it can be used to our advantage. Carbon monoxide in the regolith was detected by the analysis of the LCROSS plume, but its actual quantities and allocations around the Moon are not as clear. Additionally, there would be a significant disadvantage in the fact that, to get the carbon on the Moon, there would be the need to have a mining operation to extract it from the regolith, as it is not as straightforward as using the atmosphere on Mars. This, of course, gets a little simpler once there is a human settlement and enough human waste, but this would still take some time.

For Mars, there is no better fuel choice based on the factors discussed than methane in terms of ISRU. For that reason, it can be assigned a score of 10 on a scale of 0 to 10. For hydrogen, the only challenge is its storage cost, but apart from that, all the necessary resources are present. Therefore, it can be given a score of 8.

For the Moon, both fuels have some pros and some cons. Hydrogen still has a slight disadvantage in terms of storage but an advantage due to the fact that all the resources required are available and cooler temperatures on the Moon. For methane, it is much more challenging. The source of carbon is limited and not very well known and is harder. Therefore hydrogen can be given a score of 9 and methane a score of 7.

Part	Moon-Hydrolox	Moon-Methalox	Mars-Hydrolox	Mars-Methalox
Score	9	7	8	10

Table 22: Scoring for In Situ Production

12. Evaluation of Results

Looking at all of these aspects gives a good understanding of hydrogen and methane as fuels and an insight into their effect on the spacecraft. The analysis was broken down into six main topics that are important to consider while deciding the propellant for an engine, and the focus here was specifically on the Osiris Electrically Augmented Expander Cycle Engine and its intended use for exploration missions.

Below is the summary of the individual scores for these categories.

Part	Moon-Hydrolox	Moon-Methalox	Mars-Hydrolox	Mars-Methalox
Efficiency	10	8.105	10	8.105
System Mass	8.14	10	8.75	10
Pump Power Requirements	3.481	10	3.481	10
Storability and Long Term use	3	6	3	6
Boil Off	4.341	10	5.957	10
In Situ Production	9	7	8	10

Table 23: Summary of Scores

As mentioned in the approach in chapter 4, the score will then be multiplied into a weight that will factor in the significance of each category to the overall deciding factor. The weight will be in the range of 0 to 1.0, 0 being insignificant and 1.0 being the most significant. Below, these weights will be discussed and their reasons.

Understanding the efficiencies of these two fuels gives one of the most important factors of propellant choice for a spacecraft engine, the performance. The efficiency of a propellant combination can play an important role in many other

spacecraft design decisions too, and its influence can be a deciding factor in some cases. This would make one of the key factors in deciding the fuel, and thus, it will have a weight of 1.0.

The mass of the spacecraft is what decides if a certain spacecraft design is feasible or not in the first place. The mass of the spacecraft would also determine how much payload it can carry. A lighter inert mass means more mass available for payload, and on an exploration mission this is one of the most desirable factors. This will also affect the cost of the spacecraft directly. Therefore, it will have a weight of 1.0.

The limitation on the electrical motor and powertrain system for an electrically augmented expander engine can be huge, and it would be important to consider its impact on mass due to the importance of the electrical motor and battery during startup as well the difference in fuel pump size. But this mass penalty gets a little subdued when looking at the overall system. Additionally, better battery and motor technology and improved pump design can further narrow down the gap, and thus, make it less significant. Hence, it will have a weight of 0.5.

Storability and long-term behaviour of a fuel might not be as significant of a factor for an Earth Orbit mission, but for missions to the Moon and especially Mars, it is a significant factor to be considered for propellant management aspects; therefore, it cannot be as easily dismissed. That being said, this is one of the areas where there is significant technology and infrastructure development. And, with time, the issues related to this will start to become more and more insignificant. Accordingly, it will have a weight of 0.4.

One of the main reasons cryogenic propellants are not used, is due to their boil off. Therefore, it is important to understand the boil off behaviour so as to select a propellant that requires less thermal management and has a lesser tendency to completely be depleted during the course of the mission. Longer duration missions exacerbate this problem associated with boil off, as it gets harder to hold on to the fuel. The difference in the boil off will still be representative of the difference in behaviour shown in this study; nonetheless, it is still possible to have some advancements in thermal management approaches to narrow the differences. With this in mind, it will have a weight of 0.8 for the Moon mission and a weight of 0.9 for the Mars mission.

And lastly, it is important to understand what opportunities for In Situ Fuel production are available on the destination planetary bodies so as to develop an engine that can be part of the ecosystem of the intended settlement and is as

self-sufficient as possible. This might not be as significant at first, since currently there is no infrastructure at present for ISRU, but later, to keep up the pace of exploration, ISRU would be essential. Thus, there would have to be design decisions made for this engine with the future prospects in mind. Once set up, a self-sufficient propellant ecosystem can be the difference between long-term exploration being feasible or unfeasible. This becomes even more significant if the habitats are even further away from Earth, such as on Mars. On the Moon, to a small extent and on an initial stage, it is possible to transport some propellant from Earth to refuel, but on Mars, self-reliance can be critical as resupply missions might be insurmountable. In that case, it will have a weight of 0.9 for the Moon mission and a weight of 1.0 for the Mars mission.

The weights can further be normalised to have a total maximum sum of 1.0. This will make the final score also on a scale of 0 to 10. This can be done by dividing the weight by 6.

Therefore summarising the normalised weights:

Part	Moon-Hydrolox	Moon-Methalox	Mars-Hydrolox	Mars-Methalox
Efficiency	0.1666	0.1666	0.1666	0.1666
System Mass	0.1666	0.1666	0.1666	0.1666
Pump Power Requirements	0.0833	0.0833	0.0833	0.0833
Storability and Long Term use	0.0666	0.0666	0.0666	0.0666
Boil Off	0.1333	0.1333	0.1500	0.1500
In Situ Production	0.1500	0.1500	0.1666	0.1666

Table 24: Summary of Weights

Therefore, to calculate the final score:

$$\text{Score for X fuel for Y mission} = \sum(\text{Weight} \times \text{Score})$$

$$\begin{aligned} \text{Final Score for Hydrogen for Moon mission} &= (0.1666 \times 10) + (0.1666 \times 8.14) \\ &+ (0.0833 \times 3.481) + (0.0666 \times 3) \\ &+ (0.1333 \times 4.341) + (0.1500 \times 9) \\ &= \underline{5.440} \end{aligned}$$

$$\begin{aligned} \text{Final Score for Methane for Moon mission} &= (0.1666 \times 8.105) + (0.1666 \times 10) \\ &+ (0.0833 \times 10) + (0.0666 \times 6) \\ &+ (0.1333 \times 10) + (0.1500 \times 7) \\ &= \underline{6.631} \end{aligned}$$

$$\begin{aligned} \text{Final Score for Hydrogen for Mars mission} &= (0.1666 \times 10) + (0.1666 \times 8.75) \\ &+ (0.0833 \times 3.481) + (0.0666 \times 3) \\ &+ (0.1500 \times 5.957) + (0.1666 \times 8) \\ &= \underline{5.840} \end{aligned}$$

$$\begin{aligned} \text{Final Score for Methane for Mars mission} &= (0.1666 \times 8.105) + (0.1666 \times 10) \\ &+ (0.0833 \times 10) + (0.0666 \times 6) \\ &+ (0.1500 \times 10) + (0.1666 \times 10) \\ &= \underline{7.415} \end{aligned}$$

Note: These scores are just relative quantifiers to compare one fuel to another. The numbers by themselves do not indicate anything, but only give a representation of the difference between the two fuels. It is also important to only put scores of the same mission type next to each other to understand how both perform against each other in a similar situation.

For the Moon Mission:

$$\begin{aligned} \text{Difference in score} &= 6.631 - 5.440 \\ &= 1.191 \\ \text{Percentage difference} &= 1.191/5.440 \times 100 \\ &= \underline{\mathbf{21.89 \%}} \end{aligned}$$

Methane is better than Hydrogen as a fuel, for a mission to the Moon using the Osiris Electrically Augmented Expander Cycle Engine, according to this scoring system, by **21.89 %**.

For the Mars Mission:

$$\begin{aligned} \text{Difference in score} &= 7.415 - 5.840 \\ &= 1.575 \\ \text{Percentage difference} &= 1.575/5.840 \times 100 \\ &= \underline{\mathbf{26.97 \%}} \end{aligned}$$

Methane is better than Hydrogen as a fuel, for a mission to Mars using the Osiris Electrically Augmented Expander Cycle Engine, according to this scoring system, by **26.97 %**.

Therefore, it can be observed that for exploration missions to the Moon, a Methalox engine is a better option and even more so for missions to Mars.

13. Conclusion

For the considered use cases of the Moon and Mars missions, spacecraft with two versions of the Osiris electrically augmented expander cycle engine using hydrogen and methane as their fuel was studied. Based on six different factors, the two versions were scored. It was observed that for the Moon mission, the spacecraft with the Methalox version of the Osiris engine scored 21.89 % better than the Hydrolox version. For the Mars mission, this advantage jumped to 26.97 %. It can, therefore, be concluded that the Methalox version of the Osiris Engine is a better choice for exploration missions to both, the Moon and Mars, and any future development intended for this engine should be focused in this direction.

Two of the key areas where further development is required beyond the scope of engine development, are thermal management of boil off and ISRU technology. As was observed earlier, boil off of cryogenic propellant can be extremely large. For liquid hydrogen, this was significantly larger than liquid methane. Nonetheless, a much better thermal design is also required for keeping the boil off losses of methane as well to a minimum. ISRU is one of the key considerations for propellant selection for the Osiris engine and will form the backbone of human settlement on the Moon and Mars, but currently, no infrastructure has been set up or experimented with on these bodies. Advancements in these domains will also have to be made.

In this study, the aim was to provide a basis for choosing which fuel type should be used when further developing such an engine. While all the parameters of the study might not be representative of actual spacecraft and engine design, it gives a platform for comparison by using similar use case envelopes, and therefore, being able to compare the two fuels. Further study will now have to be carried out to create a more detailed design for the Osiris engine, but now only focussed on using Methane and Oxygen as propellants.

In the next few decades, exploration activity to the Moon and then Mars will surge in numbers. For this initial exploration to turn into long-term sustenance and regular crossings, there needs to be a space system which is reliable, reusable, versatile, cheap and can use the resources which are easily available. The Osiris electrically augmented expander cycle engine is well poised to become the propulsion for such a system, and this study is a step in developing such a system.

Appendix A - Matlab System Mass Estimation Tool

```
% Tool to Estimate System Mass
% Taha Merchant, January 2023

clc
clearvars

% Inputs

% DeltaV

prompt = "What is the DeltaV required in m/s? ";
deltaV = input(prompt); %(m/s)

% Thrust

prompt = "What is the Engine Thrust in Newtons? ";
Thrust = input(prompt); %(N)

% Combustion Chamber Pressure

prompt = "What is the Combustion Chamber Pressure in Pascal? ";
Pcc = input(prompt); %(Pa)

% Oxidiser to Fuel Ratio

prompt = "What is the Oxidiser to Fuel Ratio? ";
ofratio = input(prompt);

% Fuel

prompt = "If fuel is Liquid Hydrogen press 1, for Liquid Methane press 2,
else press 0 (assuming LOx as Oxidiser for this tool)";
fueltype = input(prompt) ;

% Propellant Densities

if fueltype==1
    rhofuel = 71 ; % (kg/m3)
elseif fueltype== 2
    rhofuel = 423 ; % (kg/m3)
else
    prompt = "What is the Density of the fuel in kg/m3? ";
    rhofuel = input(prompt); % (kg/m3)
end

rhoox = 1140 ; % (kg/m3)

% Selecting initial Inert Mass Fraction assumption
```

```

prompt = "What is the initial Inert Mass Fraction assumption? ";
delta = input(prompt);

% Specific Impulse

prompt = "What is the Isp in Seconds? ";
isp_s = input(prompt); % (s)

isp = isp_s * 9.81 ; % (m/s)

r = exp(-deltaV/isp);

lambda = r - delta ;

% Payload mass selection

prompt = "What is the Payload Mass in Kg? ";
Mpl = input(prompt); % (kg)

% Engine Mass

prompt = "What is the Engine Mass in Kg? ";
Mengine = input(prompt); % (kg)

% Selecting tank diameters
% Assume cylindrical tanks

prompt = "What is the inner Diameter of the Fuel Tank in m? ";
D_fueltank = input(prompt); %(m)

prompt = "What is the inner Diameter of the Oxidizer Tank in m? ";
D_oxtank = input(prompt); %(m)

% Selecting interstage height

prompt = "What is the Height of the Interstage in m ? ";
H_is = input(prompt); % (m)

% First Mass Estimations

M_total = Mpl/lambda ; % (kg)

M_inert = delta * M_total ; % (kg)

% Main Solving Loop

error = 42 ;

while error > 1

Mprop = ((M_inert+Mpl)/r)*(1-r) ; % (kg)

% Propellant Mass Breakdown

```

```

Mfuel = Mprop / (ofratio+1) ; % (kg)

Mox = Mprop - Mfuel ; % (kg)

M_total = M_inert + Mpl + Mprop; % (kg)

% Tank Mass

if fueltype==1
    Mfuel_tank = (9.09/rhofuel) * Mfuel ; % (kg)
else
    Mfuel_tank = (12.16/rhofuel) * Mfuel ; % (kg)
end

Mox_tank = (12.16/rhoox) * Mox ; % (kg)

%For Tanks Insualtion Mass

% Assume cylindrical tanks

% Fuel Tank Dimensions

Vfuel = Mfuel / rhofuel ; %(m3)

Vfuel_tank = 1.08 * Vfuel ; %(m3) Assuming 8% ullage volume

H_fueltank = (Vfuel_tank * 4)/ (pi * D_fueltank^2); %(m)

SA_fueltank = ((pi*D_fueltank^2)/2)+(pi*D_fueltank*H_fueltank); %(m2)

% Fuel Tank Insulation

if fueltype==1
    Mfuel_insulation = 2.88 * SA_fueltank; % (kg)
elseif fueltype== 2
    Mfuel_insulation = 1.123 * SA_fueltank; % (kg)
else
    Mfuel_insulation = 0; % (kg)
end

% Oxidiser Tank Dimensions

Vox = Mox / rhoox ; %(m3)

Vox_tank = 1.08 * Vox ; %(m3) Assuming 8% ullage volume

H_oxtank = (Vox_tank * 4)/ (pi * D_oxtank^2); %(m)

SA_oxtank = ((pi*D_oxtank^2)/2)+(pi*D_oxtank*H_oxtank); %(m2)

% Oxidiser Tank Insulation

Mox_insulation = 1.123 * SA_oxtank; % (kg)

% Thrust Bearing Structure Mass

```

```

M_thruststructure = (2.55/10000) * Thrust ; % (kg)

% Gimbal Mass

M_gimbal = 237.8 * (Thrust/Pcc)^0.9375 ; % (kg)

% Other Structural Masses

% Interstage Mass

SA_interstage = pi * D_fuel tank * H_is ; % (m2)

M_interstage = 4.95 * (SA_interstage)^1.15 ; % (kg)

% Avionics

M_avionics = 10 * (M_total)^0.361 ; % (kg)

% Wiring

M_wiring = 1.058 * ((M_total)^0.5) *(H_oxtank+H_fuel tank+H_is)^0.25 ; %
(kg)

% Total Calculated Mass

temp = M_total ;

M_total = Mengine + Mfuel + Mox + Mfuel_tank + Mfuel_insulation + Mox_tank
+ Mox_insulation + M_thruststructure + M_gimbal + Mpl + M_interstage +
M_avionics + M_wiring ; % (kg)

M_inert = Mengine + Mfuel_tank + Mfuel_insulation + Mox_tank +
Mox_insulation + M_thruststructure + M_gimbal + M_interstage + M_avionics +
M_wiring ; % (kg)

error = M_total - temp ;

end

M_total

M_inert

Mfuel

Mox

H_fuel tank

H_oxtank

```

Appendix B - Matlab Heat Flux Estimation Tool for Moon Mission

```
% Tool to estimate Heat Flux input for a Moon Mission
% Taha Merchant, December 2022

clc
clearvars

% Section 0

% User Inputs

prompt = "What is the diameter of the Hydrogen Tank in m? ";
d_hy = input(prompt);

prompt = "What is the diameter of the Methane Tank in m? ";
d_meth = input(prompt);

prompt = "What is the height of the Hydrogen Tank in m? ";
h_hy = input(prompt);

prompt = "What is the height of the Methane Tank in m? ";
h_meth = input(prompt);

% Section 1

% Script to calculate Solar Heat Flux across the solar system

% Initialise constants

sigma = 5.670374 * 10^-8 ;    % Stefan-Boltzmann constant (W/m^2*K^4)
T_sun = 5778 ;              % Temperature of the Sun (K)
R_sun = 696340000 ;        % Radius of the Sun (m)
AU = 149597870700 ;        % (m)

% Calculating total power output from the Sun

P_sun = sigma * (T_sun^4) * 4* pi * (R_sun^2);    %(W)

    % P_sun is 3.8510e+26 W

% Finding the power recieved per unit area across the solar system between
0.3 and 1.6 AU

% Storing values of r (distance from the Sun) from 0.3 AU to 1.6 AU in an
array

r_array = zeros(1301,1);
```

```

for x = 300:1600

    r_array(x-299,1) = x*AU/1000;

end

% Calculating the Solar Heat flux from 0.3 AU to 1.6AU
heat_flux_array = zeros(1301,1) ;

for y = 300:1600

    heat_flux_array(y-299,1)= P_sun/(4*pi*r_array(y-299,1)^2) ;    %
    (W/m^2)

end

% Converting the r values to AU in array to display on plot
AU_array = zeros (1301,1);

for z = 300:1600

    AU_array (z-299,1) = r_array(z-299,1)/149597870700;

end

% Plotting Solar Heat Flux vs Distance from Sun.
figure(1)
plot
(AU_array,heat_flux_array,AU_array(701),heat_flux_array(701),'o',AU_array(1
225),heat_flux_array(1225),'o')
text(AU_array(701),heat_flux_array(701), 'Earth', 'VerticalAlignment', 'bottom
', 'HorizontalAlignment', 'center')
text(AU_array(1225),heat_flux_array(1225), 'Mars', 'VerticalAlignment', 'botto
m', 'HorizontalAlignment', 'center')

title('Solar Heat Flux vs Distance from Sun')
xlabel('Distance from Sun (AU)')
ylabel('Solar Heat Flux (W/m^2)')

% Section 2

% Plotting Solar Heat Flux vs Distance from Sun for Earth to the Moon.

% Hot case is considered therefore the Moon lies between Earth and the Sun
and the spacecraft moves towards the direction of the Sun.

% Earth and Moon Radii

r_earth = 6371 ;          % (km)

```



```

r_moon = 1737 ;           % (km)

% Creating a new array to represent the space between Earth and the Moon

r_em_array = zeros(376013,1);           % (km)
heat_flux_em_array = zeros(376013,1);   % (W/m^2)
alt_array = zeros (376013,1);           % (km)

% Calculating the Solar Heat flux between Earth and the Moon

for u = 170:376182

    r_em_array(u-169) = (1-((u+r_earth)*1000)/AU)*AU;           %
    Distance of spacecraft from the Sun (km)

    heat_flux_em_array(u-169)= P_sun/(4*pi*r_em_array(u-169)^2) ;           %
    Solar Heat flux incident on the spacecraft at the particular altitude
    (W/m^2)

    alt_array(u-169) = u ;                                           %
    Distance of spacecraft from Earths surface (km)

end

figure(2)
plot (alt_array,heat_flux_em_array)

title('Solar Heat Flux between Earth and Moon vs Distance from Sun')
xlabel('Distance from Earths Surface (km)')
ylabel('Solar Heat Flux (W/m^2)')

% Section 3

% Script to calculate the Heat Flux due to Albedo from Earth

% Distance between centre of Earth and centre of the Moon

D_em = 384400;           % (km)
D_em_travel = D_em - r_earth - 170 - r_moon - 110 ;           % Subtracting the
bodies radii and orbit heights (km)

% Earths Albedo

alb_earth = 0.31 ;

% Solar Heat Flux at Earth (1 AU)

heat_flux_earth= P_sun/(4*pi*AU^2) ; % (W/m^2)

% Power of Outgoing Heat due to Albedo with respect to Distance from Earth

alt_array = zeros (376013,1);           % (km)
h_array = zeros (376013,1);           % (km)

```

```

area_array = zeros (376013,1);           % (km^2)
P_al_earth_array = zeros (376013,1);     % (W)
alb_earth_heat_flux_array = zeros (376013,1); % (W/m^2)

for w = 170:376182

    alt_array(w-169) = w ;
% (km) Distance between Earths surface and the spacecraft

    h_array(w-169) = (r_earth * alt_array(w-169))/(r_earth + alt_array(w-
169)); % (km) Height of the Sphere Cap of
Earth's surface in view of the spacecraft at that altitude

    area_array(w-169) = 2 * pi * r_earth * h_array(w-169) ;
% (km^2) Surface area of the Sphere Cap (surface area = 2*pi*r*h )

    P_al_earth_array(w-169) = (heat_flux_earth*1000000) * area_array(w-169)
* alb_earth ; % (W) Power reflected by the Earth due
to albedo for that surface area

    alb_earth_heat_flux_array(w-169)= (P_al_earth_array(w-
169)/(4*pi*((alt_array(w-169)+r_earth)^2)))/1000000; % (W/m^2) Heat flux
incident on the spacecraft at the particular altitude

end

% Plot of the heat flux incident on the spacecraft due to Earth's albedo

figure(3)
plot (alt_array,alb_earth_heat_flux_array)

title('Incident Heat Flux due to Earths Albedo vs Distance from Earths
Surface')
xlabel('Distance from Earths Surface (km)')
ylabel('Incident Heat Flux due to Earths Albedo (W/m^2)')

% Section 4

% Script to calculate the Heat Flux from Earth's IR Radiation

T_earth = 253.72 ; % Blackbody Temperature of Earth (K)

% Calculating total Infrared Power output from Earth

P_earth_IR = sigma * (T_earth^4) * 4* pi * (r_earth^2); % (W)

% Finding the IR heat flux recieved wrt to the altitude from Earth's
surface

heat_flux_IR_array = zeros (376012,1);

for v = 170:376182

```

```

    heat_flux_IR_array(v-169)= (P_earth_IR/(4*pi*((alt_array(v-
169)+r_earth)^2)))/1000000 ;

end

% Plot of The heat flux incident on the spacecraft due to Earth's IR
Radiation

figure(4)
plot (alt_array,heat_flux_IR_array)

title('Incident Heat Flux due to Earths IR Radiation vs Distance from
Earths Surface')
xlabel('Distance from Earths Surface (km)')
ylabel('Incident Heat Flux due to Earths IR Radiation (W/m^2)')

% Section 5

% Script to calculate the Heat Flux from Albedo from the Moon

% Earths Albedo

alb_moon = 0.12 ;

% Solar Heat Flux at the Moon

heat_flux_moon= P_sun/(4*pi*(AU-384400000)^2) ; % (W/m^2)

% Power of Outgoing Heat due to Albedo with respect to Distance from the
Moon

alt_moon_array = zeros (376013,1);
h_moon_array = zeros (376013,1);
area_moon_array = zeros (376013,1);
P_al_moon_array = zeros (376013,1);
alb_moon_heat_flux_array = zeros (376013,1);

temp = 1 ;

for s = 376122:-1:110

    alt_moon_array(temp) = s ;
% (km) Distance between the Moons surface and the spacecraft

    h_moon_array(temp) = (r_moon * alt_moon_array(temp))/(r_moon +
alt_moon_array(temp)); % (km) Height of the Sphere Cap
of the Moons surface in view of the spacecarft at that altitude

    area_moon_array(temp) = 2 * pi * r_moon * h_moon_array(temp) ;
% (km^2) Surface area of the Sphere Cap (surface area = 2*pi*r*h )

    P_al_moon_array(temp) = (heat_flux_moon*1000000) *
area_moon_array(temp) * alb_moon ; % (W) Power
reflected by the Moon due to albedo for that surface area

```

```

    alb_moon_heat_flux_array(temp)=
(P_al_moon_array(temp)/(4*pi*((alt_moon_array(temp)+r_moon)^2)))/1000000;
% (W/m^2) Heat flux incident on the spacecraft at the particular altitude

    temp = temp+1 ;
end

% Plot of The heat flux incident on the spacecraft due to the Moon's albedo

figure(5)
plot (alt_array,alb_moon_heat_flux_array)

title('Incident Heat Flux due to the Moons Albedo vs Distance from Earths
Surface')
xlabel('Distance from Earths Surface (km)')
ylabel('Incident Heat Flux due to the Moons Albedo (W/m^2)')

% Section 6

% Script to calculate the Heat Flux from the Moons IR Radiation

T_moon = 270.4 ;           % Blackbody Temperature of the Moon (K)

% Calculating total Infrared Power output from the Moon

P_moon_IR = sigma * (T_moon^4) * 4* pi * (r_moon^2);           %(W)

% Finding the IR heat flux recieved wrt to the altitude from the Moon's
surface

heat_flux_moon_IR_array = zeros (376013,1);

temp2=1 ;

for r = 376122:-1:110

    heat_flux_moon_IR_array(temp2)=
(P_moon_IR/(4*pi*((alt_moon_array(temp2)+r_moon)^2)))/1000000 ; % (W/m^2)

    temp2 = temp2+1 ;

end

% Plot of The heat flux incident on the spacecraft due to the Moon's IR
Radiation

figure(6)
plot (alt_array,heat_flux_moon_IR_array)

title('Incident Heat Flux due to the Moons IR Radiation vs Distance from
Earths Surface')
xlabel('Distance from Earths Surface (km)')
ylabel('Incident Heat Flux due to the Moons IR Radiation (W/m^2)')

```

```

% Section 7

% Script to calculate the Net Heat Flux across the journey

heat_flux_net_array = zeros (376013,1);

heat_flux_net_array = heat_flux_em_array + alb_earth_heat_flux_array +
heat_flux_IR_array + alb_moon_heat_flux_array + heat_flux_moon_IR_array ; %
(W/m^2) Adding all the fluxes incident on the spacecraft.

figure(7)
plot (alt_array,heat_flux_net_array)

title('Net Heat Flux across the journey vs Distance from Earths Surface')
xlabel('Distance from Earths Surface (km)')
ylabel('Net Heat Flux across the journey (W/m^2)')

% Section 8

% Script to calculate the Average Heat Flux across the journey

heat_flux_avg_total = 0;

for q = 1:376013
    heat_flux_avg_total = heat_flux_avg_total + heat_flux_net_array(q) ;
end

heat_flux_avg = heat_flux_avg_total / 376012

% Section 9

% Script to calculate the Final Heat Flux and Total Power inout into the
tanks across the journey

% Spacecraft assumed to be inside a fairing on Ascent

absorptivity_stage = 0.25 ;

heat_flux_stage = heat_flux_avg * absorptivity_stage    % (W/m^2)

surface_area_hydrogen_tank = 0.5 * (pi * d_hy * h_hy) ;           %
(m^2)

surface_area_methane_tank = 0.5 * (pi * d_meth * h_meth) ;       %
(m^2)

power_tank_hydrogen = heat_flux_stage * surface_area_hydrogen_tank % (W)

power_tank_methane = heat_flux_stage * surface_area_methane_tank  % (W)

```

Appendix C - Matlab Heat Flux Estimation Tool for Mars Mission

```
% Tool to estimate Heat Flux input for a Mars Mission
% Taha Merchant, December 2022

clc
clearvars

% Section 0

% User Inputs

prompt = "What is the diameter of the Hydrogen Tank in m? ";
d_hy = input(prompt);

prompt = "What is the diameter of the Methane Tank in m? ";
d_meth = input(prompt);

prompt = "What is the height of the Hydrogen Tank in m? ";
h_hy = input(prompt);

prompt = "What is the height of the Methane Tank in m? ";
h_meth = input(prompt);

% Section 1

% Script to calculate Solar Heat Flux across the solar system

% Initialise constants

sigma = 5.670374 * 10^-8 ;    % Stefan-Boltzmann constant (W/m^2*K^4)
T_sun = 5778 ;              % Temperature of the Sun (K)
R_sun = 696340000 ;        % Radius of the Sun (m)
AU = 149597870700 ;        % (m)

% Calculating total power output from the Sun

P_sun = sigma * (T_sun^4) * 4* pi * (R_sun^2);    %(W)

    % P_sun is 3.8510e+26 W

% Finding the power recieved per unit area across the solar system between
0.3 and 1.6 AU

% Storing values of r (distance from the Sun) from 0.3 AU to 1.6 AU in an
array

r_array = zeros(1301,1);
```

```

for x = 300:1600

    r_array(x-299,1) = x*AU/1000;

end

% Calculating the Solar Heat flux from 0.3 AU to 1.6AU
heat_flux_array = zeros(1301,1) ;

for y = 300:1600

    heat_flux_array(y-299,1)= P_sun/(4*pi*r_array(y-299,1)^2) ;    %
    (W/m^2)

end

% Converting the r values to AU in array to display on plot
AU_array = zeros (1301,1);

for z = 300:1600

    AU_array (z-299,1) = r_array(z-299,1)/149597870700;

end

% Plotting Solar Heat Flux vs Distance from Sun.
figure(1)
plot
(AU_array,heat_flux_array,AU_array(701),heat_flux_array(701),'o',AU_array(1
225),heat_flux_array(1225),'o')
text(AU_array(701),heat_flux_array(701),'Earth','VerticalAlignment','bottom
','HorizontalAlignment','center')
text(AU_array(1225),heat_flux_array(1225),'Mars','VerticalAlignment','botto
m','HorizontalAlignment','center')

title('Solar Heat Flux vs Distance from Sun')
xlabel('Distance from Sun (AU)')
ylabel('Solar Heat Flux (W/m^2)')

% Section 2

% Plotting Solar Heat Flux vs Distance from Sun for Earth to Mars.

% Earth and Mars Radii

r_earth = 6371 ;          % (km)
r_mars = 3389 ;          % (km)

%Earth and Mars Positions

```

```

earth_au = 1 ;
mars_au = 1.52366231 ;

% Distance between centre of Earth and centre of Mars

D_em = round(((mars_au - earth_au) * AU)/1000); % (km)
D_em_travel = D_em - r_earth - 500 - r_mars - 250 ; % Subtracting the
bodies radii and orbit heights (km)

% Creating a new array to represent the space between Earth and mars

r_em_array = zeros(78328258,1);
heat_flux_em_array = zeros(78328258,1);
alt_array = zeros (78328258,1);

% Calculating the Solar Heat flux between Earth and Mars

for u = 500:78328757

    r_em_array(u-499) = (1+((u+r_earth)*1000)/AU)*AU; %
Distance of spacecraft from the Sun (km)

    heat_flux_em_array(u-499)= P_sun/(4*pi*r_em_array(u-499)^2) ; % Solar
Heat flux incident on the spacecraft at the particular altitude (W/m^2)

    alt_array(u-499) = u ; %
Distance of spacecraft from Earths surface (km)

end

figure(2)
plot (alt_array,heat_flux_em_array)

title('Solar Heat Flux between Earth and Mars vs Distance from Sun')
xlabel('Distance from Earths Surface (km)')
ylabel('Solar Heat Flux (W/m^2)')

% Section 3

% Script to calculate the Heat Flux from Albedo from Earth

% Earths Albedo

alb_earth = 0.31 ;

%Solar Heat Flux at Earth (1 AU)

heat_flux_earth= P_sun/(4*pi*AU^2) ; % (W/m^2)

% Power of Outgoing Heat due to Albedo with respect to Distance from Earth

alt_array = zeros (78328258,1);

```



```

h_array = zeros (78328258,1);
area_array = zeros (78328258,1);
P_al_earth_array = zeros (78328258,1);
alb_earth_heat_flux_array = zeros (78328258,1);

for w = 500:78328757

    alt_array(w-499) = w ;
% (km) Distance between Earths surface and the spacecraft

    h_array(w-499) = (r_earth * alt_array(w-499))/(r_earth + alt_array(w-
499));
% (km) Height of the Sphere Cap of
Earths surface in view of the spacecraft at that altitude

    area_array(w-499) = 2 * pi * r_earth * h_array(w-499) ;
% (km^2) Surface area of the Sphere Cap (surface area = 2*pi*r*h )

    P_al_earth_array(w-499) = (heat_flux_earth*1000000) * area_array(w-499)
* alb_earth ;
% (W) Power reflected by the Earth due
to albedo for that surface area

    alb_earth_heat_flux_array(w-499)= (P_al_earth_array(w-
499)/(4*pi*((alt_array(w-499)+r_earth)^2)))/1000000; % (W/m^2) Heat flux
incident on the spacecraft at the particular altitude

end

% Plot of The heat flux incident on the spacecraft due to Earth's albedo

figure(3)
plot (alt_array,alb_earth_heat_flux_array)

title('Incident Heat Flux due to Earths Albedo vs Distance from Earths
Surface')
xlabel('Distance from Earths Surface (km)')
ylabel('Incident Heat Flux due to Earths Albedo (W/m^2)')

% Section 4

% Script to calculate the Heat Flux from Earth's IR Radiation

T_earth = 253.72 ;
% Blackbody Temperature of Earth (K)

% Calculating total Infrared Power output from Earth

P_earth_IR = sigma * (T_earth^4) * 4* pi * (r_earth^2);
%(W)

% Finding the IR heat flux recieved wrt to the altitude from Earth's
surface

heat_flux_IR_array = zeros (78328258,1);

for v = 500:78328757

```

```

    heat_flux_IR_array(v-499) = (P_earth_IR/(4*pi*((alt_array(v-
499)+r_earth)^2)))/1000000 ;

end

% Plot of The heat flux incident on the spacecraft due to Earth's IR
Radiation

figure(4)
plot (alt_array,heat_flux_IR_array)

title('Incident Heat Flux due to Earths IR Radiation vs Distance from
Earths Surface')
xlabel('Distance from Earths Surface (km)')
ylabel('Incident Heat Flux due to Earths IR Radiation (W/m^2)')

% Section 5

% Script to calculate the Heat Flux from Albedo from Mars

% Earths Albedo

alb_mars = 0.25 ;

% Solar Heat Flux at Mars

heat_flux_mars= P_sun/(4*pi*(AU*mars_au)^2) ; % (W/m^2)

% Power of Outgoing Heat due to Albedo with respect to Distance from Mars

alt_mars_array = zeros (78328258,1);
h_mars_array = zeros (78328258,1);
area_mars_array = zeros (78328258,1);
P_al_mars_array = zeros (78328258,1);
alb_mars_heat_flux_array = zeros (78328258,1);

temp = 1 ;

for s = 78328507:-1:250

    alt_mars_array(temp) = s ;
% (km) Distance between Mars surface and the spacecraft

    h_mars_array(temp) = (r_mars * alt_mars_array(temp))/(r_mars +
alt_mars_array(temp)); % (km) Height of the
Sphere Cap of the Mars surface in view of the spacecarft at that altitude

    area_mars_array(temp) = 2 * pi * r_mars * h_mars_array(temp) ;
% (km^2) Surface area of the Sphere Cap (surface area = 2*pi*r*h )

    P_al_mars_array(temp) = (heat_flux_mars*1000000) *
area_mars_array(temp) * alb_mars ; % (W) Power
reflected by Mars due to albedo for that surface area

```

```

    alb_mars_heat_flux_array(temp)=
(P_al_mars_array(temp)/(4*pi*((alt_mars_array(temp)+r_mars)^2)))/1000000;
% (W/m^2) Heat flux incident on the spacecraft at the particular altitude

    temp = temp+1 ;
end

% Plot of The heat flux incident on the spacecraft due to Mars' albedo

figure(5)
plot (alt_array,alb_mars_heat_flux_array)

title('Incident Heat Flux due to Mars Albedo vs Distance from Earths
Surface')
xlabel('Distance from Earths Surface (km)')
ylabel('Incident Heat Flux due to Mars Albedo (W/m^2)')

% Section 6

% Script to calculate the Heat Flux from the Mars IR Radiation

T_mars = 209.8 ;           % Blackbody Temperature of Mars (K)

% Calculating total Infrared Power output from Mars

P_mars_IR = sigma * (T_mars^4) * 4* pi * (r_mars^2);           %(W)

% Finding the IR heat flux recieved wrt to the altitude from Mars' surface

heat_flux_mars_IR_array = zeros (78328258,1);

temp2=1 ;

for r = 78328507:-1:250

    heat_flux_mars_IR_array(temp2)=
(P_mars_IR/(4*pi*((alt_mars_array(temp2)+r_mars)^2)))/1000000 ; % (W/m^2)

    temp2 = temp2+1 ;

end

% Plot of The heat flux incident on the spacecraft due to Mars' IR
Radiation

figure(6)
plot (alt_array,heat_flux_mars_IR_array)

title('Incident Heat Flux due to Mars IR Radiation vs Distance from Earths
Surface')
xlabel('Distance from Earths Surface (km)')
ylabel('Incident Heat Flux due to Mars IR Radiation (W/m^2)')

% Section 7

```

```

% Script to calculate the Net Heat Flux across the journey

heat_flux_net_array = zeros (78328258,1);

heat_flux_net_array = heat_flux_em_array + alb_earth_heat_flux_array +
heat_flux_IR_array + alb_mars_heat_flux_array + heat_flux_mars_IR_array ; %
(W/m^2) Adding all the fluxes incident on the spacecraft.

figure(7)
plot (alt_array,heat_flux_net_array)

title('Net Heat Flux across the journey vs Distance from Earths Surface')
xlabel('Distance from Earths Surface (km)')
ylabel('Net Heat Flux across the journey (W/m^2)')

% Section 8

% Script to calculate the Average Heat Flux across the journey

heat_flux_avg_total = 0;

for q = 1:78328258
    heat_flux_avg_total = heat_flux_avg_total + heat_flux_net_array(q) ;
end

heat_flux_avg = heat_flux_avg_total / 78328257

% Section 9

% Script to calculate the Final Heat Flux and Total Power inout into the
tanks across the journey

% Spacecraft assumed to be inside a fairing on Ascent

absorptivity_stage = 0.25 ;

heat_flux_stage = heat_flux_avg * absorptivity_stage      % (W/m^2)

surface_area_hydrogen_tank = 0.5 * (pi * d_hy * h_hy) ;      %
(m^2)

surface_area_methane_tank = 0.5 * (pi * d_meth * h_meth) ;    %
(m^2)

power_tank_hydrogen = heat_flux_stage * surface_area_hydrogen_tank % (W)

power_tank_methane = heat_flux_stage * surface_area_methane_tank % (W)

```

List of Figures

1	Electrically Augmented Expander Cycle [4]	18
2	General Turbo Pump Configuration for Osiris Engine [4]	20
3	Osiris Engine System Diagram and Model	21
4	Topics for Comparison	25
5	Top Level Logic flow for the Tools used	25
6	Phase Angle Diagram [17]	29
7	Hyperbolic Escape Trajectory of the spacecraft from Earth [17]	29
8	Hyperbolic Arrival Trajectory of the spacecraft to Mars [17]	31
9	Trajectory simulation of the Spacecraft at Earth Departure	32
10	Trajectory simulation of the Spacecraft Transfer Trajectory	33
11	Trajectory simulation of the Spacecraft in its final trajectory around Mars	33
12	Final ΔV Requirements	34
13	GMAT Mission definition	37
14	Moon Transfer Trajectory	38
15	ΔV Required for First Burn	38
16	ΔV Required for Second Burn	39
17	Graph of Vacuum Specific Impulse vs O/F ratio for LH ₂ /LOx, LCH ₄ /LOx and RP-1/LOx [30]	45
18	Matlab System Mass Estimation Tool Logic Flow	53
19	Input for Hydrolox Osiris Engine for Moon Mission	55
20	Output of the tool for Hydrolox Osiris Engine for Moon Mission	55
21	Input for Methalox Osiris Engine for Moon Mission	56
22	Output of the tool for Methalox Osiris Engine for Moon Mission	56
23	Input for Hydrolox Osiris Engine for Mars Mission	57
24	Output of the tool for Hydrolox Osiris Engine for Mars Mission	57
25	Input for Methalox Osiris Engine for Mars Mission	58
26	Output of the tool for Methalox Osiris Engine for Mars Mission	58
27	Plot of ΔV Total Mass plot for Hydrolox Engine	59
28	Plot of ΔV vs Inert Mass plot for Hydrolox Engine	59
29	Plot of ΔV vs Total Mass plot for Methalox Engine	60
30	Plot of ΔV vs Inert Mass plot for Methalox Engine	60
31	Plot of OF Ratio vs Total Mass for Hydrolox Engine for Moon Mission	61
32	Plot of OF Ratio vs Total Mass for Hydrolox Engine for Moon Mission	61
33	Plot of OF Ratio vs Total Mass for Methalox Engine for Moon Mission	62
34	Plot of OF Ratio vs Inert Mass for Methalox Engine for Moon Mission	62
35	Plot of OF Ratio vs Total Mass for Hydrolox Engine for Mars Mission	63
36	Plot of OF Ratio vs Inert Mass for Hydrolox Engine for Mars Mission	63

37	Plot of OF Ratio vs Total Mass for Methalox Engine for Mars Mission	64
38	Plot of OF Ratio vs Inert Mass for Methalox Engine for Mars Mission	64
39	Plot of I_{sp} vs Total Mass for Hydrolox Engine for Moon Mission . . .	65
40	Plot of I_{sp} vs Inert Mass for Hydrolox Engine for Moon Mission . . .	65
41	Plot of I_{sp} vs Total Mass for Methalox Engine for Moon Mission . . .	66
42	Plot of I_{sp} vs Inert Mass for Methalox Engine for Moon Mission . . .	66
43	Plot of I_{sp} vs Total Mass for Hydrolox Engine for Mars Mission . . .	67
44	Plot of I_{sp} vs Inert Mass for Hydrolox Engine for Mars Mission . . .	67
45	Plot of I_{sp} vs Total Mass for Methalox Engine for Mars Mission . . .	68
46	Plot of I_{sp} vs Inert Mass for Methalox Engine for Mars Mission . . .	68
47	Tank sizes for Hydrolox Engine (Left) and Methalox Engine (Right) for the Moon mission	71
48	Tank sizes for Hydrolox Engine (Left) and Methalox Engine (Right) for the Mars Mission	71
49	Performance of the Hydrogen Pump (Stage 1) at 30000 rpm [4] . . .	76
50	Performance of the Methane Pump at 20000 rpm [4]	78
51	Thrust vs Power Curve for the Hydrolox Osiris Engine [4]	79
52	Thrust vs Power Curve for the Methalox Osiris Engine [4]	79
53	Matlab Heat Flux Estimation Tool Logic Flow	90
54	Solar Heat Flux Distribution Graph	93
55	Solar Heat Flux between Earth and Moon vs Distance from Earth's Surface	94
56	Incident Heat Flux due to Earth's Albedo vs Distance from Earth's Surface	95
57	Change in Incident Heat Flux due to Earth's Albedo	96
58	Incident Heat Flux due to Earth's IR Radiation vs Distance from Earth's Surface	97
59	Incident Heat Flux due to the Moon's Albedo vs Distance from Earth's Surface	98
60	Incident Heat Flux due to the Moon's IR Radiation vs Distance from Earth's Surface	99
61	Net Heat Flux across the Journey vs Distance from Earth's Surface	100
62	Input of the Tank Size for Hydrolox Engine for Moon Mission . . .	101
63	Output of the Heat Flux and Power for Hydrolox Engine for Moon Mission	101
64	Input of the Tank Size for Methalox Engine for Moon Mission . . .	102
65	Output of the Heat Flux and Power for Methalox Engine for Moon Mission	102
66	Solar Heat Flux between Earth and Mars vs Distance from Earth's Surface	103

67	Incident Heat Flux due to Earth's Albedo vs Distance from Earth's Surface	104
68	Incident Heat Flux due to Earth's IR Radiation vs Distance from Earth's Surface	105
69	Incident Heat Flux due to Mars' Albedo vs Distance from Earth's Surface	106
70	Incident Heat Flux due to Mars' IR Radiation vs Distance from Earth's Surface	107
71	Net Heat Flux across the Journey vs Distance from Earth's Surface	108
72	Input of the Tank Size for Hydrolox Engine for Mars Mission	109
73	Output of the Heat Flux and Power for Hydrolox Engine for Mars Mission	109
74	Input of the Tank Size for Methalox Engine for Mars Mission	110
75	Output of the Heat Flux and Power for Methalox Engine for Mars Mission	110
76	First Input page for BoilFAST for LH ₂ Tank for Moon Mission . . .	111
77	Second Input page for BoilFAST for LH ₂ Tank for Moon Mission . .	112
78	Third Input page for BoilFAST for LH ₂ Tank for Moon Mission . .	112
79	Volume of Fuel vs Time for LH ₂ Tank for Moon Mission	113
80	Quantity of Fuel vs Time for LH ₂ Tank for Moon Mission	113
81	Boil Off Rates of Fuel vs Time for LH ₂ Tank for Moon Mission . . .	114
82	Heat Transfer Rates of Fuel vs Time for LH ₂ Tank for Moon Mission	114
83	First Input page for BoilFAST for LCH ₄ Tank for Moon Mission . .	115
84	Second Input page for BoilFAST for LCH ₄ Tank for Moon Mission .	115
85	Third Input page for BoilFAST for LCH ₄ Tank for Moon Mission . .	116
86	Volume of Fuel vs Time for LCH ₄ Tank for Moon Mission	116
87	Quantity of Fuel vs Time for LCH ₄ Tank for Moon Mission	117
88	Boil Off Rates of Fuel vs Time for LCH ₄ Tank for Moon Mission . .	117
89	Heat Transfer Rates of Fuel vs Time for LCH ₄ Tank for Moon Mission	118
90	First Input page for BoilFAST for LH ₂ Tank for Mars Mission . . .	118
91	Second Input page for BoilFAST for LH ₂ Tank for Mars Mission . .	119
92	Third Input page for BoilFAST for LH ₂ Tank for Mars Mission . . .	119
93	Volume of Fuel vs Time for LH ₂ Tank for Mars Mission	120
94	Quantity of Fuel vs Time for LH ₂ Tank for Mars Mission	120
95	Boil Off Rates of Fuel vs Time for LH ₂ Tank for Mars Mission . . .	121
96	Heat Transfer Rates of Fuel vs Time for LH ₂ Tank for Mars Mission	121
97	First Input page for BoilFAST for LCH ₄ Tank for Mars Mission . .	122
98	Second Input page for BoilFAST for LCH ₄ Tank for Mars Mission .	122
99	Third Input page for BoilFAST for LCH ₄ Tank for Mars Mission . .	123
100	Volume of Fuel vs for LCH ₄ Tank for Mars Mission	123

101	Quantity of Fuel vs Time for LCH ₄ Tank for Mars Mission	124
102	Boil Off Rates of Fuel vs Time for LCH ₄ Tank for Mars Mission . .	124
103	Heat Transfer Rates of Fuel vs Time for LCH ₄ Tank for Mars Mission	125
104	Example of an ecosystem with In Situ Resource Utilization [63] . .	128
105	Mars' Atmosphere as compared to Earth [64]	129
106	Subsurface ice detected by NASA's Phoenix Mars Lander's Surface Stereo Imager. Here the ice is shown sublimating between the in- terval of 4 Martian Days [68]	131
107	The Korolov Crater captured by ESA's Mars Express [69]	132
108	Comparison between the formation of gas bubbles in a lower and higher gravity environment [74]	135
109	The Sabatier Process Setup [80]	138
110	Flowchart representing the flow of resources for an ecosystem on Mars where methane is the fuel [82]	139
111	Lunar Regolith [86]	140
112	(A) Lunar North Pole and (B) Lunar South Pole. Green and Blue dots indicate detected surface water ice. [85]	141
113	Manufacturing of methane as a Fuel from carbon monoxide and water	143

List of Tables

1	Hydrolox Version Mass Breakdown	22
2	Methalox Version Mass Breakdown	23
3	Scoring for Efficiency of Fuels	46
4	Required Inputs for the Mass Estimation Tool and their Units	54
5	Outputs from the Mass Estimation tool and their units	54
6	Inputs for the Mass Estimation tool	69
7	Outputs of the Mass Estimation tool	70
8	Scoring for System Mass	73
9	Hydrogen Pump (Stage 1) Key Parameters [4]	75
10	Hydrogen Pump (Stage 2) Key Parameters [4]	75
11	Hydrogen Pump Design Parameters [4]	76
12	Methane Pump Key Parameters [4]	77
13	Methane Pump Design Parameters [4]	77
14	Scoring for Pump Power Requirements	81
15	Scoring for Storability and Long-Term Use	86
16	Inputs for the Heat Flux Estimation Tool	91
17	Outputs of the Heat Flux Estimation Tool	91
18	Inputs to the Heat Flux Estimation tool	125
19	Outputs of the Heat Flux Estimation tool	126
20	Outputs of the BoilFAST tool	126
21	Scoring for Boil Off Behaviour	127
22	Scoring for In Situ Production	144
23	Summary of Scores	145
24	Summary of Weights	147

References

- [1] John D. Clark, Ignition!: An informal history of liquid rocket propellants, Internet Archive. (1972). In Internet Archive. from https://archive.org/details/ignition_201612/page/n23/mode/2up
- [2] NASA. (2021, July 8). Moon to Mars Overview. Moon to Mars. from <https://www.nasa.gov/topics/moon-to-mars/overview>
- [3] The space economy is booming. What benefits can it bring to Earth? (2023, February 28). World Economic Forum. from <https://www.weforum.org/agenda/2022/10/space-economy-industry-benefits/#:~:text=The%20Space%20Foundation's%20The%20Space,increase%20from%20a%20year%20earlier.>
- [4] Merchant, T., Coy, & Lagemann. (2022). Osiris Electrically Augmented Expander Cycle Engine, Masters Project Report. University of Bremen.
- [5] Friedlaender, F. M., & Piper, J. (1968). Space-storable propulsion systems comparison. *Journal of Spacecraft and Rockets*. from <https://doi.org/10.2514/3.29548>
- [6] Arutyunov, V. S., Savchenko, V. G., Solomonov, B. N., Arutyunov, A. V., & Nikitin, A. (2022). The Fuel of Our Future: Hydrogen or Methane? *Methane*, 1(2), 96-106. from <https://doi.org/10.3390/methane1020009>
- [7] (2017). Usage of oxygen-and-methane propellant in liquid-propellant rocket engines. from <https://doi.org/10.18698/2541-8009-2017-12-205>
- [8] Sutton, G. P., & Biblarz, O. (2016). *Rocket propulsion elements*. John Wiley & Sons, Incorporated.
- [9] Dragon. (n.d.). www.spacex.com. from <https://www.spacex.com/vehicles/dragon/>
- [10] Falcon 9. (n.d.). www.spacex.com. from <https://www.spacex.com/vehicles/falcon-9/>
- [11] Sesnic, T. (2022). Raptor 1 vs Raptor 2: What did SpaceX change? *Everyday Astronaut*. from <https://everydayastronaut.com/spacex-raptor-engine-comparison/>
- [12] RL10 Engine — Aerojet Rocketdyne. (n.d.). from <https://www.rocket.com/space/liquid-engines/rl10-engine>

-
- [13] Electron — Rocket Lab. (n.d.). from <https://www.rocketlabusa.com/launch/electron/>
- [14] NASA. (2005). Mars Reconnaissance Orbiter. In mars.nasa.gov. from <https://mars.nasa.gov/files/mro/MRO-060303.pdf>
- [15] FreeFlyer®Software (Version 7.7.1.55976). (n.d.). [Software]. a.i. solutions. from <https://ai-solutions.com/freelyer-astrodynamic-software/>
- [16] a.i. solutions. (2023b, April 13). FreeFlyer Mission History — a.i. solutions. a.i. Solutions. from <https://ai-solutions.com/freelyer-history/>
- [17] Patched Conics Transfer. (n.d.). from https://ai-solutions.com/_freelyeruniversityguide/patched_conics_transfer.htm
- [18] (2020). 26 August 2020 release of the Apollo 15 Flight Journal. The Apollo 15 Flight Journal. from <https://history.nasa.gov/afj/ap15fj/index.html>
- [19] General Mission Analysis Tool (GMAT) (Version V2020a). (n.d.). [Software]. NASA. from <http://gmatcentral.org/>
- [20] NASA. (1978). Liquid Hydrogen as a Propulsion Fuel, 1945-1959. In ntrs.nasa.gov. from <https://ntrs.nasa.gov/citations/19790008823>
- [21] NASA. (n.d.). First in Space with Liquid Hydrogen. In www1.grc.nasa.gov. from <https://www1.grc.nasa.gov/wp-content/uploads/Centaur-First-Liquid-Hydrogen-1962.pdf>
- [22] Ariane Group. (n.d.). VINCI® ENGINE - PROPULSION SOLUTIONS FOR LAUNCHERS. www.ariane.group. from https://www.ariane.group/wp-content/uploads/2020/06/VINCI_2020_04_DS_EN_Eng_Web.pdf
- [23] RS-25 Engine — Aerojet Rocketdyne. (n.d.). from <https://www.rocket.com/space/liquid-engines/rs-25-engine>
- [24] Ariane Group. (n.d.-b). VULCAIN®2.1 ENGINE. Vulcain 2.1 Engine. from https://www.ariane.group/wp-content/uploads/2020/06/VULCAIN2.1_2020_04_PS_EN_Web.pdf
- [25] NASA. (n.d.-b). NASA T M X- 52796 FLOXIMETHANE PUMP-FED ENGINE TECHNOLOGY REVIEW. In ntrs.nasa.gov. from <https://ntrs.nasa.gov/api/citations/19700020666/downloads/19700020666.pdf>
- [26] Blue Origin. (2023, April 10). BE-4 — Blue Origin. <https://www.blueorigin.com/engines/be-4/>

-
- [27] Avio. (n.d.). Vega Family - M10 Engine. from [www.avio.com](https://www.avio.com/m-10).<https://www.avio.com/m-10>
- [28] The upper limit of specific impulse for various rocket fuels. (2016). from <https://thephysicsofspacex.files.wordpress.com/2016/07/isp-upper-limits.pdf>
- [29] Wolfram Research, Inc. (2022). Wolfram Alpha Notebook Edition. www.wolfram.com. from <https://www.wolfram.com/wolfram-alpha-notebook-edition>
- [30] Brown, C. D. (2004). Conceptual Investigations for a Methane-Fueled Expander Rocket Engine. 40th AIAA/ASME/SAE/ASEE Joint Propulsion Conference and Exhibit. from <https://doi.org/10.2514/6.2004-4210>
- [31] Methane - Density and Specific Weight vs. Temperature and Pressure. (n.d.). from https://www.engineeringtoolbox.com/methane-density-specific-weight-temperature-pressure-d_2020.html
- [32] Hydrogen - Density and Specific Weight vs. Temperature and Pressure. (n.d.). from https://www.engineeringtoolbox.com/hydrogen-H2-density-specific-weight-temperature-pressure-d_2044.html
- [33] Space Systems Laboratory - Department of Aerospace Engineering - University of Maryland. ENAE 483/788D - Principles of Space Systems Design (2022). Lecture 08 Mass Estimating Relations. from <https://spacecraft.ssl.umd.edu/academics/483F22/483F22L08.MERs/483F22L08.html>
- [34] Glatt, C. R. (1974, September 1). WAATS: A computer program for Weights Analysis of Advanced Transportation Systems. NASA Technical Reports Server (NTRS). from <https://ntrs.nasa.gov/citations/19740027176>
- [35] Macconochie, I. O. (1978, June 1). Techniques for the determination of mass properties of earth-to-orbit transportation systems. NASA Technical Reports Server (NTRS). from <https://ntrs.nasa.gov/citations/19780022221>
- [36] Heineman, W., Jr. (1971, May 1). Fundamental techniques of weight estimating and forecasting for advanced manned spacecraft and space stations. NASA Technical Reports Server (NTRS). from <https://ntrs.nasa.gov/citations/19710015949>
- [37] Willie Heineman, Jr., Mass Estimation and Forecasting for Aerospace Vehicles Based on Historical Data NASA JSC-26098, November 1994

-
- [38] NASA. (2023, April 11). Chandrayaan 2. Nssdc.Gsfc.Nasa.Gov. from <https://nssdc.gsfc.nasa.gov/nmc/spacecraft/display.action?id=2019-042A>
- [39] In Depth — Curiosity (MSL) - NASA Solar System Exploration. (n.d.). NASA Solar System Exploration. from <https://solarsystem.nasa.gov/missions/curiosity-msl/in-depth/>
- [40] R. H. Anschutz. Design Report of the RL10A-3-3 Rocket Engine. Design features of RL-10 A-3 liquid propellant rocket engine. Tech. rep. NASA, 1966. <https://ntrs.nasa.gov/citations/19670005471>
- [41] Jonas Bischof. “Detailed Design Study of an Electric Liquid Oxygen Pump”. MA thesis. City University of Applied Sciences Bremen, 2021.
- [42] Dvorsky, G. (2022, November 9). Why Hydrogen Leaks Continue to Be a Major Headache for NASA Launches. Gizmodo. from <https://gizmodo.com/nasa-hydrogen-leaks-sls-rocket-space-shuttle-1849500702>
- [43] (2015). Google Books - Gas Separation Membranes. Springer International Publishing. from https://www.google.de/books/edition/Gas_Separation_Membranes/n2u6CAAQBAJ?hl=en&gbpv=0
- [44] Hydrogen - Thermophysical Properties. (n.d.). www.engineeringtoolbox.com. from https://www.engineeringtoolbox.com/hydrogen-H2-density-specific-weight-temperature-pressure-d_2044.html
- [45] Methane - Thermophysical Properties. www.engineeringtoolbox.com. from https://www.engineeringtoolbox.com/methane-d_1420.html
- [46] (2019). Yukitaka Murakami. Metal Fatigue (2nd ed.). Academic Press. <https://www.sciencedirect.com/science/article/pii/B9780128138762000261>
- [47] Heald, Daniel A. “Some Development Problems with Large Cryogenic Propellant Systems.” SAE Transactions, vol. 68, 1960, pp. 164-68. JSTOR, <http://www.jstor.org/stable/44565125> Accessed 10 Apr.2023.
- [48] Safe Use of Hydrogen. (n.d.). Energy.gov. from <https://www.energy.gov/eere/fuelcells/safe-use-hydrogen#:~:text=For%20example%2C%20hydrogen%20is%20non,to%20enable%20its%20safe%20use.>
- [49] Methane and Health and Safety. (n.d.). www.socalgas.com. from <https://www.socalgas.com/stay-safe/methane-emissions/methane-and-health-and-safety>

-
- [50] (2011). Issues of Long-Term Cryogenic Propellant Storage in Microgravity. In ntrs.nasa.gov. from <https://ntrs.nasa.gov/api/citations/20120011680/downloads/20120011680.pdf>
- [51] Britannica, T. Editors of Encyclopaedia (2023, March 20). astronomical unit. Encyclopedia Britannica. from <https://www.britannica.com/science/astronomical-unit>
- [52] Mars Fact Sheet. (n.d.). from <https://nssdc.gsfc.nasa.gov/planetary/factsheet/marsfact.html>
- [53] Sherif, S. A. (1997). Liquid hydrogen: Potential, problems, and a proposed research program. International Journal of Hydrogen Energy, 22(7), 683-688. from [https://doi.org/10.1016/s0360-3199\(96\)00201-7](https://doi.org/10.1016/s0360-3199(96)00201-7)
- [54] Moon Fact Sheet. (n.d.). from <https://nssdc.gsfc.nasa.gov/planetary/factsheet/moonfact.html>
- [55] Albedo — EARTH 103: Earth in the Future. (n.d.) from <https://www.e-education.psu.edu/earth103/node/1002>
- [56] (2021, March 2). The Moon at thermal infrared wavelengths: a benchmark for asteroid thermal models. Www.Aanda.Org. from <https://www.aanda.org/articles/aa/pdf/2021/06/aa39946-20.pdf>
- [57] Working Group I: The Scientific Basis. (n.d.). In archive.ipcc.ch. IPCC. from <https://archive.ipcc.ch/ipccreports/tar/wg1/041.htm>
- [58] Matlab (Version v2022a). (n.d.). [Software]. MathWorks. from <https://in.mathworks.com/products/matlab.html>
- [59] Materials - Light Reflecting Factors. (n.d.). from https://www.engineeringtoolbox.com/light-material-reflecting-factor-d_1842.html
- [60] Libretexts. (2022). 6.2: Blackbody Radiation. Physics LibreTexts. from [https://phys.libretexts.org/Bookshelves/University_Physics/Book%3A_University_Physics_\(OpenStax\)/University_Physics_III_-_Optics_and_Modern_Physics_\(OpenStax\)/06%3A_Photons_and_Matter_Waves/6.02%3A_Blackbody_Radiation](https://phys.libretexts.org/Bookshelves/University_Physics/Book%3A_University_Physics_(OpenStax)/University_Physics_III_-_Optics_and_Modern_Physics_(OpenStax)/06%3A_Photons_and_Matter_Waves/6.02%3A_Blackbody_Radiation)
- [61] BoilFAST (V 1.0.0.0). (n.d.). [Software]. The University of Western Australia. from <https://www.fsr.ecm.uwa.edu.au/software/boilfast/>

-
- [62] The Space Review: The problems with lunar ISRU (page 1). (2006, September 5). Thespacereview.Com. from <https://thespacereview.com/article/697/1>
- [63] International Space Exploration Coordination Group. (2021). IN-SITU RESOURCE UTILIZATION GAP ASSESSMENT REPORT. In [globalspaceexploration.org](https://www.globalspaceexploration.org). from <https://www.globalspaceexploration.org/wordpress/wp-content/uploads/2021/04/ISECG-ISRU-Technology-Gap-Assessment-Report-Apr-2021.pdf>
- [64] Comparing the atmospheres of Mars and Earth. (n.d.). from https://www.esa.int/ESA_Multimedia/Images/2018/04/Comparing_the_atmospheres_of_Mars_and_Earth
- [65] Thronson, H., R.J. Cassady, R. Zucker, L. May, T. Cichan, L. Karanian, J. Ivey, C. Carberry (2020), The Humans to Mars Report, Explore Mars Inc. Publication, retrieved online September 5th 2020. from https://www.exploremars.org/wp-content/uploads/2020/08/H2MR_2020_Web_v1.pdf
- [66] E. Musk. (2017). Making Humans a Multi-Planetary Species. *New Space*, 5(2), 46-61. from <https://doi.org/10.1089/space.2017.29009.emu>
- [67] Conway, S.J., N. Hovius, T. Barnie, J. Besserer, S.L. Mouelic, R. Orosei, N. Anne (2012), Climate-driven deposition of water ice and the formation of mounds in craters in Mars' north polar region. *Icarus* 220, p.174-193, <http://dx.doi.org/10.1016/j.icarus.2012.04.021>
- [68] Brian Dunbar. (n.d.). NASA - Disappearing Ice In Color. from https://www.nasa.gov/mission_pages/phoenix/images/press/sol_020_024_change_dodo_v2.html
- [69] Perspective view of Korolev crater. (n.d.). from https://www.esa.int/ESA_Multimedia/Images/2018/12/Perspective_view_of_Korolev_crater
- [70] Chaffin, M., Deighan, J., Schneider, N. et al. Elevated atmospheric escape of atomic hydrogen from Mars induced by high-altitude water. *Nature Geosci* 10, 174-178 (2017). from <https://doi.org/10.1038/ngeo2887>
- [71] Chisholm, G., Zhao, T., & Cronin, L. (2022b). Hydrogen from water electrolysis. Elsevier EBooks, 559-591. from <https://doi.org/10.1016/b978-0-12-824510-1.00015-5>
- [72] Millet, P., & Grigoriev, S. N. (2013b). Water Electrolysis Technologies. Elsevier EBooks, 19-41. from <https://doi.org/10.1016/b978-0-444-56352-1.00002-7>

-
- [73] Gayen, P., Sankarasubramanian, S., & Ramani, V. (2020). Fuel and oxygen harvesting from Martian regolithic brine. *Proceedings of the National Academy of Sciences of the United States of America*, 117(50), 31685-31689. from <https://doi.org/10.1073/pnas.2008613117>
- [74] Lomax, B.A., Just, G.H., McHugh, P.J. et al. Predicting the efficiency of oxygen-evolving electrolysis on the Moon and Mars. *Nat Commun* 13, 583 (2022). from <https://doi.org/10.1038/s41467-022-28147-5>
- [75] Buseck, P. R., Dunin-Borkowski, R. E., Devouard, B., Frankel, R. M., McCartney, M. R., Midgley, P. A., Posfai, M., & Weyland, M. (2001). Magnetite morphology and life on Mars. *Proceedings of the National Academy of Sciences of the United States of America*, 98(24), 13490-13495. from <https://doi.org/10.1073/pnas.241387898>
- [76] Charvin, P., Abanades, S., Flamant, G., & Lemort, F. (2007). Two-step water splitting thermochemical cycle based on iron oxide redox pair for solar hydrogen production. *Energy*, 32(7), 1124-1133. from <https://doi.org/10.1016/j.energy.2006.07.023>
- [77] Idriss, H., Scott, M., & Subramani, V. (2015). Introduction to hydrogen and its properties. Elsevier EBooks, 3-19. from <https://doi.org/10.1016/b978-1-78242-361-4.00001-7>
- [78] Formisano, V., Atreya, S. K., Encrenaz, T., Ignatiev, N., & Giuranna, M. (2004). Detection of Methane in the Atmosphere of Mars. *Science*, 306(5702), 1758-1761. from <https://doi.org/10.1126/science.1101732>
- [79] Junaedi, C. (2011, July 17). Compact and Lightweight Sabatier Reactor for Carbon Dioxide Reduction. NASA Technical Reports Server (NTRS). from <https://ntrs.nasa.gov/citations/20120016419>
- [80] Castellani B, Gambelli AM, Morini E, Nastasi B, Presciutti A, Filipponi M, Nicolini A, Rossi F. Experimental Investigation on CO2 Methanation Process for Solar Energy Storage Compared to CO2-Based Methanol Synthesis. *Energies*. 2017; 10(7):855. from <https://doi.org/10.3390/en10070855>
- [81] Alam, S. J., Depcik, C., Burugupally, S. P., Hobeck, J. D., & McDaniel, E. (2022). Thermodynamic modeling of in-situ rocket propellant fabrication on Mars. *IScience*, 25(5), 104323. from <https://doi.org/10.1016/j.isci.2022.104323>

-
- [82] Muscatello, A. C. (2012, January 9). Mars in Situ Resource Utilization Technology Evaluation. NASA Technical Reports Server (NTRS). from <https://ntrs.nasa.gov/citations/20120001775>
- [83] Akhmanova, M; Dement'ev, B; Markov, M (1978). "Possible Water in Luna 24 Regolith from the Sea of Crises". *Geochemistry International*. 15 (166).
- [84] Colaprete, A., Schultz, P. G., Heldmann, J. L., Wooden, D. H., Shirley, M. D. F., Ennico, K., Hermalyn, B., Marshall, W. L., Ricco, A. J., Elphic, R. C., Goldstein, D., Summy, D., Bart, G. D., Asphaug, E., Korycansky, D., Landis, D. R., & Sollitt, L. (2010). Detection of Water in the LCROSS Ejecta Plume. *Science*, 330(6003), 463-468. from <https://doi.org/10.1126/science.1186986>
- [85] Li, S., Lucey, P. G., Milliken, R. E., Hayne, P. O., Fisher, E. M. C., Paige, D. A., Hurley, D. M., & Elphic, R. C. (2018). Direct evidence of surface exposed water ice in the lunar polar regions. *Proceedings of the National Academy of Sciences of the United States of America*, 115(36), 8907-8912. from <https://doi.org/10.1073/pnas.1802345115>
- [86] NASA. (1969, July 20). Close-up view of astronauts foot and footprint in lunar soil. images.nasa.gov. <https://images.nasa.gov/details/as11-40-5880>